

Impact of breeding innovations in canopy architecture and function on yield formation in winter wheat

Von der Naturwissenschaftlichen Fakultät der
Gottfried Wilhelm Leibniz Universität Hannover

zur Erlangung des Grades
Doktorin der Naturwissenschaften (Dr. rer. nat.)

genehmigte Dissertation
von
Carolin Lichthardt, M.Sc.

2020

Referent: Prof. Dr. sc. agr. Hartmut Stützel

Korreferent: Prof. Dr. rer. nat. Thomas Debener

Korreferentin: Prof.in Dr. rer. hort. Traud Winkelmann

Tag der Promotion: 13.03.2020

für Mama und Papa

ABSTRACT

Wheat (*Triticum aestivum* L.) is one of the most important staple crops worldwide and there is an urgent need to develop high-yielding and resilient new cultivars and to elevate the breeding progress. This thesis presents a retrospective analysis of the breeding progress of the last 50 years aiming to identify innovations in physiological traits with great relevance for future breeding.

Intercepting radiation and the radiation use efficiency (RUE) determine biomass production, which is the more promising influencing factor for total grain yield in comparison to biomass partitioning (harvest index). The first objective within this thesis was to discover the genetic variation in relative light interception and RUE and to understand the underlying architectural and physiological functions of the canopy determining the source of assimilate production. From another perspective, grain yield formation can also be seen as a constant interplay between sink and source components, as the assimilates produced by the source are allocated to the sink organs of the crop. Therefore, the second objective was an in-depth analysis of the interdependencies between sinks and sources and possible limiting factors within that network. Furthermore, a genetic analysis of the physiological and yield related traits was performed. The identification of the genetic regions relevant for the source compartments, which partly enabled the yield increase and their potential effect, was the third objective of this thesis.

During three experimental seasons, canopy traits were assessed in the field by measuring the relative leaf chlorophyll content (via SPAD measurements), the proportion of green leaf material, light interception and leaf area index (LAI) non-destructively. Using these traits, relative light interception, RUE, green canopy duration (GCD), green leaf area integral and the light extinction coefficient were derived. The field trials were conducted with 220 cultivars of which 174 represent the German breeding history. For the evaluation of the dependencies of the canopy parameters and final grain yield, correlations and causal effects between the variables were investigated. Additionally, the progress of each parameter with the year of release of each cultivar was assessed to detect relevance of the traits during breeding progress. A genome wide association study (GWAS) with single markers and additionally with chromosomal segments (haploblocks) was performed to detect co-evolutionary processes between sink and source traits and detect causal genetic regions.

The broad-sense heritability of all measured and derived physiological traits ranged from 7-66%, with the highest values for RUE, SPAD and the average LAI and the lowest for the extinction coefficient. Relative light interception and RUE were identified as two independent traits, which showed high explanatory power for grain yield (30% and 64%, respectively).

Previous studies already indicated the importance of RUE for future breeding progress, but to our knowledge, this is the first study representing more details regarding the underlying traits and concrete causal agents (SPAD and GCD). Investigating the breeding progress, we found that grains per spike showed the most pronounced progress in the breeding history besides total yield (0.45% per year). This trait showed the strongest correlation with final yield among the yield components ($r=0.54$). However, the variation of grains per spike was significantly associated with the variation of SPAD and GCD. The investigations of the network of sinks and sources substantiate the relevance of SPAD and GCD, which both explained substantial variation in grain yield (40% and 42%, respectively). However, the physiological link between the sink and sources lies at stages relevant for grains per spike in contrary to the expected association between grain weight and the canopy persistence. Our results suggest that the potential longevity of the green canopy is predetermined at the time point when the number of grains is fixed. The GWAS underpinned the association of breeding progress in canopy longevity as we observed a shift in allele frequencies. Furthermore, highly significant associations were observed for single marker effects of which some were overlapping with high haplotype variances. Especially a region spanning over 40 Mbp on chromosome 6A was associated with canopy height and also parameters describing the canopy architecture, persistence and thereby light interception. The results present important findings which can be applied in the network of genomic, phenomics and crop modelling and provide new application possibilities for large scale field phenotyping.

Keywords: *winter wheat, physiological breeding, phenotyping, light interception, light utilization, grain number, green canopy duration, SPAD, sink and source, co-evolution, breeding progress, GWAS, haplotype association*

KURZFASSUNG

Weizen (*Triticum aestivum* L.) ist eines der wichtigsten Grundnahrungsmittel weltweit und es besteht die dringende Notwendigkeit, ertragreiche und widerstandsfähige Sorten zu züchten. Die vorliegende Doktorarbeit präsentiert eine retrospektive Analyse des Zuchtfortschritts der letzten 50 Jahre mit dem Ziel, physiologische Züchtungsinnovationen mit großer Relevanz für zukünftige Züchtungen zu identifizieren.

Die aufgenommene Sonneneinstrahlung und die Strahlungsnutzungseffizienz (RUE) bestimmen die Biomasseproduktion der Pflanze, welche wiederum einen höheren Einfluss auf den Ertrag verspricht als im Vergleich dazu die Biomasseverteilung (Ernte Index). Im ersten Teil dieser Arbeit wurde die genetische Variation in der relativen Lichtaufnahme und RUE untersucht, um die zugrundeliegenden architektonischen und physiologischen Funktionen des Bestandes zu verstehen, welche die Quelle der Assimilatproduktion darstellen. Aus einer anderen Perspektive kann die Ertragsbildung auch als ständiges Zusammenspiel von Senken und Quellen („*sink*“ und „*source*“) gesehen werden: die von der „*source*“ produzierten Assimilate werden in die „*sinks*“ verlagert. Im zweiten Teil dieser Arbeit wurden die Wechselwirkungen zwischen „*sink*“ und „*source*“ und möglicher limitierender Faktoren innerhalb dieses Netzwerks analysiert. Im dritten Teil dieser Arbeit wurde eine genetische Analyse der physiologischen und ertragsbezogenen Merkmale durchgeführt.

Über drei aufeinanderfolgende Jahre wurden in Feldversuchen Bestandesmerkmale erfasst, indem der relative Blattchlorophyllgehalt (SPAD Messungen), der Anteil an grünem Blattmaterial, die Lichtaufnahme und der Blattflächenindex (LAI) zerstörungsfrei gemessen wurden. Aus diesen Merkmalen wurden relative Lichtaufnahme, RUE, grüne Bestandesdauer (GCD), grünes Blattflächenintegral und der Lichtextinktionskoeffizient abgeleitet. Die Feldversuche wurden mit 220 Sorten durchgeführt, von denen 174 die deutsche Züchtungsgeschichte abbilden. Zur Beurteilung der Abhängigkeiten der Bestandparameter und des Ertrags wurden Korrelationen und kausale Effekte zwischen den Variablen untersucht. Zusätzlich wurde der Fortschritt jedes Parameters mit dem Zulassungsjahr der Sorten bewertet, um die Relevanz der Merkmale für den Zuchtfortschritt zu ermitteln. Eine genomweite Assoziationsstudie (GWAS) mit Einzelmarkern und chromosomalen Segmenten (Haploblocks) wurde durchgeführt um ko-evolutionäre Prozesse zwischen „*sink*“ und „*source*“ Merkmalen zu untersuchen und kausale Regionen auf dem Genom zu identifizieren.

Die Heritabilität aller gemessener und abgeleiteter physiologischen Merkmale reichte von 7% bis 66%. Die höchsten Werte wurden für RUE, SPAD und den durchschnittlichen LAI errechnet, die niedrigsten für den Extinktionskoeffizienten. Relative Lichtaufnahme und RUE wurden als zwei unabhängige Merkmale identifiziert, welche eine hohe Aussagekraft für den Kornertrag zeigten (30% bzw. 64%).

Frühere Studien zeigten bereits eine Bedeutung von RUE für den zukünftigen Zuchtfortschritt, aber nach unserem Kenntnisstand ist die vorliegende Arbeit die erste Studie, die Details über die zugrundeliegenden Merkmale enthält und konkrete Kausalfaktoren (SPAD und GCD) identifiziert. Bei der Untersuchung des Zuchtfortschritts haben wir festgestellt, dass die Anzahl Körner pro Ähre neben dem Gesamtertrag (0,45% pro Jahr) den stärksten Zuchtfortschritt zeigten. Unter den Ertragskomponenten zeigte dieses Merkmal die stärkste Korrelation mit dem Kornertrag ($r = 0,54$). Die Variation der Körnerzahl pro Ähre steht wiederum signifikant mit der Variation von SPAD und GCD in Beziehung. Die Untersuchungen des Netzwerks von „sink“ und „source“ belegen die Relevanz von SPAD und GCD, die beide erhebliche Variation im Kornertrag (40% bzw. 42%) erklärten. Der physiologische Zusammenhang zwischen „sink“ und „source“ wurde demnach der Entwicklungsphasen zugeordnet, die für die Körnerzahl pro Ähre relevant ist. Unsere Ergebnisse deuten darauf hin, dass die potenzielle Langlebigkeit eines grünen Bestandes zu dem Zeitpunkt vorbestimmt wird, zu dem die Anzahl der Körner festgelegt wird. Die GWAS untermauerte die Assoziation des Zuchtfortschritts in der Bestandesdauer, da wir eine Verschiebung der Allelhäufigkeiten beobachteten. Darüber hinaus wurden hochsignifikante Assoziationen für einzelne Marker-Effekte beobachtet, von denen sich einige mit hohen Haplotyp-Effekten überschneiden. Insbesondere ein Bereich, der sich über 40 Mbp auf dem Chromosom 6A erstreckt, war mit der Höhe des Bestandes und auch mit Parametern assoziiert, die die Architektur des Bestandes und die Bestandesdauer und damit die Lichtaufnahme beschreiben. Die Ergebnisse präsentieren wichtige Erkenntnisse die im Netzwerk der Genomik, Phänomik und Pflanzenmodellierung angewendet werden können. Diese Doktorarbeit eröffnet einen neuen Weg für die Hochdurchsatz-Phänotypisierung im Zeitalter der digitalen Züchtung.

Schlagworte: Winterweizen, physiologische Pflanzenzüchtung, Lichtaufnahme, Lichtnutzung, Körnerzahl pro Ähre, Bestandesdauer, SPAD, „sink“ und „source“, Ko-Evolution, Zuchtfortschritt, GWAS, Haplotyp-Assoziation

CONTENT

Widmung.....	I
Abstract.....	II
Zusammenfassung.....	IV
List of Tables.....	IX
List of Figures.....	XI
Abbreviations.....	XIV

Chapter 1

<i>General introduction</i>	1
Wheat production and breeding – a short history.....	2
Physiological breeding – a powerful approach to improve wheat.....	4
Application of genotypic information – the step forward.....	6
Objectives.....	7

Chapter 2

<i>Green canopy duration and SPAD at heading are the most important indicator for light interception and utilization and thereby relevant for breeding progress of German winter wheat</i>	8
Abstract.....	9
Introduction.....	10
Material and Methods.....	12
Plant material and field trial.....	12
Measuring and deriving canopy parameters.....	13
Yield measurements.....	20
Statistical analyses.....	20
Structural equation model.....	21
Breeding progress.....	23
Results.....	24
High accuracy of RUE _{Eg} , canopy duration and SPAD values at heading in explaining variation in grain yield despite seasonal effects.....	26
SPAD values at heading explain variation in RUE and LAI explains variation in radiation interception.....	27
Suboptimal conditions at vegetation start caused variation in importance of vegetative canopy characteristics for grain yield.....	29

SPAD _{BBCH59} is most relevant for RUE _{gr} and the persistence of the canopy, GCD is most relevant for light interception.....	31
Grain number is affected by SPAD at heading and the canopy duration and grain weight is not affected by any canopy characteristic.....	32
Breeding progress reflects environmental differences and plasticity of modern cultivars.....	33
Discussion.....	36
Usefulness of photosynthetic capacity and the persistence of the canopy for breeding purpose.....	36
The role of canopy architecture in achieving high yield.....	37
Valuable results from path analysis reveal relevance of canopy parameters.....	38
Source characteristics around and after anthesis are relevant for grain number but not individual grain weight.....	38
Progress of yield trough RUE and relative light interception.....	39
Conclusions.....	40
Chapter 3	
<i>Co-evolution of sink and source in the recent breeding history of winter wheat in Germany</i>	41
Abstract.....	42
Introduction.....	43
Material and Methods.....	45
Plant material.....	45
Experimental design and growing conditions.....	45
Yield measurements.....	46
Physiological measurements.....	46
Statistical analyses.....	47
Quantification of the breeding progress.....	48
Genome-wide association study.....	48
Results.....	50
Environmental effects on yield component traits and source characteristics.....	50
The main factor relevant for yield formation, grains per spike, is determined by the photosynthetic activity around anthesis and affects the canopy longevity.....	51
Breeding progress was most pronounced in grains per spike and green canopy duration.....	54
Significant marker-trait associations for GCD and biomass.....	57

Discussion.....	60
Significant breeding progress in biomass, HI, grains per spike, SPAD and GCD.....	60
GCD and grain yield: correlation does not imply causation.....	61
Relevance of GCD for breeding.....	62
Genetic associations of GCD.....	62
Conclusions.....	64
Chapter 4	
<i>Genetic structures of physiological parameters relevant for yield formation and breeding progress in Germany.....</i>	65
Abstract.....	66
Introduction.....	67
Material and Methods.....	68
Plant material and experimental conditions.....	68
Parameters for genetic association.....	68
Genotyping.....	69
Genome wide association with single markers.....	70
Genome wide association with chromosomal segments.....	70
Results.....	71
Single marker – trait association.....	71
Haplotype – trait association.....	73
Discussion.....	76
Chapter 5	
<i>Discussion.....</i>	77
Supplementary Material.....	81
References.....	103
Curriculum Vitae.....	113
List of Publications.....	114
Danksagung.....	115

LIST OF TABLES

Table 2.1	List of measured and estimated physiological parameters.	p. 19
Table 2.2	Summary of parameters describing the canopy characteristics, BLUE values, genetic variance and heritability calculated based on the linear mixed model in formula (16), *= data only from 2017, += repeatability.	p. 25
Table 2.3	Pearson correlation coefficients of all parameters with grain yield within the three seasons and overall with the BLUE values, shading indicates the ranking of the coefficients within the season (shading= top four associations among the canopy traits).	p. 26
Table 2.4	Estimated values for the causal relationships explaining the yield components by the source model.	p. 32
Table 2.5	Breeding progress of the yield, canopy and architectural parameters. Absolute and relative breeding progress was derived from sliding window means. Absolute breeding progress is the slope of the linear regression line fitted for the parameter in dependency of the year of release. The relative breeding progress is expressed in percent [%] as the ration between the trait value of 2010 and 1970. Grey numbers: $R^2 < 0.25$, bold numbers: $R^2 > 0.75$.	p. 34
Table 3.1	Breeding progress of the main yield and stay green parameters dissected into the development within each growing season separately and calculated for all seasons together (overall). Absolute and relative breeding progress was derived from sliding window means. Units for absolute breeding progresses are: grain yield: $t\ ha^{-1}$; harvest index (HI): unitless; biomass: $g\ m^{-2}$; straw: $t\ ha^{-1}$; thousand grain weight (TGW): g; grains m^{-2} : quantity; spikes m^{-2} : quantity; grains $spike^{-1}$: quantity; maximal leaf area index (LAI _{max}): unitless; green canopy duration (GCD): $^{\circ}Cd$; leaf area duration (LAD): $^{\circ}Cd$; and SPAD: unitless. Relative breeding progress is expressed in percent (%).	p. 56

Table 4.1	List of the 20 traits used for the genetic associations.	p. 68
Table 4.2	Summary of significant marker-trait associations, in parentheses: number of associations per chromosome.	p. 71
Table 4.3	Multi-trait associations of single marker effects.	p. 72
Table 4.4	Multi-trait associations of local GEBV variances.	p. 73

LIST OF FIGURES

- Figure 2.1** Theoretical path diagram indicating the causal relationships between source parameters and final grain yield. Black boxes indicate endogenous response variables, white boxes the predictor variables. p. 21
- Figure 2.2** Theoretical path diagram for interdependencies between sink and sources. Black boxes indicate endogenous response variables, white boxes the predictor variables. The models were tested with respect to the derived source model. p. 22
- Figure 2.3** Proportion of variance in percent explained by the variance components of the model (equation 19). p. 24
- Figure 2.4** Linear relationship between the radiation use efficiency and the underlying parameters k and SPAD at heading (a) and between the mean relative light interception and the leaf area index and k (b). The regression line was only plotted, when the relationship was significant (p -value ≤ 0.05). The \widehat{gI}_{mean} - outlier in 2016 was the cultivar Helios which was performing not very well in both replications in 2015. However, removing the cultivar from the regression analyses does not have any considerable effects (data not shown). p. 28
- Figure 2.5** Measured data of LAI and the relative light interception at several dates throughout the seasons (b) and the corresponding correlation of the values with the final grain yield (a). p. 30
- Figure 2.6** Model with fitted observed variables for interdependencies between source characteristics. Black boxes indicate endogenous response variables, white boxes the predictor variables. Only significant standardized path coefficients for each causal relationship ($p < 0.05$) and standardized path coefficients are displayed if larger than 0.1. R^2 values for the response variables indication the prediction accuracy of the explanatory variables. The width of the path represents the magnitude of the standardized coefficients and dashed arrows indicate the additional dependencies suggested by the structural equation model. p. 31

-
- Figure 2.7** Fitted models for the causal relationships between yield components and underlying source traits based on the complete and adjusted underlying source model (compare Fig. 2.5). Black boxes indicate endogenous response variables, white boxes the predictor variables.
- p. 33
- Figure 2.8** Sliding window plots showing the breeding progress of RUE_{gf} (a), \widehat{gI}_{mean} (b), \widehat{gLAI}_{mean} (c) and k (d). Each dot represents a mean value of 10 cultivars, the coloured area represents the standard deviation. The slopes of the linear regressions are referred to as absolute breeding progress and the relative breeding progress is the ratio between the values from 2010 and 1970.
- p. 35
-
- Figure 3.1** Boxplots of the yield, yield components and green canopy parameters presenting the mean values per cultivar and season for the 174 cultivars representing the breeding history. Different lower-case letters within the plots indicate significant differences between seasons. Abbreviations are listed in Table 1.
- p. 51
- Figure 3.2** Relationships between grain yield and (A) harvest index (HI); (B) biomass; and (C) grains per spike. Each point represents the mean values of a cultivar in three growing seasons. In total, 174 cultivars representing the breeding history were used.
- p. 52
- Figure 3.3** Relationships between (A) grains per spike and SPAD; (B) green canopy duration and grain per spike; and (C) grain yield and green canopy duration. Each point represents the mean values of a cultivar in three growing seasons. In total, 174 cultivars representing the breeding history were used.
- p. 53
- Figure 3.4** Sliding window plots showing breeding progress in grain yield per season (A-C) and on average (D). Each dot represents a mean value of a group of 10 cultivars and the coloured area represents their standard deviations. The slopes of the linear regression lines (black line) are referred to as absolute breeding progress and the relative breeding progress is the ratio between the values in 2010 and 1970.
- p. 54
- Figure 3.5** Sliding window plots showing breeding progress of harvest index (A-D) and biomass (E-H). For detail, see the caption of Fig. 3.4.
- p. 55

-
- Figure 3.6** Sliding window plots showing breeding progress of grain per spike. For detail, see the caption of Fig. 3.4. p. 55
- Figure 3.7** Sliding window plots showing breeding progress of SPAD (A-C) and green canopy duration (D-G). For detail, see the caption of Fig. 3.4. p. 57
- Figure 3.8** Heat maps of pairwise LD of the SNP-markers with significant marker-trait-associations for (A) biomass on chromosome 3A and (B) green canopy duration (GCD) on chromosome 6A. SNP-markers among the top 100 $-\log(p\text{-values})$ for each analysed trait on these chromosomes are also shown. p. 58
- Figure 3.9** Green canopy duration (GCD) of cultivars in relation to their number of GCD alleles in the selected region between 400 and 441 Mbp on chromosome 6A. Point colours representing the year of release and grey points are the cultivars with unknown year of release. Red points indicate the mean GCD for cultivars carrying the major allele ($x=0$) or the minor allele ($x=1$) p. 59
-
- Figure 4.1** Single marker – trait associations on chromosome 6A (A) and overlapping LD blocks (B). A bar indicates that for the trait the local GEBV variance is among the top 10. p. 75

ABBREVIATIONS

BBCH59	Heading date
BBCH87	Hard dough stage
Bh	Breeding history
BLUE	Best linear unbiased estimator
FDR	False discovery rate
g	Fraction of green leaf area
GCD	Green canopy duration
GEBV	Genomic estimated breeding value
gf	Grain filling
gI	Relative light intercepted by the green canopy
\widehat{gI}_{int}	Relative light interception integral
\widehat{gI}_{dur}	Duration of relative light interception
\widehat{gI}_{mean}	Mean relative light interception
GLA ₅₀	Thermal time at which the green leaf area drops to 50%
gLAI	Green leaf area index, canopy size capable for photosynthesis
\widehat{gLAI}_{int}	Green LAI integral
\widehat{gLAI}_{dur}	Green LAI duration
\widehat{gLAI}_{mean}	Mean GLAI
\widehat{gLAI}_{BBCH59}	Green LAI at BBCH59
GWAS	Genome wide association studies
H ²	Broad-sense heritability
HI	Harvest index
I/I ₀	Transmission (I= transmitted radiation, I ₀ = total incident radiation)
iPAR	Intercepted radiation
k	Extinction coefficient
LAD	Leaf area duration
LAI	Leaf area index
LAI _{max}	Maximal leaf area index
LD	Linkage disequilibrium
Mbp	Mega base pairs (1 000 000 base pairs)

N	Nitrogen
N _{min}	Soil mineral nitrogen
PAR	Incident light (PAR= photosynthetically active radiation)
QTL	Quantitative trait loci
Rht	Reduced height (loci)
RUE	Radiation use efficiency
SEM	Structural equation modelling
SNP	Single nucleotide polymorphism
TGW	Thousand grain weight
TT	Thermal time

CHAPTER 1

General introduction

Allein ein ganzes Menschenalter würde nicht hinreichen, jedes Meisterstück der göttlichen Kunst in dem Reich der Natur nur zu erzählen, viel weniger, nach Würde zu betrachten.

Carl von Linné (1707 - 1778)

WHEAT PRODUCTION AND BREEDING - A SHORT HISTORY

For more than 10 000 years wheat is one of the main sources of calories for large parts of the world's population (Feuillet *et al.*, 2008). The staple crop is produced globally as it is adopted to various environments (Feuillet *et al.*, 2008; Rasheed and Xia, 2019) and hence deeply connected to various cultures in the temperate latitudes.

Early farmers in the Near Eastern Fertile Crescent started the domestication process of wheat when they cultivated wild diploid wheat species which were gradually replaced by closely related tetra- and hexaploid varieties. Hexaploid wheat (*Triticum aestivum* L., genome= AABBDD, $2n= 42$) remained as the one species with major economic importance not least because of its polyploid character which creates certain adaptive advantages. About 5000 years ago, the modern wheat species emerged from the allopolyploidization of the AB genome from a tetraploid ancestor (*Triticum turgidum* L., genome= AABB, $2n= 28$) and the D genome from a diploid grass *Aegilops tauschii* (Marcussen *et al.*, 2014). Such a duplication or triplication of homologous genes results in a genetic buffering effect which facilitates a great ability to adapt to different climatic conditions. This results among others in a broad range of photoperiod and vernalization requirements leading to the differentiation between two cultivation types: winter and spring wheat (Dubcovsky and Dvorak, 2007).

Throughout its cultivation, many evolutionary steps were induced to improve the agronomic characteristics and adjust it to dietary preferences. Domestication started by continuously selecting seeds of non-shattering spikes for the next sowing. Traits like free-threshing, an increased seed size, a reduced number of tillers, more erect growth and reduced seed dormancy are characteristic of the domesticated wheat that we produce today (Dubcovsky and Dvorak, 2007). Most of the improvements to ancient wheat took place during early phases of domestication followed by a long period of cultivating wheat in extensive farming systems. Farmers continuously selected the best seed for the next sowing but systematic breeding did not emerge until the 17th century. From then on, regional specific varieties emerged from existing landraces (Langridge, 2018; Balfourier *et al.*, 2019). Developments during the second half of the twentieth century, the "Green revolution", triggered remarkable gains in yield, pest and disease resistances and lodging and shifted breeding improvements to a new level. In the case of wheat, the introgression of the semi-dwarf growth habit into wheat varieties around the world, mediated by the dwarfing genes (i.e. Reduced height loci, Rht-B1 and Rht-D1), enabled the development of new high-yielding varieties. They were characterized by reduced height, resistance to lodging through a more stable stem and several resistances to diseases such as stem rust (Borlaug, 2007; Knopf *et al.*, 2008).

The adoption of these improved varieties was accompanied by a substantial increase in nitrogen fertilizer application and an overall intensification of agricultural production in the 1960's (Evenson and Gollin, 2003). Between 1960 and 2000 these developments facilitated an unprecedented increase of global yields with a solely breeding-induced increase of on average 1% per annum. As a consequence, poverty and under-nutrition were reduced in large parts of the world and also the food price decreased up to the early 21st century (Pingali, 2012). The worldwide wheat production was almost trebled (also by e.g. increasing the area for cultivating wheat) from about 200 million tons in 1960 to close to 600 million tons in 2000 (FAO, 2019).

In Germany, wheat (mainly winter wheat) nowadays grows on close to one third of the arable land (over 3 million ha) and represents the main staple food in Germany. It is the number one export product of all agricultural commodities and over 10 million tons of wheat were exported in 2016, nearly half of what was totally produced (42% from over 24 tons totally harvested in 2016). As the country is among the top 10 wheat exporters, the German wheat market is of great importance for the world wheat supply. Furthermore, it is a valuable source of income for farmers because high quality wheat is most profitable among cereals (BMEL, 2019).

The intensification of the agricultural production starting with the Green Revolution has guaranteed a high quality and high quantity wheat supply and also farm incomes but it also brought problematic aspects (Tilman, 1998). Detrimental effects on ground waters and the atmosphere by the release of greenhouse gases, the loss of soil fertility and a decreasing crop genetic diversity are just some of the stated drawbacks of the intensification of agricultural production (Tilman, 1998).

Additionally, climate change already altered growing conditions and will have further negative consequences in the future if unabated. With the proposed temperature increase, the evapotranspiration will rise and thereby heat and water stress will increase (Lüttringhaus *et al.*, 2019). The frequency and intensity of extreme weather events will increase and it has been estimated that droughts and heat waves caused an average national yield reduction of 9-10 % (Lesk *et al.*, 2016). At the same time, the projected increase of the world's population accompanied by changes in the dietary patterns and demographic changes, today's production is not enough to meet the demand (Serraj *et al.*, 2018). For future developments in wheat, a second green revolution is claimed by many researchers that wish to increase people's access to food, nutrition, and the sustainability of agroecological systems (Wollenweber *et al.*, 2005; Pingali, 2012).

In summary, the major challenges of the modern agriculture are: reducing the environmental impact, adopting to climate change and extreme weather conditions, coping with limited resources (e.g. land, fertilizer, water) and political restrictions for plant protection and finally increase the yield to feed the constantly growing world population. Given these challenges, today's plant breeders should focus on the increase of the *cultivate-ability* under the given conditions while simultaneously increasing yield (Borlaug, 2007).

To reach these complex aims, a deep understanding of the physiology underlying yield formation is necessary and the approach "physiological breeding" has been developed (Reynolds and Langridge, 2016). Furthermore, a combination of advancements in the disciplines of physiology, plant genomics and modelling should support the progress (Wollenweber *et al.*, 2005).

PHYSIOLOGICAL BREEDING - A POWERFUL APPROACH TO IMPROVE WHEAT

There is a pronounced requirement of resilient, tolerant and high-yielding varieties. To develop suitable lines, a deep understanding of the yield physiology is necessary to introduce the right adaptive traits into the broadly-adapted, high-yielding agronomic background (Reynolds *et al.*, 2011; Reynolds, 2012). The core of physiological breeding is to (1) define characteristics, namely the relevant physiological traits, (2) screen genetic resources for the specific traits or introduce the trait of interest into adapted material and (3) perform complementary crosses. This concept is rooted in the understanding of yield as the product of total biomass on the one side and the harvest index (HI), biomass partitioning, on the other side. Consequently, complementary crosses are performed between lines with high performance on the biomass side and lines with high performance on the HI side (Reynolds *et al.*, 2017).

In the next lower hierarchical level, biomass can be characterised as the source component and HI comprises parameters relevant for yield formation, namely the sink strength and size. Sink and source related traits can be assigned to different phases during the development. During the reproductive phase, from floral initiation till anthesis, the number of spikes, number of spikelets per spike and the number of grains per spikelet are determined. During that phase, the source is mainly characterised by traits affecting light interception. After anthesis follows the grain filling and the sink component "individual grain weight" measured by the thousand grain weight (TGW) is determined. Relevant source traits characterise the radiation use efficiency (RUE), namely canopy photosynthetic capacity, but also the persistence of the canopy (stay-green) (Reynolds *et al.*, 2012). The physiological perspective on yield formation enables a target-oriented breeding of lines suitable to specific growing conditions and a strategic combination of certain traits leads to an accumulation of complementary alleles (Reynolds *et al.*, 2017).

Every sink (grain number and grain weight) and source (light interception and RUE) related characteristic in the physiological network has the potential to increase yield (Reynolds *et al.*, 2017; Furbank *et al.*, 2019). It is a proven method to investigate the historical development of breeding lines and focus on the crucial characteristics which facilitated the yield progress of modern cultivars. In many cases, the number of grains has been determined as the most relevant trait affecting yield progress (Fischer, 2011). Therefore, it has been proposed, that breeding after the Green Revolution led to a selection gain mainly on the sink side. Since over 30 years it is a widely shared notion among breeders and crop physiologists that HI was more in focus than biomass itself (Reynolds *et al.*, 2011). Nevertheless, progress on the source side has also been shown by some studies and in parallel with the advancement of phenotyping techniques, the frequency increases (Furbank *et al.*, 2019). Additionally, a limitation of the HI has been proposed, as it might reach a theoretical restriction of the sink organs in relation to the structure of the plant supporting the sink (Austin *et al.*, 1980). In the last decades, parameters describing the accumulation of assimilates and formation of biomass have gained more attention. The feasibility of non-destructive measurements of traits like leaf area index, light interception and vegetation indices based on photogrammetry or spectral data supported the development (Cabrera-Bosquet *et al.*, 2016; Furbank *et al.*, 2019). However, the concrete interdependencies especially of the traits subordinated of RUE and light interception in wheat have not been investigated in great detail; yet this is essential for physiological breeding.

In addition to the parameter itself, the interdependencies are also of great relevance. Empirical correlation, (multiple) linear regression analyses or path analyses are possible methods to assess causal relationships between networks of intercorrelated variables (Lamb *et al.*, 2011; Molero *et al.*, 2019). Furthermore, a co-evolution can be assumed, if traits relevant for yield formation, sources and sinks, are physiologically linked and were prone to selection over numerous selection cycles. Investigations on the previous progress in potentially linked phenotypes provide additional insight in the interdependencies.

If the traits and the corresponding value for yield formation are defined, the set-up of an ideotype could help to guide physiological breeding. Although the predominant strategy in breeding for a long time was to cross the “best with the best”, ideotype-breeding has already been proposed 50 years ago. With a more divers profile of requirements for modern varieties and an increasing awareness of the physiological yield formation, the ideotype approach has gained prominence (Furbank *et al.*, 2019). One story of success is the “super” rice development based on an ideotype with a yield increase of up to 15% (Peng *et al.*, 2008).

APPLICATION OF GENOTYPIC INFORMATION - THE STEP FORWARD

Already prior to the advancements in phenotyping techniques, the development in genotyping was driven forward by the community of researchers in molecular breeding. With the progress in molecular technologies facilitating high-throughput genotyping, its application became also routine in wheat breeding (Ganal *et al.*, 2019). Especially for qualitative traits determined by few or single genes, marker assisted selection is widely applied. The application of diagnostic markers saves resources of extensive phenotype screens, facilitates marker assisted backcrossing, gene introgression, gene pyramiding and enhance selection accuracy (Rasheed and Xia, 2019). Functional markers have the advantage, that the phenotype can be accurately predicted as the sequence polymorphism, which is tracked by the marker, lies within the functional gene. Nevertheless, the analysis of sets of several not-necessarily functional markers allows genome wide association studies (GWAS), quantitative trait loci (QTL) mapping and genomic selection which have a great potential in assessing quantitative inherited traits like yield potential, stress adaptability and other physiological and more complex traits (Ganal *et al.*, 2019). The accuracy of investigations in complex quantitative traits relies on marker density, marker type, size of training populations and the heritability. A prominent impairment for the prediction of complex quantitative traits is the effect of the specific environment on trait expression, the genotype by environment interaction. However, combining the knowledge of physiological trait networks offers great potential to increase prediction accuracy for quantitative traits. Crop growth models represent such networks as they can predict the crops' performance under certain environmental conditions. The potential of such a combination of crop growth models with genomic prediction has been evaluated recently (Cooper *et al.*, 2016; van Eeuwijk *et al.*, 2019). Also, the utilization of certain specific physiological traits as secondary parameters in the genomic prediction model has been successful in increasing the prediction accuracy (Rutkoski *et al.*, 2016; Juliana *et al.*, 2019). These approaches apply phenotypic data, often from high-throughput phenotyping, to improve genomic prediction of yield under specific environmental conditions and it is of crucial importance to be aware of the relevance of that physiological trait for yield. From another perspective, concrete QTL for physiological traits, the genotypic data, can be applied to improve functional plant models (Yin *et al.*, 2004). This provides insights in the performance of the crop under environmental stress estimated from the performance of a specific genotype (Hammer *et al.*, 2006; Chenu *et al.*, 2009) and presents a valuable tool for ideotype breeding (Furbank *et al.*, 2019). The identification of significant genotype – phenotype associations for the relevant physiological traits is the first step to make this procedure possible. Another prerequisite is a high heritability of the trait. If a specific genomic region can be identified, a population segregating in that locus should be tested under contrasting environmental conditions, to evaluate the genotype by environment interaction (Yin *et al.*, 2004).

Investigations in the genetic basis of physiological traits also could provide insights in possible co-localizations or pleiotropic effects. The findings can be of great importance for breeding, especially if antagonists are genetically linked and detrimental characteristics of breeding lines are unintentionally selected e.g. the negative effect of *Rht-D1b* on flowering traits relevant for hybrid seed production (Boeven *et al.*, 2016). To completely understand the network of physiological traits relevant for yield formation and to ensure their applicability, it is also of crucial importance to investigate the genetic basis of these parameters.

OBJECTIVES:

As explained above, winter wheat breeding highly important for global food security and climate change adaptation. Physiological breeding provides a framework to systematically improve and speed up the breeding progress. In my dissertation I analyzed a set of modern and historical wheat cultivars in one field trail to identify the causal agents for the progress in yield which has already been realised in the last 50 years (cultivars released between 1966 and 2013). The following three chapters provide valuable information for the first step of physiological breeding: the identification of relevant characteristics underlying the final yield development and evaluate their usability for future improvement of winter wheat cultivars. The specific objectives of the chapters are:

- The investigation of the complete set of physiological canopy characteristics related to light interception and utilization, their relevance for yield formation and progress during breeding (chapter 2).
- To elucidate the concrete interdependencies of sink and source components and investigate, whether an interdependency was accompanied by a parallel development in the breeding progress (chapter 3).
- The investigation of the genetic structures underlying physiological parameters relevant for yield formation (chapter 4).

CHAPTER 2

Green canopy duration and SPAD at heading are the most important indicator for light interception and utilization and thereby relevant for breeding progress of German winter wheat

Carolin Lichthardt¹, Tsu-Wei Chen¹, Andreas Stahl², Hartmut Stützel¹

¹Institute of Horticultural Production Systems, Leibniz University Hannover, Hannover, Germany

²Department of Plant Breeding, IFZ Research Centre for Biosystems, Land Use and Nutrition, Justus Liebig University, Giessen, Germany

ABSTRACT

Radiation interception and use efficiency determine the biomass production and are important traits for further improvement of winter wheat yield. Underlying characteristics of radiation interception and radiation use efficiency (RUE) are the phenology and the canopy parameters leaf area index (LAI), canopy transmissivity, durability of the canopy and photosynthetic efficiency. To guide the usability of these physiological parameters for breeding, the dependencies of the traits and the relevance for yield formation were assessed.

Using 220 winter wheat cultivars grown in field experiments conducted in three consecutive years (2015-2017), we present a mathematical framework which estimates the physiological functions of the canopy by a simple field phenotyping protocol. Canopy traits, e.g. LAI, canopy light interception, relative leaf chlorophyll content and canopy greenness were weekly measured non-destructively from vegetative to grain filling stages. Based on these traits, relative light interception, RUE, green canopy duration, green leaf area integral, canopy chlorophyll content and light extinction coefficient (k) were derived. Broad-sense heritability of all measured and derived physiological traits ranged from 7-66%. Relative light interception and RUE were two independent traits, which showed high explanatory power for grain yield (30% and 64%, respectively). Using a structural equation modelling approach, the network of physiological traits could explain the variation in relative light interception by 63% and the variation in RUE with 46%. The parameters with the highest relative path coefficients were the average LAI for light interception and relative leaf chlorophyll content for RUE. Since all parameters in our field phenotyping protocol can be estimated by remote sensing using for instance reflectance data from aerial imaging or multispectral sensors, our framework provides a new avenue for large scale field phenotyping in the era of digital breeding.

INTRODUCTION

Physiological understanding of yield formation may provide insights into strategies for crop improvement. Grain yield of winter wheat can be described as the product of the total biomass production and its allocation to the grains (harvest index, HI). Furthermore, the former can be described as the sum of the incident light (PAR), the relative light intercepted by the green (photosynthetically active) canopy (gI) and the radiation use efficiency (RUE) for each day of the duration of crop growth (Reynolds *et al.*, 2012; Cabrera-Bosquet *et al.*, 2016). Any of these physiological parameters (gI, RUE and HI) can contribute to the increase of grain yield, which is an urgent need in the case of winter wheat (Reynolds *et al.*, 2017). It is universal that the production of staple food needs to be increased and stabilized, and crop scientists must find the most effective key levers to facilitate these aims. New strategies to meet the prospected demand of staple food for the increasing world population and to be prepared for challenges of climate change need to be developed (Hickey *et al.*, 2019).

For a target improvement of winter wheat yield, the weighting of the physiological parameters in explaining yield and yield components is of crucial importance. Historically, winter wheat breeding has intensively improved the HI, whereas changes in total biomass were not observed so frequently (Reynolds *et al.*, 2012). Nowadays, further progress in HI is unlikely, because the systematic improvement has declined since the 1990s and the HI is assumed to be limited (Austin *et al.*, 1980; Foulkes *et al.*, 2009; Reynolds *et al.*, 2013). Therefore, it appears to be more promising to focus on increasing the total biomass production by light interception and utilization (Reynolds *et al.*, 2009; Reynolds *et al.*, 2017; Molero *et al.*, 2019; Asseng *et al.*, 2019; Furbank *et al.*, 2019; Richards *et al.*, 2019).

The amount of intercepted light and the RUE rely on numerous physiological traits characterising the canopy and representing the source of assimilate production. Light interception over time is determined by the persistence of the canopy and its interception efficiency (gI), which is related to the leaf area index (LAI) and the extinction coefficient of the canopy (k). RUE describes the total dry matter per unit intercepted light during the complete growing period (Reynolds *et al.*, 2013) which in turn depends on the photosynthetic capacity and the gradient of light transmission through the canopy, and can also be related to k (Gitelson and Gamon, 2015; Asseng *et al.*, 2019).

The high relevance of RUE after anthesis in breeding progress has been shown in retrospective for cultivar collections of Mediterranean (Acreche *et al.*, 2008), Argentinian (Calderini *et al.*, 1997), UK (Shearman *et al.*, 2005) and Australian wheat collections (Sadras and Lawson, 2011).

However, the concrete relevance of the physiological traits underlying light interception and utilization especially for western European winter wheats remains unclear (Asseng *et al.*, 2019).

The present study aims to investigate the canopy traits underlying radiation interception (the persistence, gI , LAI and k) and utilisation (photosynthetic capacity and k) for yield formation. Previous investigations have shown, that yield formation is mainly influenced by the physiological constitution of the canopy at anthesis and during grain-filling (Acreche *et al.*, 2008; Fischer, 2011; Tang *et al.*, 2017). Therefore, the present study mainly focuses on the generative phase, the grain filling (gf) and the following equation describes the grain yield formation during that phase:

$$\text{Yield} = \text{RUE}_{\text{gf}} \times \sum_i^{\text{gf}} (gI_i \times \text{PAR}_i) \quad (1)$$

where i and gf denote each day during grain filling, from heading date to 50% relative light interception. The complete biomass produced during grain filling is allocated to the grains and the RUE is considered as constant.

To completely understand the causal dependencies between the physiological traits and total grain yield, we applied a path analysis – structural equation modelling (SEM). Furthermore, the study presents detailed investigations of the formation of the yield components and the corresponding dependency on underlying physiological traits. The number of grains per spike depends on the size and productivity of the leaves around anthesis, the target date for the final grain number (Guo *et al.*, 2015), as source limitation around anthesis drives floret abortion (Wang *et al.*, 2003; Guo *et al.*, 2018). Therefore, a causal relationship between the quality and quantity of the leaf area around anthesis and the grain number per spike can be expected. Final grain weight depends on the capacity of the source during the grain filling processes, the canopy photosynthesis, the size of the canopy and the senescence of the canopy. An extended canopy duration has been described to boost grain filling (Serrago *et al.*, 2013). Causal agents for grain weight should therefore be the photosynthetic performance, green leaf area index and the green canopy duration. Moreover, the progress of the relevant traits in the breeding history in Europe (mainly Germany) will be assessed. Measurements characterising the canopy were performed non-destructively throughout three years of field experiments especially during the grain filling phase, but also prior to heading to quantify the canopy development. The environmental differences during the conducted experiments further allowed to distinguish between strategies to facilitate a high yield of the modern cultivars. This gives insight into the response capacity of the cultivars to environmental instabilities.

MATERIAL AND METHODS

Plant material and field trial

In the present study we examined 220 winter wheat cultivars (Table S2.1). The collection consisted of 191 cultivars representing cultivars relevant for the European (especially German) breeding history (*Bh*- sub-set), and 29 international materials and exotic breeding lines obtained from the German gene bank (<https://gbis.ipk-gatersleben.de>) (*Div*- sub-set). Cultivars in the breeding history subset were released between 1966 and 2013. The subset comprised five hybrids and 186 lines of which 17 were recommended for organic production. For detail see Lichthardt *et al.*, 2020 and Voss-Fels *et al.*, 2019.

All cultivars were investigated in field trials over three consecutive years (2014-2015, 2015-2016 and 2016-2017) at the research station in Ruthe near Hannover (52°14'44.1"N 9°49'03.4"E, clayey silt soil type). The cultivars were sown in plots with 330 viable seeds m⁻² and in 15 rows with 2 m plot width (13.33 cm row spacing) and plot sizes of 12 m², 10 m² and 9.4 m² in the three consecutive years, respectively. The plots were arranged in a randomized block design with two replications each year. Cultivars were randomized within four sub-groups according to the flowering time and plant height (early and short; early and tall; late and short; late and tall). Herbicides, fungicides and growth regulators were applied according to standard application in intensive wheat production in Germany. The plots were treated with optimal nutrient supply by fertilizing in three applications a total amount of 220 kg N/ha subtracted by the mineral nitrogen (N_{min}) measured at the beginning of the growing year in the root zone (Wehrmann and Scharpf, 1979) (exact amounts in Table S2.2). The treatments were applied to complete trial, when most of the cultivars had reached the relevant stage for application. The experiment was conducted on different fields each year but the preceding crop was always maize.

Temperature, rainfall and radiation were recorded with hourly resolution by a weather station close to the study site. Temperature sum was defined as the accumulated daily mean temperatures, starting from the day of sowing with 0°C as base temperature (Fig. S2.1 and Table S2.3).

Measuring and deriving canopy parameters

Phenology

As wheat self-pollinates in the closed (cleistogamous) flower, the exact date of anthesis is difficult to determine in a field trial of this dimension. Therefore, we recorded the easily assessable heading date (BBCH59 (Meier, 2018) in °Cd) for all cultivars in one replication per year as a proxy for the start of the grain filling phase.

Senescence

Due to the fungicide treatment, leaf and ear diseases, including powdery mildew, rust, *Septoria* species and *Fusarium*, were successfully suppressed. Therefore, all cultivars were close to 100% green at heading date. After heading, the declining proportion of green leaf area [%] was visually scored every one to two weeks.

To quantify the dynamics in the senescence patterns, a logistic power function with two parameters was used to describe the relationships between the fraction of green leaf area (g , [%]) and thermal time (TT , [°Cd]):

$$\hat{g}_{TT} = \frac{1}{1 + \left(\frac{TT}{GLA_{50}}\right)^s} \quad (2)$$

GLA_{50} is the thermal time [°Cd], at which the green leaf area drops to 50% and s (unitless) describes the steepness of the curve. For details see Lichthardt *et al.*, 2020. \hat{g}_{TT} is the estimated fraction of green leaf area at any time point (TT), the “^” will in the following always indicate the estimated function value.

The persistence of the green leaf material was measured by the parameter GCD (green canopy duration) which was defined as the thermal timespan [°Cd] from heading until 50% loss of greenness of the whole canopy:

$$GCD = TT_{\hat{g}_{50\%}} - TT_{BBCH59} \quad (3)$$

Leaf area index

The leaf area index (LAI) was assessed by non-destructive sensor measurements in every plot starting around BBCH59 and was repeated approximately every two weeks. The LAI-2200 plant canopy analyser (LI-COR Biosciences, Lincoln, NE, USA) was applied to assess the LAI of the complete canopy by placing one sensor above and one sensor below the canopy. Both sensors were attached to a stand and the above and below measurement were taken simultaneously. In addition to the complete canopy, the top layer (above the flag leaf) was measured separately in 2017 for all cultivars at two consecutive dates after canopy closure. For this purpose, one of the LAI sensors was placed below the flag leaf (the exact height was recorded) to measure the LAI of the flag leaves, parts of the stem and spikes. LAI measurements were conducted irrespective of daytime and weather, namely sky conditions. According to the manufacturer's recommendations, a scattering correction was performed for the measurements done at clear or changing sky conditions in order to overcome the underestimation of the LAI due to measurement errors caused by direct solar radiation (Kobayashi *et al.*, 2013).

To account for the greenness of the measured leaf area and only measure the photosynthetically functional leaf tissue per unit ground area, the total LAI values (LAI_{TT} , including green and yellow/brown leaves) were multiplied with the estimated scores of % green (value of eq. 2 for each measurement, \hat{g}_{TT}):

$$gLAI_{TT} = LAI_{TT} \times \hat{g}_{TT} \quad (4)$$

Thereby the parameter ($gLAI_{TT}$) represents the canopy size capable for photosynthesis. To quantify the development of the green leaf area index, we fitted a two-parametric logistic function of the thermal time (TT , [°Cd]):

$$\widehat{gLAI}_{TT} = \frac{gLAI_{max}}{1 + e^{(b \times TT) - c}} \quad (5)$$

The regression formula was linearized and the parameters were estimated with the $lm()$ function from the package *stats* in the *R environment* (R Core Team, 2019) with b being the slope and c the intercept of the linear formula

$$\ln\left(\frac{gLAI_{max}}{gLAI_{TT}} - 1\right) = c + b \times TT \quad (6)$$

The fitting was performed with a minimum of 4 data points for gLAI, by that restriction approx. 9% of the data were excluded.

Based on equations (5) and (6), a LAI integral was calculated from heading date, TT_{BBCH59} , until the temperature sum of 50% gLAI, $TT_{\widehat{\text{gLAI}}_{50\%}}$, to evaluate the cultivar differences in size and persistence of the green leaf area:

$$\widehat{\text{gLAI}}_{\text{int}} = \int_{TT_{\text{BBCH59}}}^{TT_{\widehat{\text{gLAI}}_{50\%}}} \widehat{\text{gLAI}}_{TT} \quad (7)$$

To measure the persistence of the green leaf area, the gLAI duration ($\widehat{\text{gLAI}}_{\text{dur}}$) was defined as the temperature sum from heading till 50% loss of green leaf area index

$$\widehat{\text{gLAI}}_{\text{dur}} = TT_{\widehat{\text{gLAI}}_{50\%}} - TT_{\text{BBCH59}} \quad (8)$$

In addition, the mean gLAI for the duration of available green leaf area was calculated as

$$\widehat{\text{gLAI}}_{\text{mean}} = \frac{\widehat{\text{gLAI}}_{\text{int}}}{\widehat{\text{gLAI}}_{\text{dur}}} \quad (9)$$

and the gLAI at heading date was estimated accordingly (b (slope) and c (intercept) estimated with equation (5) and (6)):

$$\widehat{\text{gLAI}}_{\text{BBCH59}} = \frac{\text{gLAI}_{\text{max}}}{1 + e^{(b \times TT_{\text{BBCH59}}) - c}} \quad (10)$$

Relative chlorophyll content

As a proxy for the photosynthetic activity, the relative chlorophyll content of the flag-leaf was measured in 2016 and 2017 by a hand-held SPAD-meter (SPAD 502, Minolta, Japan). The values can be interpreted as representatives of the canopy photosynthetic capacity. For each genotype and replication, five flag-leaves were measured at the widest section at (for most of the cultivars) three dates after heading. The SPAD value close to heading date was extracted from all measure values as a measure for the photosynthetic constitution of the canopy at heading ($\text{SPAD}_{\text{BBCH59}}$ [-]).

Radiation interception

Relative canopy light interception was recorded approximately every two weeks in each plot. The plots were measured each time with both sensors (LAI and light interception) on the same day or in few cases on the following day. The measurements were performed with quantum sensors measuring photosynthetically active radiation (PAR) in the wavelength range from 400 to 700 nm above (I_0 , [$\mu\text{mol m}^{-2} \text{s}^{-1}$]) and below the canopy (I , [$\mu\text{mol m}^{-2} \text{s}^{-1}$]). A line sensor (LI-191R, LI-COR Biosciences, Lincoln, NE, USA) was placed in parallel to the rows at the bottom of the canopy and a point sensor (LI-190R, LI-COR Biosciences, Lincoln, NE, USA) was placed as close as possible to the measured plot above the canopy. Above and below canopy measurements were recorded simultaneously and were repeated three times in each plot. Mean values of the three measurements were calculated and corrected by a matching measurement of point and line sensor. For measurements with a coefficient of variation larger than 0.4, the corresponding outlier value was deleted. For each plot up to eight repeated measurements could be performed. The relative canopy light interception was also measured for the top layer in 2017. For this, the line sensor was placed below the flag leaf (the exact height was recorded) to measure the light intercepted by the flag leaves, stem parts and spikes. Light interception was always only measured between 11 am and 2 pm in order to reduce the possible effect of the daytime (Impens and Lemeur, 1969).

The proportion of light intercepted by the green leaves of the canopy was calculated by multiplying the intercepted radiation (1 minus the transmission, calculated as $\frac{I}{I_0}$) with the estimated greenness of the canopy estimated based on the temperature sum of the measurements date (\hat{g} , eq. 2)

$$gI_{TT} = \left(1 - \frac{I_{TT}}{I_{0TT}}\right) \times \hat{g}_{TT} \quad (11)$$

In the following, we fitted a two-parametric logistic sigmoid function for the light intercepted by green leaf material and the thermal time (TT, [$^{\circ}\text{Cd}$]):

$$\hat{g}I_{TT} = \frac{gI_{\max}}{1 + e^{(b \times TT) - c}} \quad (12)$$

The regression formula was linearized and the parameters were estimated based on the linear equation (compare eq. 6). The fitting was performed with a minimum of 4 data points, by that restriction we excluded about 5% of the data. The relative light interception during the grain filling phase was estimated based on this equation. An integral was calculated from heading date until the temperature sum of 50% gI , $\hat{g}I_{50\%}$.

$$\widehat{gI}_{\text{int}} = \int_{\text{TT}_{\text{BBCH59}}}^{\text{TT}_{\widehat{gI}_{50\%}}} \widehat{gI}_{\text{TT}} \quad (13)$$

Accordingly, the duration of light interception was calculated as follows

$$\widehat{gI}_{\text{dur}} = \text{TT}_{\widehat{gI}_{50\%}} - \text{TT}_{\text{BBCH59}} \quad (14)$$

and the average relative light interception during that period was

$$\widehat{gI}_{\text{mean}} = \frac{\widehat{gI}_{\text{int}}}{\widehat{gI}_{\text{dur}}} \quad (15)$$

The intercepted radiation (iPAR_{gf} [MJ/m^2]) was calculated as the sum of the light intercepted each day (relative light interception multiplied with the incident PAR) of the individual timespan from heading date of the cultivar until \widehat{GLI} was reduced to 50 %:

$$\text{iPAR}_{\text{gf}} = \sum_{\text{day of BBCH59}}^{\text{day of } \widehat{gI}_{50\%}} \widehat{gI}_{\text{day}} \times \text{PAR}_{\text{day}} \quad (16)$$

The fraction of PAR was determined by multiplying the total radiation with the factor 0.46 (Nagaraja Rao, 1984).

Based on these parameters it was possible to calculate a radiation use efficiency of the grain filling phase, RUE_{gf} [g/MJ], by dividing the produced grain yield by the intercepted radiation.

$$\text{RUE}_{\text{gf}} = \frac{\text{Yield}}{\text{iPAR}_{\text{gf}}} \quad (17)$$

Architectural characteristics

The height of the canopy was recorded for all cultivars in two replications per year at the start of the grain filling phase (around anthesis). In 2017 additionally the height of the top layer, from the position of the flag leaf to the top, was recorded.

To get a measure for the vertical profile of light distribution in the canopy, the light extinction coefficient k [-] was calculated using Monsi and Saeki's (1953) adaptation of the Beer-Lambert law for plant canopies (Monsi and Saeki, 2005):

$$k = \frac{-\ln\left(\frac{I}{I_0}\right)}{\text{LAI}} \quad (18)$$

, where I_0 is the incident PAR [$\mu\text{mol m}^{-2} \text{s}^{-1}$] from above the canopy and I [$\mu\text{mol m}^{-2} \text{s}^{-1}$] is the radiation at the bottom of the canopy as described above (eq. 11). Variation in k can be attributed to the canopy architecture, namely the leaf angle distribution. For steeper inclination of the leaves in the canopy, k is small and more light penetrates through the canopy, whereas canopies with mainly horizontal leaves show a high k (Monsi and Saeki, 2005; Zhang *et al.*, 2014).

The coefficient was calculated for every parallel measurement of LAI and relative light interception for the complete canopy reaching up to seven dates within the years and for each cultivar. The extinction coefficient was also calculated for the corresponding values of the top layer measured in 2017. Because of the linear relationship between $\ln\left(\frac{I}{I_0}\right)$ and LAI, it was possible to detect outliers based on a given model with the function *outlierTest* from the package *car* in *R*. 6% of the data points were lost in the data set for the complete canopy and 14% in the data set of the top layer due to the outlier test.

All physiological parameters are summarised in Table 2.1.

Table 2.1: List of measured and estimated physiological parameters

Parameter	Symbol	Unit	Explanation	Equation
Phenology				
Heading date	BBCH59	°Cd	Start of grain filling period	
Greenness				
Green canopy duration	GCD	°Cd	Persistence of green leaf material, from heading to 50% green	(3)
Leaf area index				
Green LAI integral	$\widehat{\text{gLAI}}_{\text{int}}$	°Cd	Size and persistence of the green leaf area	(5) and (7)
Green LAI duration	$\widehat{\text{gLAI}}_{\text{dur}}$	°Cd	Persistence of the green leaf area	(5) and (8)
Mean GLAI	$\widehat{\text{gLAI}}_{\text{mean}}$	-	$\widehat{\text{gLAI}}_{\text{int}}$ divided by the duration	(5), (6) and (7)
Green LAI at BBCH59	$\widehat{\text{gLAI}}_{\text{BBCH59}}$	-	Available green leaf area estimated for heading date	(7), (8) and (9)
Photosynthetic performance				
SPAD close to BBCH59	SPAD _{BBCH59}	-	Estimated photosynthetic activity at heading date	
Radiation interception				
Relative light interception integral	$\widehat{\text{gl}}_{\text{int}}$	°Cd	Relative light interception of the green leaf mass integrated from heading to 50% relative light interception	(12) and (13)
Duration of relative light interception	$\widehat{\text{gl}}_{\text{dur}}$	°Cd	Duration of the relative light interception of the green leaf mass	(12) and (14)
Mean relative light interception	$\widehat{\text{gl}}_{\text{mean}}$	-	$\widehat{\text{gl}}_{\text{int}}$ divided by the duration	(13), (14) and (15)
Intercepted radiation	iPAR _{gf}	MJ/m ²	Intercepted radiation (absolute) from heading to 50% relative light interception	(12) and (16)
Radiation use efficiency	RUE _{gf}	g/MJ	Radiation use efficiency of the grain filling period, from heading to 50% relative light interception	(16) and (17)
Architectural traits				
Extinction coefficient	k	-	Light extinction coefficient, leaf angle distribution	(18)
Extinction coefficient of top layer	k _{top}	-	Light extinction coefficient of the top layer (flag leaf and above), measured only in 2017	(18)
Canopy height	height	cm	Height of the complete canopy	
Height of top layer	height _{top}	cm	Height of the top layer (flag leaf and above), measured only in 2017	

Yield measurements

To determine the primary yield components, a sample of one row (50 cm in length) per plot was cut shortly before combine harvesting the plots. Numbers of spikes and TGW (g) of these samples were used to determine spikes per m² and grains per spike and m². Plot grain yield (t/ha) and TGW (g) were determined by harvesting the plots completely with a combine harvester.

Statistical analyses

The phenotypic data collected in the field experiment was evaluated with the following mixed model:

$$P_{ijkl} = \mu + c_i + y_j + cy_{ij} + YR_{jk} + YRG_{jkl} + e_{ijkl} \quad (19)$$

where P_{ijkl} was the phenotypic observation of the i^{th} cultivar (i = cultivar number 1 – 220, factorial) in the j^{th} year (j = 2015, 2016 and 2017, factorial) in the k^{th} complete replication and l^{th} incomplete sub-group (l = early and short; early and long late and short; late and short). The model was used to estimate adjusted means for each cultivar in each year with lower case letters indicating fixed factors (cultivar and year) and capital letters indicating random effects (replication, and group). The observation was dissected into the general mean, μ , the genetic effect of the i^{th} cultivar, c_i , the effect of the j^{th} year, y_j , the interaction between the cultivar and the year, cy_{ij} , the interaction of the year and the replication YR_{jk} , the interaction of the year, replication and sub-group, YRG_{jkl} and the residual e_{ijkl} . The model was fit to the data with the *lmer* function of the *lme4* package in the R environment (Bates *et al.*, 2015). Significant differences between cultivars, years and the interactions were examined with the *anova* function. Parameter correlations were calculated based on the best linear unbiased estimators (BLUE) which were calculated using the *lsmean* function based on the model (eq. 19) (Lenth, 2016).

Broad-sense heritability H^2 of the physiological parameters were calculated over n years and r replications according to the formula:

$$H^2 = \frac{\sigma_c^2}{\left(\sigma_c^2 + \frac{\sigma_{cY}^2}{n} + \frac{\sigma_e^2}{er}\right)} \quad (20)$$

where σ_c^2 , σ_{cY}^2 and σ_e^2 are the genetic variance component, the interaction variance component between genotype and year and the residual variance component, respectively.

Structural equation model

To completely understand the dependencies between canopy architectural traits, light interception, light utilization and yield formation, structural equation modelling (SEM) was employed. SEM is a path analysis method which allows to test direct and indirect theoretical causal relationships within networks of many variables (Lamb *et al.*, 2011). The evaluation of the SEM reveals the strength and significance of the causal relationships and elucidates the interdependencies of the physiological traits underlying grain yield formation. To apply SEM, a prior knowledge of the relationships between the model components is required. The diagram in Figure 2.1 represents the hypothetical model of causal relationships between source traits in focus of this study. This initial model aims to explain grain yield from the interception and utilization of radiation. In the underlying hierarchy, the light interception ($iPAR_{gf}$) depends on the duration of light interception (\widehat{gI}_{dur} [°Cd]), the average relative light interception (\widehat{gI}_{mean}) and the average PAR irradiation per °Cd [$M\ m^{-2}\ °Cd^{-1}$] which was derived by calculating

$$\text{average PAR} = \frac{\sum_{\text{day of BBCH59}}^{\text{day of } \widehat{gI}_{50\%}} PAR_{\text{day}}}{\widehat{gI}_{dur}} \tag{21}$$

(\widehat{gI}_{dur} is derived in eq. 14). The average relative light interception (\widehat{gI}_{mean}) in turn is determined by the leaf area index (\widehat{gLAI}_{mean}) and interception efficiency (light extinction coefficient: k). The radiation use efficiency of the grain filling phase (RUE_{gf}) depends on the photosynthetic constitution of the canopy ($SPAD_{BBCH59}$) and on the transmissibility of the canopy described by k (Fig. 2.1).

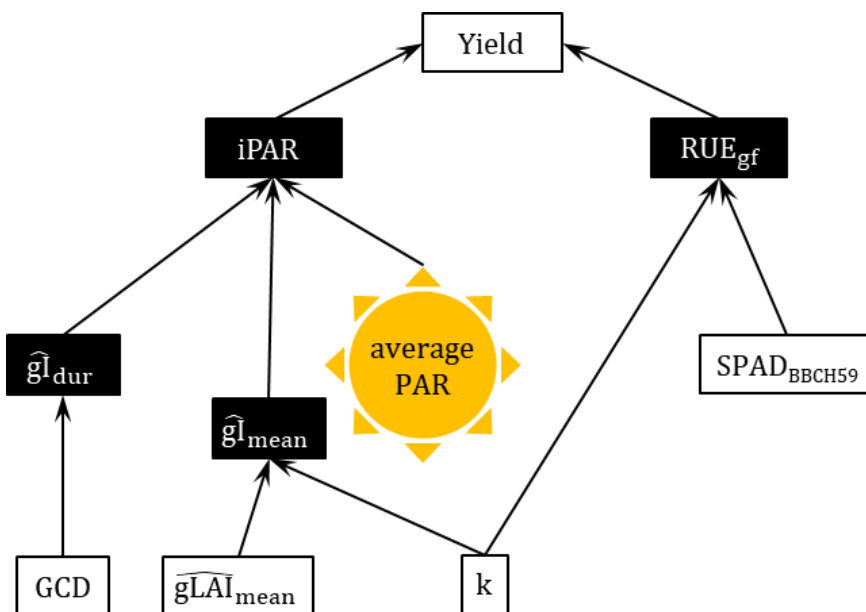


Figure 2.1: Theoretical path diagram indicating the causal relationships between source parameters and final grain yield. Black boxes indicate endogenous response variables, white boxes the predictor variables.

The path diagram was tested in a piecewise structural equation model with the *psem()* function from the R package piecewiseSEM based on the following equations:

$$\begin{aligned} \text{Grain yield} &= \text{iPAR} + \text{RUE}_{\text{gf}} \\ \text{iPAR} &= \widehat{\text{gI}}_{\text{dur}} + \widehat{\text{gI}}_{\text{mean}} + \text{average PAR} \\ \widehat{\text{gI}}_{\text{mean}} &= \widehat{\text{gLAI}}_{\text{mean}} + k \\ \text{RUE}_{\text{gf}} &= \text{SPAD}_{\text{BBCH59}} + k \\ \widehat{\text{gI}}_{\text{dur}} &= \text{GCD} \end{aligned}$$

The model fit was evaluated by the Akaike Information Criterion (AIC) and the individual the p-values ($p < 0.05$) and the R^2 gave hints on the strength and the significance of each individual causal relationship. Based on these criteria, the model was adjusted to reach the best fit to the data.

To test the interdependencies for the yield components, the following equations were added to the derived source model one by one:

$$\begin{aligned} \text{(a) Grains per spike} &= \text{SPAD}_{\text{BBCH59}} + \widehat{\text{gLAI}}_{\text{BBCH59}} \\ \text{(b) TGW} &= \text{SPAD}_{\text{BBCH59}} + \widehat{\text{gLAI}}_{\text{BBCH59}} + \text{GCD} \end{aligned}$$

The initial relationship between canopy characteristics and the yield components are presented in Figure 2.2. The final result-model was developed by adding the suggested additional significant associations and retaining significant predictor variables, which resulted in a better-fitting model.

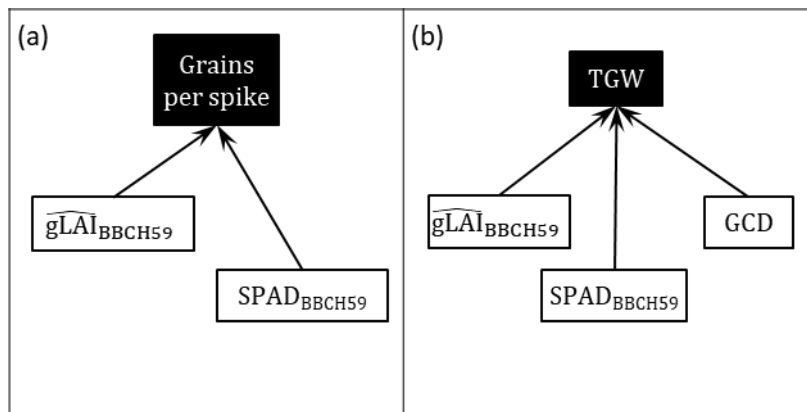


Figure 2.2: Theoretical path diagram for interdependencies between sink and sources. Black boxes indicate endogenous response variables, white boxes the predictor variables. The models were tested as supplements to the derived source model.

Breeding progress

To assess the breeding progress of winter wheat, the development of the parameters was investigated for the subset of 191 cultivars representing the breeding progress in Europe, mainly Germany (Table S2.1). A sliding window approach was used with the window being moved from the old toward the more recently released cultivars on the scale of the year of release by one cultivar each step. The cultivars were ordered by the year of release and window means were calculated for constant window sizes of ten cultivars. The slope of the linear regression of the window means for each parameter and the year of release was defined as the absolute breeding progress. The relative four-decade breeding progress was calculated as the ratio between the trait value of 2010 and 1970 ($\frac{f(2010)}{f(1970)}$). The breeding progress was calculated for each experimental year separately (mean values of two replications) and based on the BLUE values to investigate the progress independent of the year-effect.

RESULTS

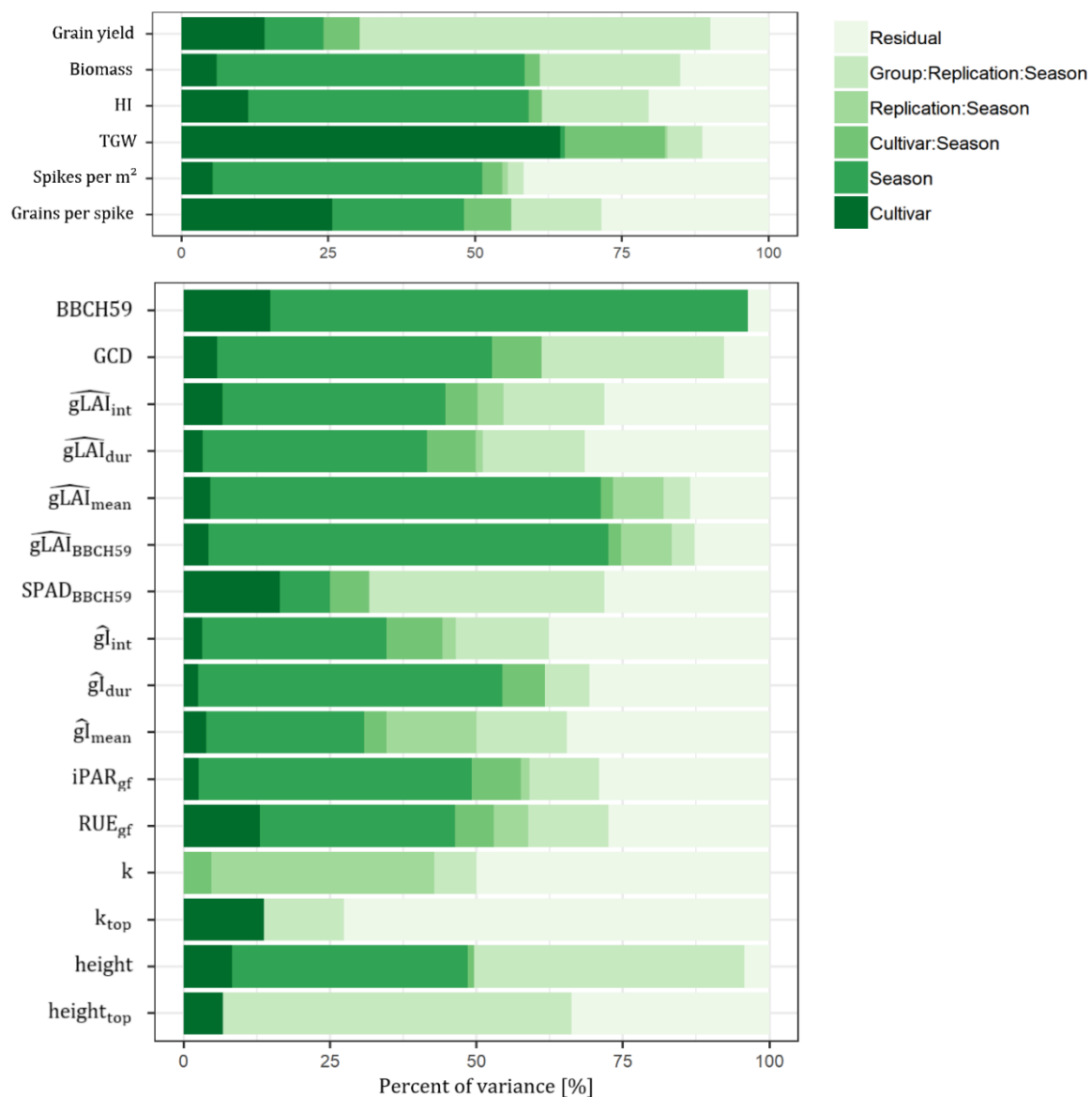


Figure 2.3: Proportion of variance in percent explained by the variance components of the model (equation 19).

For all investigated parameters we observed significant genetic differences. In addition, all trait values differed significantly between years except for $SPAD_{BBCH59}$, \widehat{gLAI}_{int} and \widehat{gI}_{int} , \widehat{gI}_{mean} and TGW. Moreover, we observed significant cultivar by year interactions for all traits except k (data not shown). Figure 2.3 shows the proportion of variance explained by the different components of the model (eq. 19) which was applied to investigate the multi-seasonal data. The residual variance showed great variation ranging from only a few percent for heading date up to almost 75% for the light extinction coefficient of the top layer. The broad-sense heritability also varied considerably with 0 and very low values for the light extinction coefficient of the top layer, \widehat{gLAI}_{dur} , \widehat{gI}_{int} , the relative and absolute light interception (\widehat{gI}_{mean} and $iPAR_{gf}$) and k , indicating a great variation of these traits not related to the genotype.

High heritabilities were observed for the canopy characteristics RUE_{gf} ($H^2= 0.66$), GCD ($H^2= 0.58$), $SPAD_{BBCH59}$ ($H^2= 0.61$) or \overline{gLAI}_{mean} ($H^2= 0.61$) (Table 2.2). These traits showed a more stable expression across the experiments which indicates their suitability for selection and breeding activities.

Table 2.2: Summary of parameters describing the canopy characteristics, BLUE values, genetic variance and heritability calculated based on the linear mixed model in formula (19), * = data only from 2017, † = repeatability

Trait	Range (BLUE values)			Broad-sense heritability
	min	max	mean \pm sd	
Grain yield [t/ha]	4.8	9.48	7.9 \pm 0.95	0.79
Biomass [g/m ²]	997.13	2071.54	1597.71 \pm 154.45	0.64
HI	0.39	0.59	0.50 \pm 0.03	0.74
Yield parameters				
TGW [g]	33.13	51.35	42.7 \pm 3.36	0.89
Spikes per m ²	437.28	919.54	606.2 \pm 67.32	0.40
Grains per spike	23.08	51.12	39.11 \pm 4.98	0.76
Phenology				
BBCH59 [$^{\circ}$ Cd]	1311.59	1601.03	1493.99 \pm 43.99	0.92
Greenness				
GCD [$^{\circ}$ Cd]	462.37	769.25	649.85 \pm 54.17	0.58
Leaf area index				
\overline{gLAI}_{int}	2 569.76	4 378.65	3 477.81 \pm 313.11	0.50
\overline{gLAI}_{dur} [$^{\circ}$ Cd]	466.22	659.44	587.91 \pm 29.10	0.29
\overline{gLAI}_{mean}	4.67	7.55	5.98 \pm 0.42	0.61
\overline{gLAI}_{BBCH59}	4.88	7.98	6.35 \pm 0.44	0.60
Photosynthetic performance				
$SPAD_{BBCH59}$	43.88	58.90	51.70 \pm 3	0.61
Radiation interception				
\widehat{gl}_{int}	442.45	616.83	548.17 \pm 33	0.25
\widehat{gl}_{dur}	497.53	695.93	617.19 \pm 30.96	0.25
\widehat{gl}_{mean}	0.78	0.92	0.89 \pm 0.0218	0.39
$iPAR_{gf}$ [MJ/m ²]	239.83	346.06	299.93 \pm 17.85	0.25
RUE_{gf} [g/MJ]	1.85	3.20	2.67 \pm 0.27	0.66
Architectural traits				
k	0.5	0.61	0.55 \pm 0.02	0.07
k_{top} *	0.28	1.14	0.54 \pm 0.1	0.28†
height [cm]	74.14	125.25	90.16 \pm 7.75	0.89
$height_{top}$ [cm]*	20	48.5	30.32 \pm 4.78	0.28†

High accuracy of RUE_{gf}, canopy duration and SPAD values at heading in explaining variation in grain yield despite seasonal effects

The parameter correlation of BLUE values with the final grain yield were investigated based on Pearson's correlation coefficient (Table 2.3). Among the primary yield components, the correlation of grain number per spike exceeds the correlation of TGW and spike number with grain yield.

Table 2.3: Pearson correlation coefficients of all parameters with grain yield within the three seasons and overall with the BLUE values, shading indicates the ranking of the coefficients within the season (shading= top four associations among the canopy traits)

Trait	Pearson correlation coefficients for parameter correlation with grain yield			
	2015	2016	2017	BLUE values
Biomass [g/m ²]	0.85	0.82	0.79	0.86
HI	0.71	0.63	0.36	0.66
Yield parameters				
TGW [g]	0.40	-0.14	0.32	0.18
Spikes per m ²	n.s.	n.s.	n.s.	n.s.
Grains per spike	0.40	0.58	0.33	0.54
Phenology				
BBCH59 [°Cd]	n.s.	0.41	0.19	0.27
Greenness				
GCD [°Cd]	0.66	0.14	0.56	0.65
Leaf area index				
\overline{gLAI}_{int}	0.34	0.40	0.43	0.49
\overline{gLAI}_{dur} [°Cd]	0.29	n.s.	0.41	0.39
\overline{gLAI}_{mean}	0.22	0.40	0.24	0.33
\overline{gLAI}_{BBCH59}	0.21	0.36	0.19	0.29
Photosynthetic performance				
SPAD _{BBCH59}	-	0.59	0.49	0.63
Radiation interception				
\widehat{gI}_{int}	0.42	0.21	0.49	0.55
\widehat{gI}_{dur}	0.38	n.s.	0.40	0.41
\widehat{gI}_{mean}	0.36	0.61	0.36	0.53
iPAR _{gf} [MJ/m ²]	0.41	0.27	0.45	0.51
RUE _{gf} [g/MJ]	0.70	0.80	0.67	0.8
Architectural traits				
k	n.s.	-0.16	-0.14	-0.16
k _{top}	-	-	n.s.	-
height [cm]	-0.69	-0.53	-0.34	-0.66
height _{top} [cm]	-	-	-0.39	-0.58

This indicates that the number of grains was most relevant for yield formation in this experiment. The utilization of radiation has a greater relevance for yield formation than the interception ($r = 0.8$ vs. $r = 0.5$ for the average correlation of yield with RUE_{gf} and $iPAR_{gf}$, respectively). There was no clear relationship between interception and utilization of radiation, i.e. low correlation values between RUE_{gf} and $iPAR_{gf}$ or \widehat{gI}_{mean} (data not shown). Among the canopy traits, the highest correlations with the final grain yield were observed for RUE_{gf} , GCD and $SPAD_{BBCH59}$ with $r > 0.6$ for each of these three parameters. Generally, the results indicate that the constitution of the leaves around anthesis and the persistence had the greatest importance for the yield formation together with the overall radiation use efficiency during grain filling and a reduced importance of the radiation interception.

Interestingly, the top-ranking parameters also explained variation in yield with high accuracies in each of the investigated years, despite the significant cultivar by year interaction of the traits. This shows, that the ranking with respect to relevance for yield remained constant, while the single cultivar expression might interact with the seasonal effect. Moreover, the data show that the canopy architecture (light extinction coefficient k) and the LAI only have a marginal importance for yield formation in general. In parallel, the extinction coefficient of the top layer also shows no effect on yield formation. However, it is conspicuous that in the year 2016, where the GCD had a low accuracy in explaining grain yield, the \widehat{gLAI}_{mean} gained in importance and additionally the \widehat{gI}_{mean} explained variation in yield with a higher accuracy in that year.

SPAD values at heading explain variation in RUE and LAI explains variation in radiation interception

Figure 2.4 presents the linear relationships between RUE_{gf} and \widehat{gI}_{mean} with the corresponding underlying physiological traits for each season and overall. For RUE_{gf} the results indicate that the photosynthetic capacity (assessed via SPAD) has a higher accuracy in explaining variation in grain yield than the extinction coefficient, although the coefficients of determination are generally low ($R^2 < 0.33$). For the average relative light interception, the relationship is stronger ($R^2 < 0.46$). However, also here, the extinction coefficient does not explain variation in light interception. This indicates that based on the coefficient of determination of the linear regression, there is no clear relationship between the measure of canopy architecture and the light interception and utilisation (Fig. 2.4). Interestingly, the year 2016 is again conspicuous in the relevance of the leaf area index, here \widehat{gLAI}_{mean} shows a greater ability to explain variation in light interception in comparison to the other seasons.

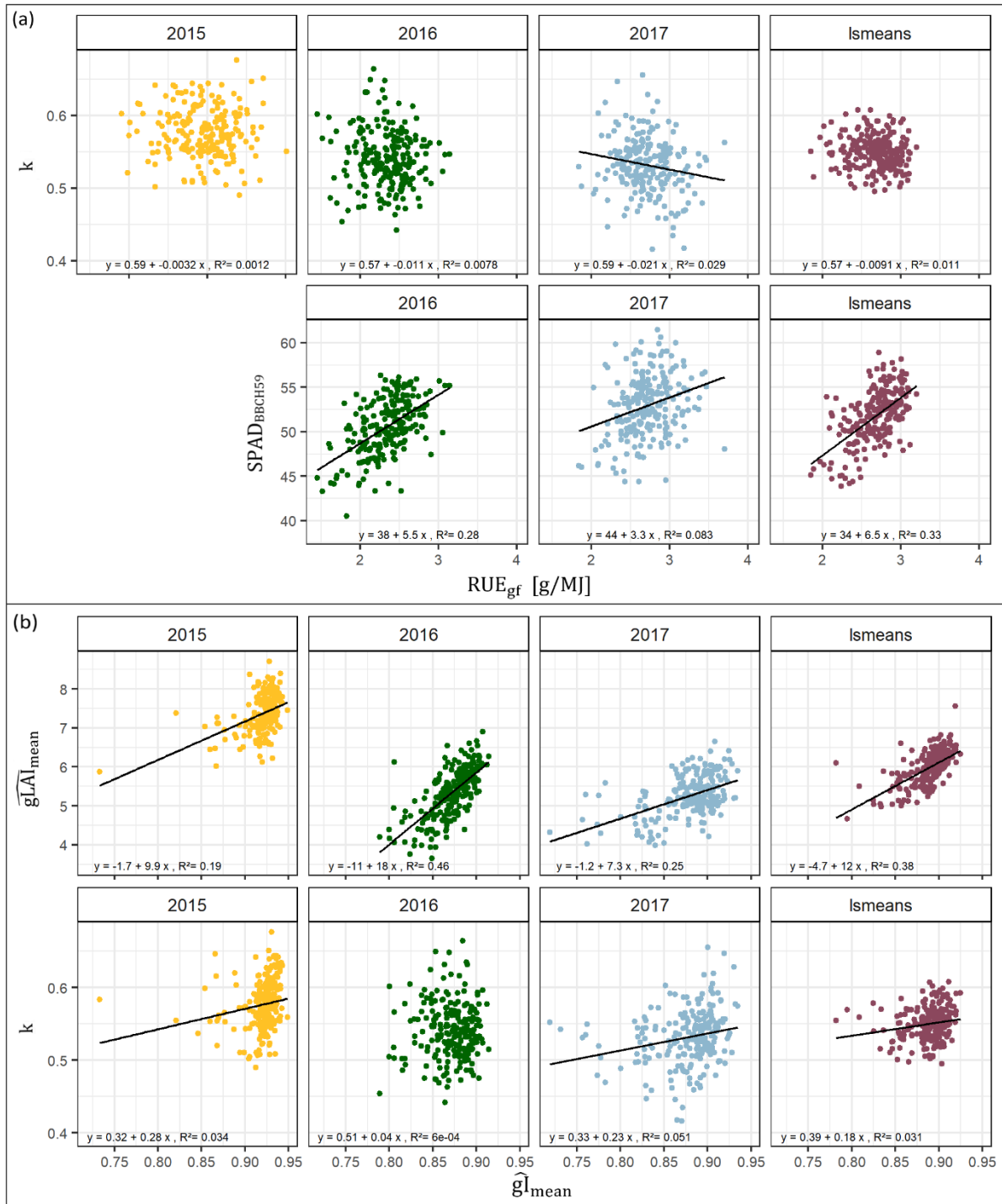


Figure 2.4: Linear relationship between the radiation use efficiency and the underlying parameters k and SPAD at heading (a) and between the mean relative light interception and the leaf area index and k (b). The regression line was only plotted, when the relationship was significant (p -value ≤ 0.05). The \widehat{gI}_{mean} - outlier in 2016 was the cultivar Helios which was performing not very well in both replications in 2015. However, removing the cultivar from the regression analyses does not have any considerable effects (data not shown).

Suboptimal conditions at vegetation start caused variation in importance of vegetative canopy characteristics for grain yield

The 220 cultivars were investigated in three years of field experiments under contrasting environmental conditions. The characteristics could be recognized in the trait expression and should therefore be described in detail. The first year, **2015** was not conspicuous in terms of weather conditions, but the nitrogen content of the soil was particularly high. The residual nitrogen in the soil in spring made the first application redundant (Table S2.2). These conditions were reflected in the biomass production, as the cultivars developed close to 30% more total biomass and LAI in comparison to 2016 and 2017 (data not shown). Subsequently, the grain filling duration was the longest in this year, which can be associated with the high amount of resources to be allocated to the seed (Table S2.3). The following year, **2016**, was characterised by a very warm autumn, a cold and wet spring and high radiation especially during the grain filling period (Table S2.3). Because of extreme conditions during winter and spring (warm autumn and cold winter: higher risk for winter kill, wet February: low nitrogen levels in the soil due to leaching and withdrawal of nitrogen by the plants) led to a greater differentiation of cultivars in terms of canopy characteristics. The additionally higher total amount of incoming radiation in that year then led to a more efficient interception of light, so that the canopy duration was not crucial anymore and had no meaning for yield development in that year. Figure 2.5 shows the measured LAI and relative light interception values and the corresponding correlations of these values with the final grain yield. It is obvious that the dependencies differ in 2016 in comparison to the other two years and that the measured values have a greater relevance for the final yield formation. The LAI values at vegetative growth explained the variation in grain yield with Pearson correlation coefficients of up to $R^2 = 0.6$ (Fig. 2.5(a)).

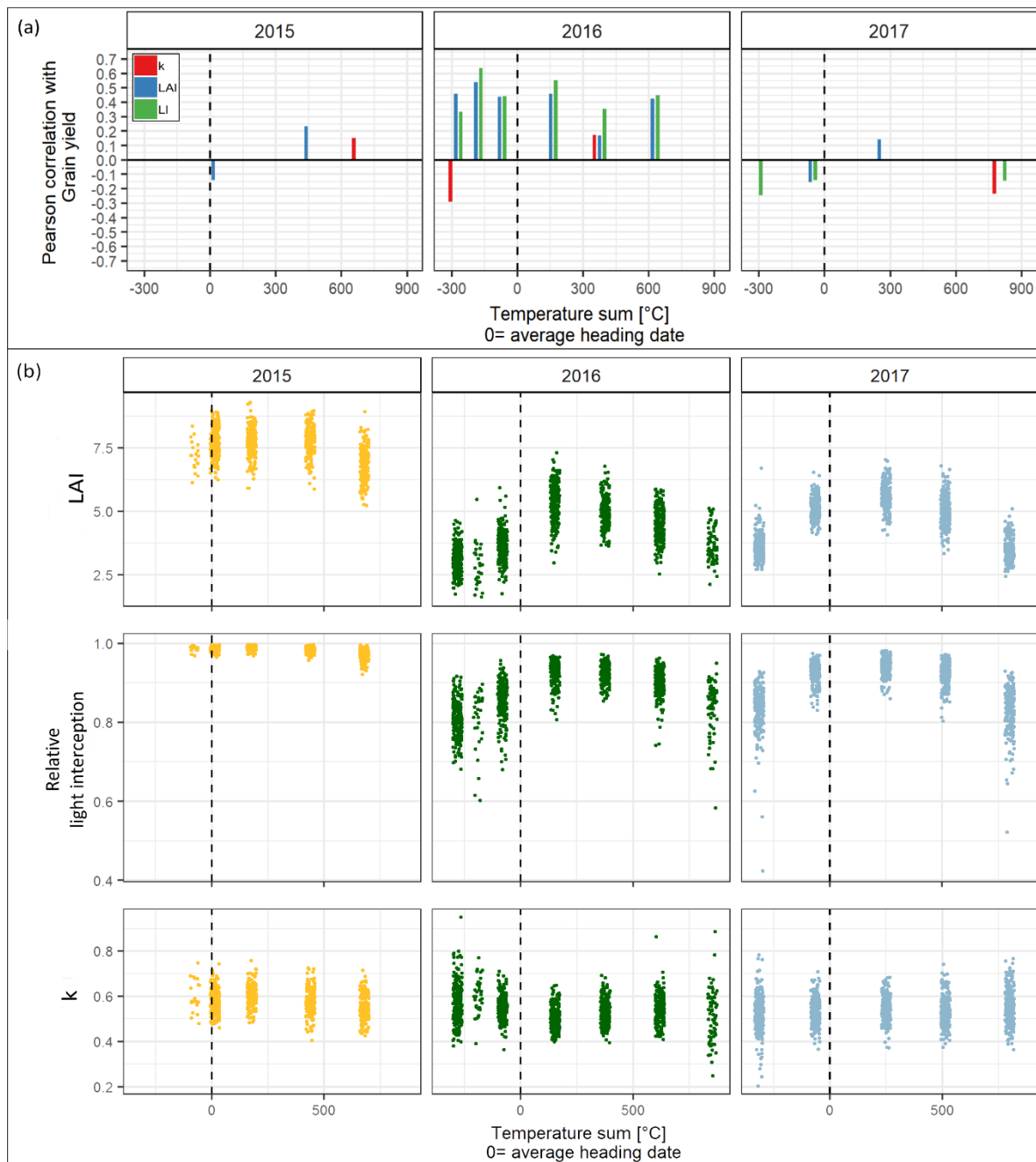


Figure 2.5: Measured data of LAI and the relative light interception at several dates throughout the seasons (b) and the corresponding correlation of the values with the final grain yield (a).

Additionally, the relative light interception and the extinction coefficients at vegetative stages also showed significant correlations with the final grain yield in that year. This indicates an ability of the cultivars to react to environmental conditions. 2017 was characterised by a very warm spring and on average the least radiation (Table S2.3). Interestingly, in this year the cultivars reached maturity on average in the shortest duration, 36 days, because of high temperatures in June and July, but nevertheless, the canopy duration had again a higher meaning to the final yield.

SPAD_{BBCH59} is most relevant for RUE_{gf} and the persistence of the canopy, GCD, is most relevant for light interception

The assumed causal relationships of the traits related to light interception and utilization and those two with the final grain yield, were tested with a structural equation model based on the BLUE values over all seasons. The results clearly supplement the simple correlation of the parameters. Since the initial fit did not represent the data well (*Fisher's C* = 317.116, *p-value* = 0, 50 degrees of freedom, *AIC* = 357.116), the model was adjusted by investigating the significant unstandardized coefficients. Figure 2.6 shows the adjusted model and all significant path coefficients greater than 0.1. Smaller but still significant causal effect, were the effects of \widehat{gI}_{mean} (0.08), \widehat{gLAI}_{mean} (-0,05) and GCD (0.03) on grain yield and of \widehat{gLAI}_{mean} (0.03) on $iPAR_{gf}$. With the additional paths (dashed arrows), the model fits the data reasonably well as indicated by the *p-value* > 0.05, and lower *AIC* and *Fisher's C* values (*Fisher's C* = 41.111, *p-value* = 0.13, 32 degrees of freedom, *AIC* = 99.111).

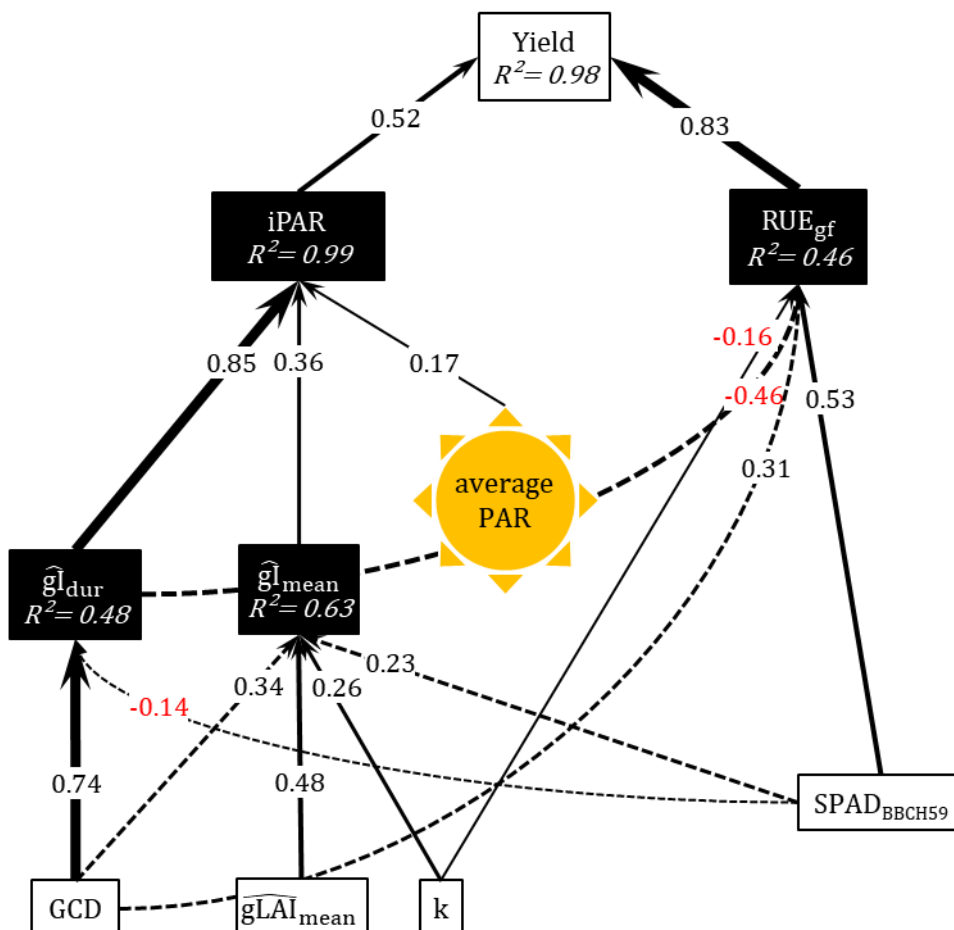


Figure 2.6: Model with fitted observed variables for interdependencies between source characteristics. Black boxes indicate endogenous response variables, white boxes the predictor variables. Only significant standardized path coefficients for each causal relationship ($p < 0.05$) and standardized path coefficients are displayed if larger than 0.1. R^2 values for the response variables indicate the prediction accuracy of the explanatory variables. The width of the path represents the magnitude of the standardized coefficients and dashed arrows indicate the additional dependencies suggested by the structural equation model.

The additional paths increased the accuracy of the total model and also the prediction accuracy for the response variables: for RUE_{gf} from $R^2= 0.35$ to $R^2= 0.46$, for \widehat{gI}_{dur} from $R^2= 0.46$ to $R^2= 0.48$ and for \widehat{gI}_{mean} from $R^2= 0.43$ to $R^2= 0.63$. The model supports the expected dependencies (the canopy duration and interception efficiency affect $iPAR_{gf}$ and the photosynthetic capacity and the penetration of light through the canopy affect RUE_{gf}). Additionally, it suggests causal effects of $SPAD_{BBCH59}$ on the relative light interception (pos.) and its duration (neg.) and causal effects of the \widehat{gI}_{dur} (neg.) and the GCD (pos.) on the RUE_{gf} . This affirms the relevance of $SPAD_{BBCH59}$ and the duration of the green leaf material for the biomass production during grain filling, the yield formation. The results indicated that for the present data set, the radiation use efficiency is most relevant for yield formation and that this parameter largely depends on the photosynthetic capacity but also the persistence of the assimilating leaf material. The persistence is at the same time the most relevant parameter in the network of the traits affecting the light interception. Interestingly, in addition to GCD and $SPAD_{BBCH59}$, the model further reveals that the \widehat{gLAI}_{BBCH59} and k , which showed low correlation coefficients with grain yield and low heritabilities, as valuable characteristics. The influence of LAI and k on the light interception and utilization efficiency should obviously not be neglected.

Grain number is affected by $SPAD$ at heading and the canopy duration and grain weight is not affected by any canopy characteristic

Regarding the primary yield components, the evaluation of the structural equation model to describe the effects of the canopy characteristic on grains per spike revealed that exchanging the \widehat{gLAI}_{BBCH59} with the GCD improved the model fit. These causal effects were able to explain 26% of the variation (Table 2.4, Fig. 2.7 (a)) in comparison to 24% if \widehat{gLAI}_{BBCH59} and $SPAD_{BBCH59}$ were assumed to affect grain per spike (Fig. 2.2).

Table 2.4: Estimated values for the causal relationships explaining the yield components by the source model.

Response	Predictor	Estimate	Std. error	DF	Critical value	P-value	Standardized estimate
Grains per spike	$SPAD_{BBCH59}$	0.6547	0.105	217	6.2372	0	0.39 ***
	GCD	0.0189	0.0058	217	3.246	0.0014	0.21 **
	GCD	0.0037	0.0048	216	0.7536	0.4519	0.0589
TGW	\widehat{gLAI}_{BBCH59}	-0.0346	0.5491	216	-0.063	0.9498	-0.0046
	$SPAD_{BBCH59}$	0.1192	0.0819	216	1.4558	0.1469	0.1066

This indicates that the present leaf area has no significant effect on the grain number, the quantity of the source seems to have no effect, the quality has a greater importance. Additionally, there is a causal link of the canopy duration to the grain number. For the grain weight, no significant coefficient was detected for any of the canopy traits as causal agent (Table 2.4, Fig. 2.7 (b)). This result illustrates that the grain weight is independent of the source characteristics during grain filling.

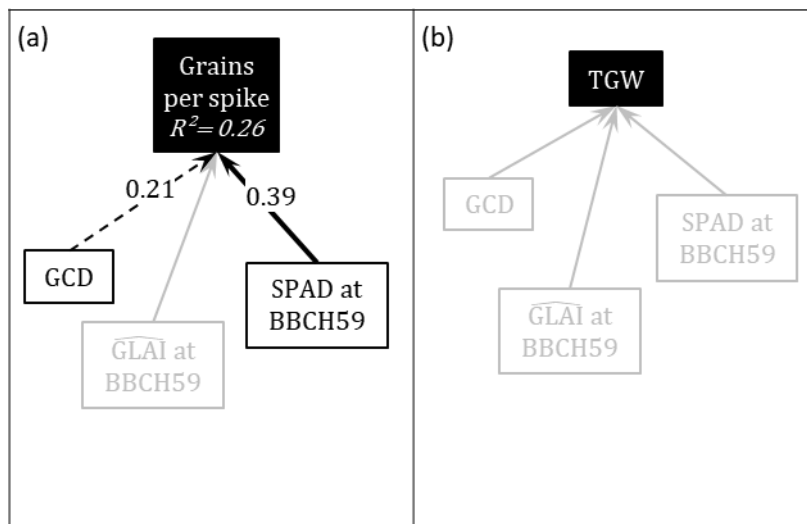


Figure 2.7: Fitted models for the causal relationships between yield components and underlying source traits based on the complete and adjusted underlying source model (compare Fig. 2.5). Black boxes indicate endogenous response variables, white boxes the predictor variables.

Breeding progress reflects environmental differences and plasticity of modern cultivars

For all investigated yield, physiological and architectural parameters also the progress with the year of release was investigated for each experimental year and overall based on the BLUE values (Table 2.5). The R^2 values in the table show the goodness of fit of the linear regression of the sliding window means for each parameter and the year of release (compare Fig. 2.8). The highest relative breeding progress was observed for the final grain yield (23.5%, 0.04 t/ha/a) but also the other traits showed significant progress with the year of release. The present subset of cultivars showed similar progress in biomass and HI (both around 10%), whereas the progress in HI varied greater between seasons. The data shows, that in a year with overall high biomass production due to environmental issues, the modern cultivars outcompete the old ones in an even greater extend in terms of biomass partitioning (HI). This reflects a degree of adaptability of the modern cultivars (Table 2.5: HI 15% increase in 2015). Among the yield components the number of sink organs, grains per spike showed the most pronounced increase (17.2% on average and even 22.7 % in 2015).

Table 2.5: Breeding progress of the yield, canopy and architectural parameters. Absolute and relative breeding progress was derived from sliding window means. Absolute breeding progress is the slope of the linear regression line fitted for the parameter in dependency of the year of release. The relative breeding progress is expressed in percent [%] as the ration between the trait value of 2010 and 1970. Grey numbers: $R^2 < 0.25$, bold numbers: $R^2 > 0.75$.

	2015				2016				2017				BLUE values			
	$f(1970)$	absolute	R^2	relative	$f(1970)$	absolute	R^2	relative	$f(1970)$	absolute	R^2	relative	$f(1970)$	absolute	R^2	relative
Grain yield [t/ha]	7.61	0.06	0.9	29.45	6.72	0.04	0.86	21.42	6.49	0.03	0.80	19.45	6.94	0.04	0.92	23.74
Biomass [g/m ²]	1850.32	5.44	0.7	11.77	1416.80	3.69	0.52	10.43	1281.80	3.3	0.45	10.34	1516.30	4.15	0.66	10.95
HI	0.41	0.0016	0.79	15.62	0.48	0.0012	0.77	9.72	0.51	0.0012	0.58	9.12	0.47	0.0013	0.79	11.25
Yield parameters																
TGW [g]	40.30	0.09	0.49	9.30	42.73	n.s.			41.19	0.05	0.41	5.34	41.40	0.05	0.29	4.54
Spikes per m ²	823.04	-1.7	0.19	-8.26	501.09	0.87	0.15	6.98	518.28	n.s.			614.18	n.s.		
Grains per spike	29.57	0.17	0.73	22.73	37.16	0.16	0.44	17.6	38.55	0.13	0.58	13.68	35.10	0.15	0.65	17.61
Phenology																
BBCH59 [°Cd]	1475.79	-0.62	0.25	-1.67	1606.80	0.282	0.07	0.7	1444.81	-0.43	0.09	-1.20	1509.13	-0.26	0.05	-0.68
Greenness																
GCD [°Cd]	601.71	2.98	0.8	19.78	699.84	0.7697	0.39	4.4	504.71	1.98	0.54	15.67	602.09	1.91	0.75	12.67
Leaf area index																
\widehat{gLAI}_{int}	3629.75	11.71	0.54	12.90	3088.89	8.8005	0.33	11.4	2975.46	6.46	0.25	8.68	3232.78	9.02	0.50	11.16
\widehat{gLAI}_{dur} [°Cd]	501.21	1.22	0.60	9.75	636.34	-0.2187	0.05	-1.37	570.98	0.98	0.46	6.84	569.15	0.67	0.49	4.70
\widehat{gLAI}_{mean}	7.23	0.0054	0.16	3.01	4.86	0.0156	0.46	12.85	5.23	n.s.			5.78	0.0075	0.33	5.19
\widehat{gLAI}_{BBCH59}	7.72	0.0066	0.22	3.40	5.18	0.0164	0.46	12.69	5.50	n.s.			6.14	0.0079	0.34	5.15
Photosynthetic performance																
SPAD _{BBCH59}					49.04	0.0718	0.47	5.85	50.29	0.11	0.55	8.40	49.66	0.09	0.59	7.14
Radiation interception																
\widehat{gI}_{int}	500.13	1.19	0.46	9.50	579.83	0.3718	0.1	2.56	499.69	1.06	0.44	8.45	526.06	0.88	0.59	6.68
\widehat{gI}_{dur} [°Cd]	545.68	1.15	0.46	8.42	673.32	n.s.			576.30	0.883		6.13	597.93	0.71	0.58	4.77
\widehat{gI}_{mean}	0.91	0.0003	0.25	1.19	0.86	0.0005	0.46	2.16	0.87	0.0005	0.21	2.15	0.88	0.0004	0.40	1.83
iPAR _{gf} [MJ/m ²]	289.07	0.70	0.49	9.62	317.85	0.2447	0.16	3.08	253.98	0.55	0.48	8.70	286.65	0.50	0.62	7.03
RUE _{gf} [g/MJ]	2.68	0.011	0.68	16.53	2.13	0.0095	0.79	17.76	2.60	0.0058	0.56	8.85	2.47	0.01	0.84	14.23
Architectural traits																
k	0.56	0.0005	0.24	3.33	0.57	-0.0009	0.68	-6.02	0.53	n.s.			0.55	-0.0001	0.08	-1.03
k _{top}									0.51	0.0009	0.12	6.91				
height [cm]	104.67	-0.20	0.58	-7.59	94.82	-0.2534	0.74	-10.69	85.85	-0.20	0.64	-9.22	95.57	-0.22	0.72	-9.17
height _{top} [cm]									31.46	-0.07	0.36	-8.98				

The RUE_{gf} showed a highly significant breeding progress of 14.2% on average whereas the intercepted radiation only moderately improved with the year of release (Table 2.5 and Fig. 2.8(a) and (b)). In parallel, the duration, the integral and the average relative light interception showed only moderate progress.

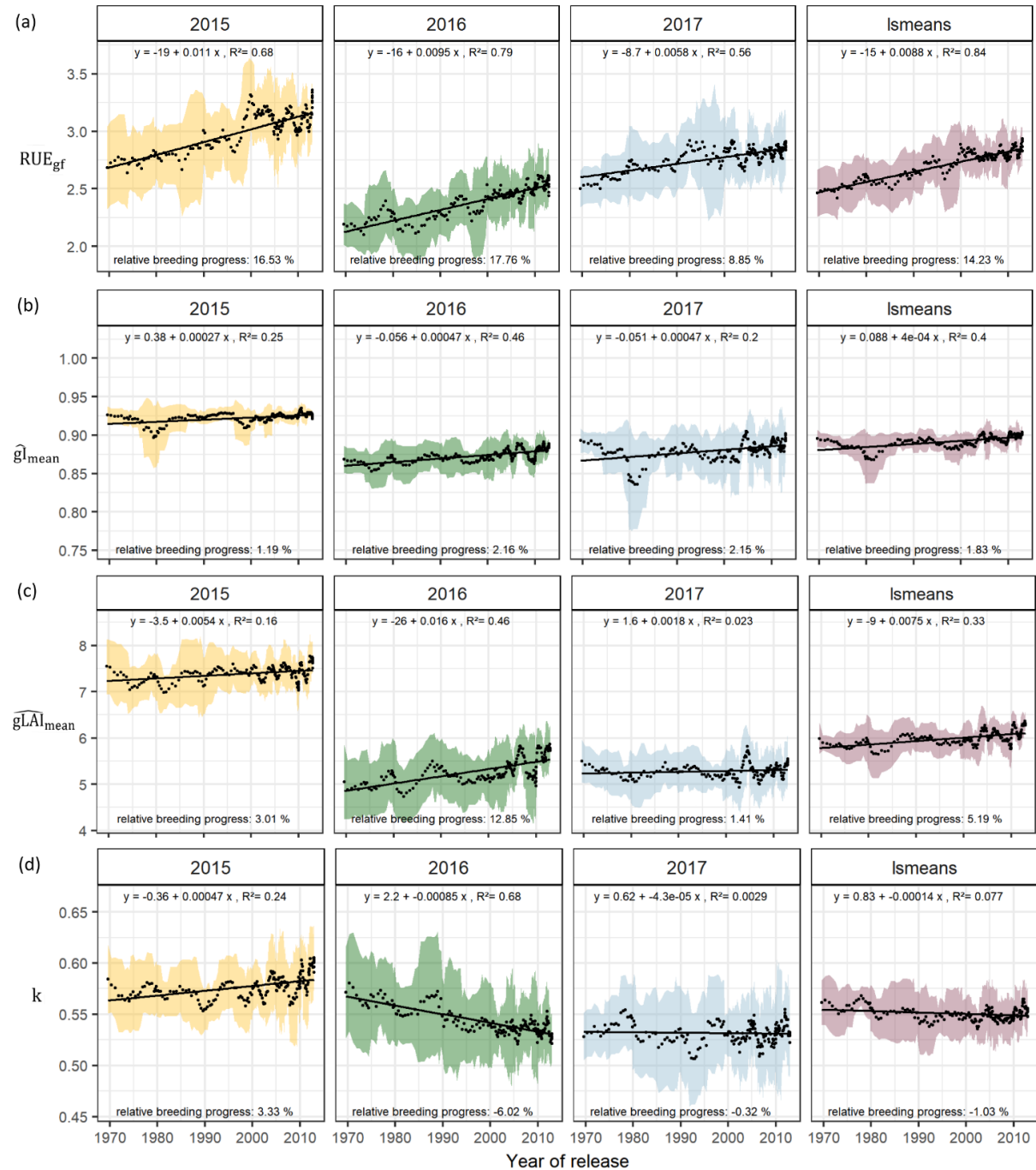


Figure 2.8: Sliding window plots showing the breeding progress of RUE_{gf} (a), $\widehat{g}l_{mean}$ (b), $\widehat{g}LAI_{mean}$ (c) and k (d). Each dot represents a mean value of 10 cultivars, the coloured area represents the standard deviation. The slopes of the linear regressions are referred to as absolute breeding progress and the relative breeding progress is the ratio between the values from 2010 and 1970.

Furthermore, the \widehat{gLAI}_{dur} , \widehat{gLAI}_{mean} , the extinction coefficient k of the complete canopy and of the top layer showed no, not significant or very little breeding progress (Table 2.5 and Fig. 2.8(c) and (d)). On the contrary, GCD and the \widehat{gLAI}_{int} show significant breeding progress of >10%. Interestingly, for most of the parameters the progress is constant between years, but some are conspicuous. In the year 2016, a significant progress in the \widehat{gLAI}_{BBCH59} was observed instead of a breeding progress in GCD. This observation can be related to the relevance of each of these parameters for yield formation in that year, as the LAI also has gained importance. In addition, it becomes apparent here, that also the extinction coefficient k shows a significant breeding progress in only this year. As described above, the modern cultivars developed a higher LAI at vegetative stages which was obviously associated with a more erect leaf orientation (smaller k) compared to the old ones. The subsequently increased efficiency to intercept light was also reflected in the higher breeding progress of RUE_{gf} in that year compared to the others (Table 2.5 and Fig. 2.8(c)).

DISCUSSION

Usefulness of photosynthetic capacity and the persistence of the canopy for breeding purpose

It is increasingly important to unravel the interdependencies between the physiological traits to enable the development of modern high yielding varieties. As grain yield is a very complex quantitative trait, selection for underlying physiological traits with relevance for yield formation is a highly recommended strategy for plant breeders, especially as high-throughput techniques in plant phenotyping rapidly progress (Schulthess *et al.*, 2017; Furbank *et al.*, 2019). Complementary crosses, namely crossings between lines with high biomass production on one side and high HI on the other side is a more promising strategy, than just crossing two high yielding lines without knowing their physiological characteristics (Reynolds *et al.*, 2017). The present study revealed SPAD and GCD as most promising candidate traits to tackle radiation interception and utilization and thereby identify genotypes with efficient biomass production.

Measuring physiological traits of hundreds of genotypes is challenging under field conditions, especially for photosynthetic activity. Non-destructive sensor measurements have been developed to be able to assess canopy characteristics, which often make use of close relationships between traits (Furbank *et al.*, 2019). For example, there is strong evidence of a positive relation between leaf chlorophyll content and leaf photosynthetic capacity (Wu *et al.*, 2009). Leaf chlorophyll content is, in turn, closely associated with non-destructive reflectance measurements, e.g. measured by a handheld chlorophyll meter (Bannari *et al.*, 2007) like the SPAD as applied in this study.

The measurements have been used widely to investigate the chlorophyll content and thereby the photosynthetic performance but also to determine the nitrogen status of the canopy to guide fertilizing strategies (Bannari *et al.*, 2007; Xiong *et al.*, 2015; Furbank *et al.*, 2019). However, there is also evidence, that the measurements are non-linearly related to chlorophyll content and an interacting effect of environmental factors (e.g. irradiance) and the N-status of the leaves on the measurement (Xiong *et al.*, 2015). The applicability might therefore be questioned. Despite that, the present study revealed a high heritability of the SPAD values, indicating a comparatively low environmental influence. The value of this optical instrument for breeding purposes should therefore not be underestimated. An advancement in estimating the photosynthetic performance via reflectance data should rather be the improvement of the throughput of the measurements, which can be met by innovative phenotyping solutions. Aerial imaging and multispectral sensing are promising tools for phenotyping of photosynthetic related parameters of the canopy (Furbank *et al.*, 2019; Zhang *et al.*, 2019).

The role of canopy architecture in achieving high yield

We expected that besides the photosynthetic capacity, also the size of the canopy, the vertical profile of leaf orientation affecting the penetration of light and the persistence of the canopy are relevant for biomass accumulation. It has been suggested that a more erect canopies is beneficial for grain yield; a higher RUE could be realised with more leaves exposed to sun light (Richards *et al.*, 2019). Principally, this study reveals that the architecture of the canopy and the size (LAI) are not as relevant as the photosynthetic capacity and the persistence. Also, the specific measurements of the top layer did not show relevance in explaining the grain yield. However, under certain conditions the weighting in the relevance shifts and the investigated collection of cultivars revealed that modern cultivars carry a higher plasticity to cope with environmental constrains. Richards *et al.*, 2019, summarized that the beneficial effect of a either plano- or erectophile canopy largely depends on the specific agronomic and climatic conditions (e.g. row spacing, length of growing period and potential LAI). The capacity of responsiveness in physiological traits to environmental constrains to facilitate stability in yield should be highly beneficial in terms of future growing conditions under climate change. This phenomenon is supported by the investigations on the general setup of the genome of modern in comparison to older breeding lines, which show, that the genetic variation was not reduced through breeding (Cavanagh *et al.*, 2013; Voss-Fels *et al.*, 2019).

Valuable results from path analysis reveal relevance of canopy parameters

The structural equation model presents a suitable method to investigate and outline the relationships of the canopy characteristics, as also the parameters with low heritability but still relevance particularly through their plasticity are included here. Regarding the canopy architecture, the SEM could uncover dependency while the person correlations were not significant. Interestingly, the effect of the canopy architecture parameter k is positive on light interception and at the same time negative on the RUE_{gf} . Canopies with more erect leaves (small k) especially in the upper layer are known to have less light-saturated leaves in comparison to more horizontal arranged leaves (larger k) (Furbank *et al.*, 2019; Richards *et al.*, 2019). The present data obviously shows that more erect leaves have a beneficial effect on the RUE_{gf} and a negative effect on the light interception, as more light can penetrate the canopy (less light intercepted). Additionally, a contradictory effect was observed for the effect of the duration parameters on RUE_{gf} . Whereas the GCD has a positive influence, the \widehat{GLI} duration affects RUE_{gf} negatively. This phenomenon indicates that an extended persistence of the green canopy (irrespective of size and light interception) supports the utilization of light, while the extended interception of light would inhibit RUE_{gf} . This portends a possible surplus of light intercepting leaf material after anthesis.

Source characteristics around and after anthesis are relevant for grain number but not individual grain weight

The investigations of the dependencies of the source characteristics affecting the yield components revealed that the number of grains per spike is dependent on the quality and the persistence of the canopy (and not the size), whereas the thousand grain weight was not affected by any of the source characteristics. Obviously, there was no limitation of the specific weight of each grain due to assimilation during grain filling and it can be assumed that the assimilates to be stored in the grain were already produced. The direction of the physiological link between number of grains and the canopy persistence is conspicuous and might be questioned. It is unlikely that grain number is adjusted depending on the persistence of the canopy during grain filling because grain number is already fixed around anthesis. On the contrary, this result would rather indicate the causality to be inversely, an effect of the grain number on the canopy duration. The concrete dependencies between sinks and sources of grain yield also revealed a pre-determination of the canopy persistence at the stage, when the grain number is fixed (Lichthardt *et al.*, 2020).

Progress of yield through RUE and relative light interception

The present investigations not only revealed the causal agents for yield formation in general, but could also highlight, which parameters were of great relevance to facilitate of breeding progress in the last 50 years of German breeding history. The significant improvement in grain yield was accompanied by progress in several of the underlying traits. Breeding progress was observed for both the biomass and HI, despite of the general opinion that HI has already reached its optimum in the 1980's (Austin *et al.*, 1980; Reynolds *et al.*, 2009). It seems to be a general belief, that the harvest index has not been improved since the green revolution at that it might already be at its theoretical optimum. However, Würschum *et al.*, 2017, showed that the breeding efforts have shifted the focus towards newly identified height reducing genes (Rht24) and therefore further improvement of the biomass partitioning within the canopy might be feasible. It is of crucial importance, that the HI still stays in focus when breeding for increase in biomass (Reynolds *et al.*, 2017).

Furthermore, breeding progress was observed for light interception and utilisation, whereas the latter was more pronounced. Regarding the underlying traits, again SPAD_{BBCH59} and GCD are apparent but also the integral of the green leaf area showed a substantial significant progress. With respect to the link between the source and the sink components a co-evolution was prosed between grain number and especially the two parameters SPAD_{BBCH59} and GCD (Lichthardt *et al.*, 2020). The canopy architecture did not change on average with breeding, although the plant height was significantly reduced.

An increased leaf area index and biomass had to be arranged on a shorter stem in the modern cultivars, but the data shows no change in the light extinction. The k stabilizes around 0.55 and the light interception was already for the old cultivars close to 1 (complete interception) and no substantial improvement could be expected. With an extinction coefficient of 0.55, 95% of light interception is mathematically reached at a LAI of 5.44 (according to eq. 18) and a higher LAI does not increase the interception of light. The present study shows LAI values of up to 8 and it can be assumed, that some of that leaf material is not required by the plants to adequately support the growing grains. The LAI can a breeding target, but it could also be tackled by agricultural management (e.g. fertilization).

CONCLUSION

The present study reveals the persistence of the canopy and the SPAD values around anthesis as most relevant in the network of characteristics explaining the light interception and utilisation. Previous studies did already indicate the importance of RUE for future breeding progress, but to our knowledge, this is the first study representing more details regarding the underlying traits and identifies concrete causal agents (SPAD and GCD) to be applied in breeding. This study presents the complete network of the traits underlying light interception and utilization during grain filling and their dependencies. However, low heritabilities and genotype by year interaction of many of the canopy parameters might cause instability. Therefore, only SPAD and GCD are indeed usable for breeding and could guide to an improvement of relative light interception and RUE. If at the same time breeder care for the degree of genetic variation in the germplasm (e.g. by using wild relatives to introduce favourable traits), the physiological plasticity should be ensured and therefore facilitate stability in yield. Additionally, the significant decrease of k with the year of release in 2016 provides evidence that the canopy architecture is adjusted in modern cultivars to increase the light interception at lower LAI values.

CHAPTER 3

Co-evolution of sink and source in the recent breeding history of winter wheat in Germany

Carolin Lichthardt¹, Tsu-Wei Chen¹, Andreas Stahl², Hartmut Stützel¹

¹Institute of Horticultural Production Systems, Leibniz University Hannover, Hannover, Germany

²Department of Plant Breeding, IFZ Research Centre for Biosystems, Land Use and Nutrition, Justus Liebig University, Giessen, Germany

Published in:

Frontiers in Plant Science, Section: Plant Breeding (2020),

DOI: 10.3389/fpls.2019.01771

<https://www.frontiersin.org/articles/10.3389/fpls.2019.01771/full>

ABSTRACT

Optimizing the interplay between sinks and sources is of crucial importance for breeding progress in winter wheat. However, the physiological limitations of yield from source (e.g. green canopy duration, GCD) and sink (e.g. grain number) are still unclear. Furthermore, there is little information on how the source traits have been modified during the breeding history of winter wheat. This study analysed the breeding progress of sink and source components and their relationships to yield components. Field trials were conducted over three years with 220 cultivars representing the German breeding history of the past five decades. In addition, genetic associations of QTL for the traits were assessed with genome-wide association studies. Breeding progress mainly resulted from an increase in grain numbers per spike, a sink component, whose variations were largely explained by the photosynthetic activity around anthesis, a source component. Surprisingly, despite significant breeding progress in GCD and other source components, they showed no direct influence on thousand grain weights, indicating that grain filling was not limited by the source strength. Our results suggest that, 1) the potential longevity of the green canopy is predetermined at the time point that the number of grains is fixed; 2) a co-evolution of source and sink strength during the breeding history contribute to the yield formation of the modern cultivars. For future breeding we suggest to choose parental lines with high grain numbers per spike on the sink side, and high photosynthetic activity around anthesis and canopy duration on the source side, and to place emphasis on these traits throughout selection.

INTRODUCTION

The final grain yield of winter wheat is the result of the number of grains and the grain weight which are determined by the primary yield components: spike number per unit area, grain number per spike and thousand grain weight (TGW) (Fischer, 2011). The formation of different yield components can be interpreted as the result of the interplay between sinks and sources. Sink size of the developing yield organs is determined by the number of spikes per unit area, grains per spike and a specific sink size per grain (resulting in TGW). Source size is related to the production of photo-assimilates, namely the size, the photosynthetic capacity and the duration of the leaf area, which drive spike development and grain filling (Jagadish *et al.*, 2015).

The interplay between sinks and sources has an impact on yield formation which becomes apparent from double ridge stage (first spikelet ridges visible) to the end of grain filling. In the very early phase, from double ridge to terminal spikelet stages, a source limitation may result in a reduced spikelet number (Guo *et al.*, 2018). Around anthesis, spikelet fertility is affected and the physiological process of floret abortion could be activated, thereby reducing the grain number. The physiological factors relevant for source limitation at anthesis are (1) the canopy leaf area, which maximizes light interception, and (2) photosynthetic capacity per leaf area which maximizes the utilization of light energy for production of plant mass. It has been shown that limitation of source strength (e.g. by shading of leaves around anthesis) reduces grain number per spike (Wang *et al.*, 2003). Furthermore, the crop growth rate around anthesis could also be associated with grain number (Bancal, 2008; Guo *et al.*, 2018). This indicates a negative effect of source limitation around anthesis on the formation of the sink size, namely grain number. After the seed number is determined, a reduction in source limitation can be achieved physiologically by extending the canopy longevity, or the capacity to stay green. Source limitation during the grain filling phase (after anthesis) can reduce the TGW (Foulkes *et al.*, 2009; Guo and Schnurbusch, 2015; Liang *et al.*, 2018), indicating a negative effect of the source limitation after anthesis on the sink size, namely grain weight.

An ongoing debate is whether grain yield is sink or source limited. Complementary crosses between genotypes with high sink capacity and those with high source capacity resulted in progeny with substantial yield improvement (Reynolds *et al.*, 2017), suggesting the co-limitation of source and sink on yield. It has been suggested that the selection of crossing partners based on physiological traits is a promising strategy to achieve a higher crop productivity via breeding, which is not least facilitated by the increasingly automated phenotyping techniques (Foulkes *et al.*, 2009; Reynolds and Langridge, 2016; Reynolds *et al.*, 2017; Furbank *et al.*, 2019).

A precise description of the sink and source characteristics of possible genetic resources for future winter wheat varieties is, together with the application of genomic tools, a purposive strategy to promote the genetic gain via strategic complementary crosses. Functional interdependencies of physiological traits often depend on pleiotropic relationships or interactions of relevant genetic loci. Therefore, patterns of co-evolution during breeding history between interacting sinks and sources can be assumed (Schulthess *et al.*, 2017; Alonso *et al.*, 2018). In order to meet the projected demand for food and the challenges of climate change (Reynolds *et al.*, 2009; Ray *et al.*, 2013), possible linchpins to further increase the yield potential of new cultivars can be found by investigating physiological and genetic interdependencies between yield, yield components and their links to source and sink components.

The co-limitation of sink and source implies that breeding progress of them should be achieved parallelly. However, the concrete interactions of source characteristics with the sink traits and thereby its role in breeding progress of winter wheat is unclear, especially for the capacity of the canopy to stay green (Jagadish *et al.*, 2015). Since stay-green prolongs the time for carbon assimilation and increases the source for grain filling (Lawlor and Paul, 2014), it can be hypothesized that, under source limited conditions, breeding progress in stay-green trait is linked to the breeding progress in TGW. The beneficial effect of stay-green traits on grain yield, especially TGW, has been demonstrated and summarized by several research groups (Wu *et al.*, 2012; Gregersen *et al.*, 2013; Xie *et al.*, 2016). Additionally, previous studies have shown the link between increased leaf area index (LAI) or extended longevity of the leaf area and yield increase in modern varieties (Tian *et al.*, 2011; Sanchez-Garcia *et al.*, 2015). However, these studies did not elaborate, whether grain number or TGW are affected by the delayed senescence, so that the functional interface between sink and source remains unclear. Additionally, especially for the central European wheat cultivars, the interdependencies of sink and source characteristics have to our knowledge not yet been tested in greater detail. Interestingly, there is evidence of a non-causal association between source and sink activities during grain filling and a possible link between a delayed senescence and sink size, namely grain number (Yin *et al.*, 2009; Liang *et al.*, 2018). In summary, one would at first glance assume a direct effect of the stay-green trait on thousand grain weight but there could also be a link from grain number to an extended availability of photosynthetic active materials.

The present study aims to decipher the source-sink interdependencies between the yield components during grain filling and to evaluate the contributions of German breeding progress on the sink and source characteristics after anthesis. We used 220 cultivars, 174 of which were released in Germany between 1966 and 2013, representing the breeding history of the last five decades.

All cultivars were grown over three consecutive seasons (2014-2017) to study the breeding progress of the source strength (leaf area index, relative chlorophyll content and canopy longevity) and the sink strength (spike number, grain per spike and grain weight). We hypothesized that high yield of modern wheat cultivars is realised by both a higher grain number and higher TGW with the first being associated with the photosynthetic capacity and leaf area at flowering, whereas the latter is linked to the increase in canopy longevity to assure the source for grain filling. Furthermore, a genome wide association study (GWAS) was conducted to identify the significant quantitative trait loci (QTL) to facilitate marker-assisted selection.

MATERIAL AND METHODS

Plant materials

Breeding history of German winter wheat was represented by a collection of 174 wheat cultivars released between 1966 and 2013. These cultivars, including 5 hybrids and 169 pure lines, are recommended for conventional production and represent all baking quality classes “E”, “A”, “B” and “C” (very high to very low baking quality). They were selected based on the country of cultivar registration (always including Germany) and an agronomic and economical importance in Germany. Each decade in the breeding history was represented by more than 20 cultivars and 66% of the collection was released in the last two decades (Fig. S3.1). Additionally, 46 diverse accessions obtained from the German seed bank (<https://gbis.ipk-gatersleben.de>) were included to enlarge the genetic diversity and improve the reliability of the genome-wide association study (see later section). In total, 220 cultivars were used in this study and the complete list of cultivar names, year and country of registration, breeder, quality classification and the assignment to the subsets is provided in Table S2.1. All cultivars of the breeding history subset of this study were included in the main experiment of the study described by Voss-Fels *et al.*, 2019.

Experimental design and growing conditions

Field trials were conducted in three seasons (2014-2015, 2015-2016 and 2016-2017) at the research station in Ruthe near Hannover (52°14'44.1"N 9°49'03.4"E, clayey silt soil type). All 220 cultivars were sown in plots with 330 viable seeds m² and in 15 rows in 2 m plot width (13.33 cm row spacing). The plot sizes were 12 m², 10 m² and 9.4 m² in the three consecutive years, respectively. Plots were arranged in a randomized block design with two replications and cultivars were randomized within four sub-groups according to the flowering time and plant height (early and short; early and tall; late and short; late and tall) based on previous knowledge (tall= >100cm height).

Due to the field design, applications were conducted on all plots when most cultivars reached the relevant stage for application and they were all treated once. The plots were treated according to standard agrochemical application in intensive wheat production in Germany. Mineral nitrogen (N) fertilizer was supplied in three applications with a target value of 220 kg N/ha including the soil mineral nitrogen (N_{\min}) measured at the beginning of the growing season in the root zone (Wehrmann and Scharpf, 1979). In each season, growth regulators were applied once at stem elongation stage and fungicides were applied at stem elongation, flag leaf appearance and beginning of flowering. The treatment of growth regulator followed the recommendation of regional advisors with expertise in winter wheat production to be in step of the actual best-practice. Weed and insect control were applied according to the requirements. A summary of the crop protection is provided in Table S3.2 and the weather conditions during the experimental periods are summarized in Figure S3.2.

Yield measurements

Shortly before harvesting the plots, a sample of one row (50 cm in length) was cut to determine the harvest index (HI) by the ratio of grain yield (g m^{-2}) to total dry biomass (g m^{-2}). Numbers of spikes and TGW (g) of these samples were used to determine spikes per m^2 and grains per spike and m^2 . Plot grain yield and TGW were determined by harvesting the complete plots with a combine harvester. Plot biomass was calculated by dividing the grain yield by the harvest index.

Physiological measurements

Heading date (BBCH59, (Witzenberger *et al.*, 1989)) was recorded for all cultivars in one replication per year. Additionally, the hard-dough (BBCH87) was recorded in one replication each year. Because the investigation is a time-consuming process, the hard-dough was only recorded for a subset of 20 cultivars, which were selected to represent the variation in maturity. Due to the fungicide treatment, leaf and ear diseases, including powdery mildew, rust, *Septoria spp.* and *Fusarium*, were successfully controlled. Therefore, all cultivars were close to 100% green at the heading stage. After heading, the declining fraction of green leaf area (%) was visually scored every one to two weeks. Around the heading date (approx. 230 days after sowing), the leaf area index was maximal and was measured by a plant canopy analyser (LAI-2200C, Li-COR, Lincoln, Nebraska USA).

To quantify the dynamics in the senescence pattern, a logistic power function with two parameters was used to describe the relationships between the fraction of green leaf area (y , %) and the thermal time (TT , °Cd):

$$y = \frac{1}{1 + \left(\frac{TT}{GLA_{50}}\right)^s} \quad (1)$$

GLA_{50} is the temperature sum (°Cd), at which the green leaf area drops to 50% and s describes the steepness of the curve (Fig. S3.3). Temperature sum is defined as the cumulative sum of the daily mean temperatures, starting from the day of sowing with 0°C as base temperature. Green canopy duration (GCD, °Cd) was defined as the difference between GLA_{50} and the thermal time at heading date (TT_{heading}):

$$GCD = GLA_{50} - TT_{\text{heading}} \quad (2)$$

In addition, leaf area duration (LAD) was defined as the product of the maximal leaf area index (LAI_{max}) and duration of it, namely the integral of the logistic curve from heading to harvest:

$$LAD = \int_{TT_{\text{heading}}}^{TT_{\text{harvest}}} \frac{1}{1 + \left(\frac{TT}{GLA_{50}}\right)^s} \times LAI_{\text{max}} \quad (3)$$

LAI_{max} is a measure for the canopy development until heading and a proxy of the biomass accumulation prior to grain filling. GCD is defined as the duration of the availability of photosynthetic leaves from heading to 50% leaf senescence (Fig. S3.3). LAD is the integral of the green leaf area from heading to harvest weighted by the maximal canopy size (LAI_{max}), in other words the product of the integrated canopy duration and the canopy size. The photosynthetic activity is difficult to assess in a large scale field experiment. Therefore, the SPAD values of the flag-leaf were measured as a proxy for the photosynthetic activity in 2016 and 2017. For each genotype and replication, five flag leaves were measured at the widest section around the heading dates of that genotype (± 10 days).

Statistical analyses

The phenotypic data collected in the field experiment was evaluated with the following mixed model

$$P_{ijkl} = \mu + c_i + \gamma_j + c\gamma_{ij} + YR_{jk} + YRG_{jkl} + e_{ijkl}, \quad (4)$$

where P_{ijkl} was the phenotypic observation of the i^{th} cultivar ($i = \text{cultivar number } 1 - 220, \text{ factorial}$) in the j^{th} year ($j = 2015, 2016 \text{ and } 2017, \text{ factorial}$) in the k^{th} complete replication and the l^{th} incomplete sub-group ($l = \text{early and short; early and long late and short; late and short}$). Fixed factors are indicated by lowercase letters, capital letters indicate random effects.

The observation was dissected into the general mean, μ , the genetic effect of the i th cultivar c_i , the effect of the j th season y_j , the interaction of the cultivar and the season cy_{ij} , the interaction of the sub-group, the replication and the season GRY_{jkl} , the interaction of the replication and the season RY_{jl} and the residual e_{ijkl} . The model was fit to the data with the *lmer* function of the *lme4* package in the R environment (Bates *et al.*, 2015; R Core Team, 2017). Significant differences between cultivars, seasons and the interactions were examined with the *anova* function. The best linear unbiased estimators (BLUE) for each cultivar and cultivar within each year were calculated using the *lsmean* function from the *lsmeans* package (Lenth, 2016). Analyses of the cultivar's performances within each year and across the years was performed based on the estimated BLUEs and were also used the phenotypic values in the marker – trait associations in the genome-wide association study.

Broad-sense heritability H^2 of the physiological and yield components within the breeding history – subset was calculated over n environments and r replications according to the formula:

$$H^2 = \frac{\sigma_c^2}{\left(\sigma_c^2 + \frac{\sigma_{cY}^2}{n} + \frac{\sigma_e^2}{nr}\right)} \quad (5)$$

where σ_c^2 , σ_{cY}^2 and σ_e^2 are the genetic variance component, the interaction variance component between genotype and environment and the residual variance component (equation (4)), respectively. To estimate the variance components, the model in equation (4) was set as completely random.

Quantification of the breeding progress

The population of 174 cultivars was used to quantify the breeding progress in winter wheat. The *absolute breeding progress* (increase per year) was the slope of the linear regression line between the year of release and the parameter of interest. The linear regressions were calculated based on sliding window means, where the window for mean calculation is moving on the scale of the year of release with a constant window size of 10 cultivars with cultivars ordered by the year of release. Means and standard deviation of the parameters in each window were calculated. Using the linear regression equation of the absolute breeding progress, the *relative four-decades breeding progress* (%) of the parameters was described by the ratio between the trait values of 2010 and 1970. It is an estimate for the superiority of the modern cultivar in percent (in the following referred to as *relative breeding progress*). The breeding progress was investigated for each experimental year separately (BLUE values per cultivar and year) and on average (BLUE values per cultivar).

Genome-wide association study

Genome wide association study (GWAS) was performed to identify marker-trait-associations of the single nucleotide polymorphisms (SNPs) associated with the parameters which were putatively improved with breeding. Leaf DNA samples of the total collection of 220 accessions were genotyped with the 135K Affymetrix TGWEXCAP Array carrying a total of 136,780 SNP markers (TraitGenetics, Gatersleben, Germany). The complete set of markers was applied to detect clusters of genetically related individuals within the R package *adegenet* (Jombart, 2008). A discriminant analysis of principal components (DAPC) was performed. Via a k-means clustering of initial calculated principle components, five groups were identified. These groups were then implemented as covariates in the mixed model which was applied to estimate the genome wide association.

To anchor the SNP markers to physical positions, 136,780 SNP probes were aligned to the *T.aestivum* genome (IWGSC release iwgsc_refseqv1.0 assembly soft-masked version (IWGSC, 2018) using BLASTN 2.2.31 (Camacho *et al.*, 2009). Markers were excluded if their SNP probe sequence could not be aligned with high stringency to a unique physical position on the reference sequence (E-value $\leq 10^{-5}$). The results were filtered with the following criteria 1) uniquely mapped 2) no gap, and 3) minimum 1 base mismatch, to obtain a total of 92,464 anchored SNP markers. After quality control by filtering monomorphic markers with > 10% missing values or a minor allele frequency < 5%, a selection of 45,370 high-quality, polymorphic SNPs remained in the data set for further analyses. On average 2,130 markers per chromosome were applied for the genome-wide scan for marker-trait associations. The size of the area on the chromosome covered with markers ranged from 473 Mbp (chromosome 6D) to 829 Mbp (chromosome 3B) and hence the marker density lied between one marker per 1.6 Mbp (chromosome 4D) and one marker per 0.2 Mpb (chromosome 5B). The minor allele frequency ranged from 0.19 (chromosome 3D) to 0.28 (chromosome 6A). The allelic associations were calculated for genotypic trait values (BLUE values) of yield, HI, biomass, grains per spike, SPAD, LAI_{max} and GCD with the polygenic function in the R package *genABEL* by implementing the population structure and the genome wide kinship matrix (Aulchenko *et al.*, 2007). The Bonferroni method ($p < 0.05$) and the false discovery rate (FDR 10%) were considered as thresholds for significant marker-trait-associations.

RESULTS

Environmental effects on yield component traits and source characteristics

All traits showed significant differences between the 174 wheat cultivars representing the breeding history (Table S3.3, $p < 0.05$). Between the growing seasons all parameter values differed significantly except TGW, grains per m² and SPAD. The interaction between growing season and cultivar was significant for all traits except for biomass, HI, spikes per m² and grains per m².

In 2015 the mean grain yield of all cultivars was around 17% higher than in 2016 and 2017, but the HI was lower in 2015 compared to 2016 and 2017 (Fig. 3.1 A, B). This was probably due to the high nitrogen availability during the early vegetative growth in 2015 (Table S2.2), the high ratio of daily radiation to mean temperature (data not shown) and an overall lower mean temperature (Table S3.4), which significantly enhanced the vegetative growth indicated by 27% more total biomass (Fig. 3.1 C) and 33% more straw (Fig. 3.1 D). In parallel, spike number, determined by the physiological processes related to tillering and tiller reduction during the vegetative development, was about 30% higher in 2015 (Fig. 3.1 G). However, the higher spike number in 2015 was accompanied by a 17% lower number of grains per spike (Fig. 3.1 H). The total amount of grains per unit area, which is the product of the number of spikes and number of grains per spike, remained only slightly higher in 2015 (not significant) than in the other seasons (Fig. 3.1 F). This indicates a higher robustness of this sink trait, or vice versa a higher plasticity of spike number and grains per spike with respect to environmental conditions.

The maximal leaf area index (LAI_{max}), SPAD and the canopy longevity parameters, including green canopy duration (GCD, eqn. 2) and leaf area duration (LAD, eqn. 3), were taken as the parameters describing source capacity. All parameters showed significant cultivar and cultivar by year effects, and, except for SPAD, significant differences between years (Table S3.3). For the source parameters, the heritabilities were lower than that for yield and grains per spike (0.50, 0.66, 0.51 and 0.57 for LAI_{max}, SPAD, LAD and GCD, respectively, Table S3.5), indicating a high environmental variance of the traits.

Conditions for vegetative growth were more favourable in 2015 resulting in a 28% higher maximum LAI than in the other two seasons (Fig. 3.1 I). In 2017, the canopy longevity parameters LAD and GCD showed significantly lower values due to high temperatures in the later generative phase (Fig. 3.1 J, 3.1 K and S3.2). High LAD values in 2015 can be attributed to the high maximal LAI values.

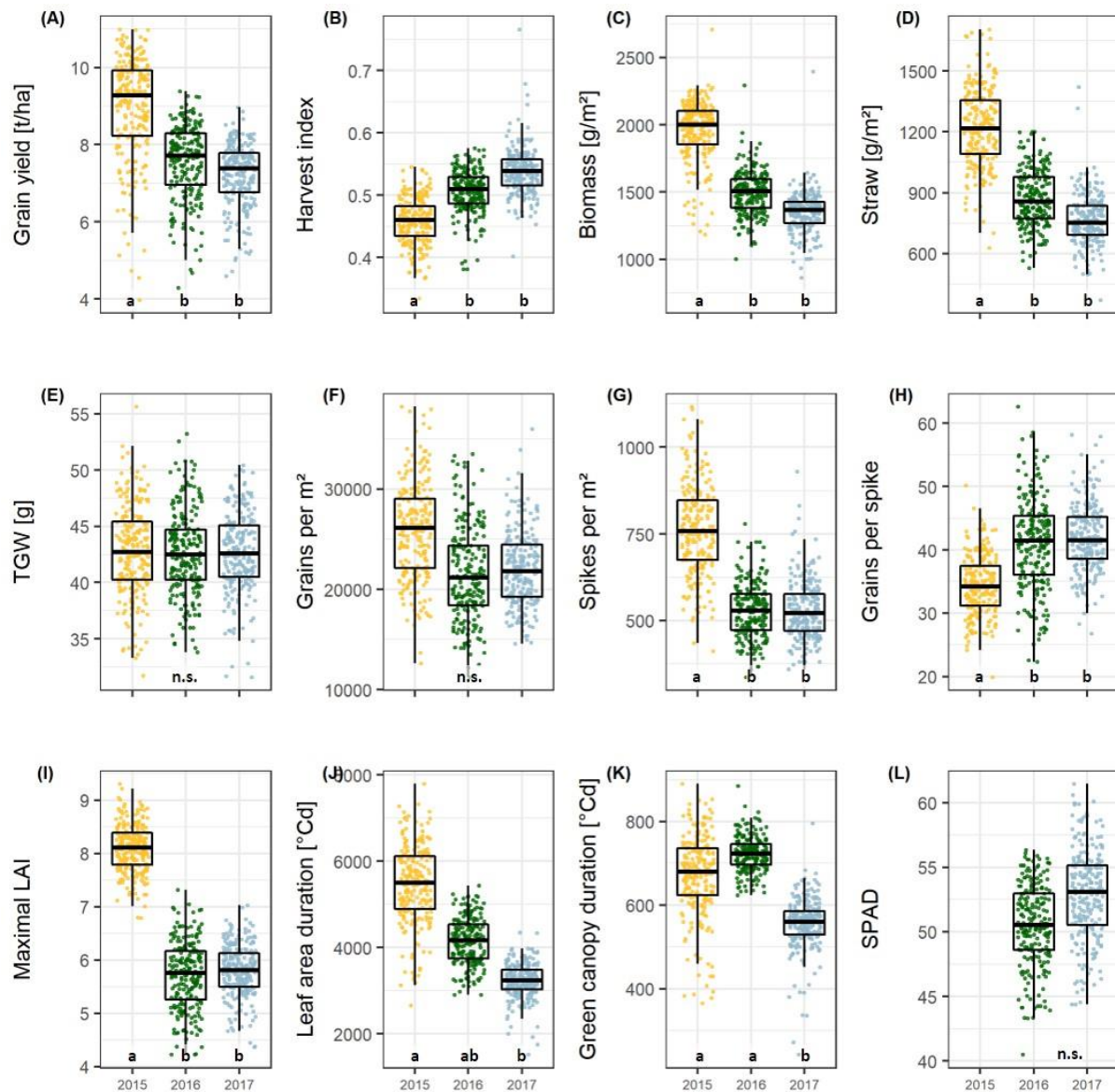


Figure 3.1: Boxplots of the yield, yield components and green canopy parameters presenting the mean values per cultivar and season for the 174 cultivars representing the breeding history. Different lower-case letters within the plots indicate significant differences between seasons. Abbreviations are listed in Table 1.

The main factor relevant for yield formation, grains per spike, is determined by the photosynthetic activity around anthesis and affects the canopy longevity

HI and biomass explain variations in grain yield with high accuracies, indicated by the high correlation values on average (Fig. 3.2 A and B) and for each of the growing seasons (Fig. S3.4). The interdependencies of the source characteristics (LAI_{max} , SPAD, LAD and GCD) and these yield parameters indicate that both, the photosynthetic activity (SPAD) and the longevity of the canopy (GCD) are of importance for yield formation.

However, a positive relationship between wheat leaf photosynthesis and leaf chlorophyll content has been widely observed (Wu *et al.*, 2009) and the leaf chlorophyll content, in turn, is closely associated with non-destructive measurements with the hand-held digital chlorophyll meter SPAD (SPAD 502, Minolta, Japan) (Bannari *et al.*, 2007)

HI, the ratio of grain yield to total biomass, correlates mainly with the GCD, whereas the total biomass can be not only associated to the size of photosynthetic leaf material, but also by activity (SPAD-values) of assimilate production around anthesis (Fig. S3.4).

Grain yield can be dissected into thousand grain weight and grain number per unit area, the latter being the product of grains per spike and spike number per unit area. However, the genotypic differences in grain yield could not be explained by the genotypic variation in spike number and TGW of the studied cultivars (Fig. S3.4). In contrast, grains per spike explained the variation in grain yield with a Pearson coefficient of correlation (r) of up to 0.54 averaged over all seasons (Fig. S3.4, Fig. 3.2 C).

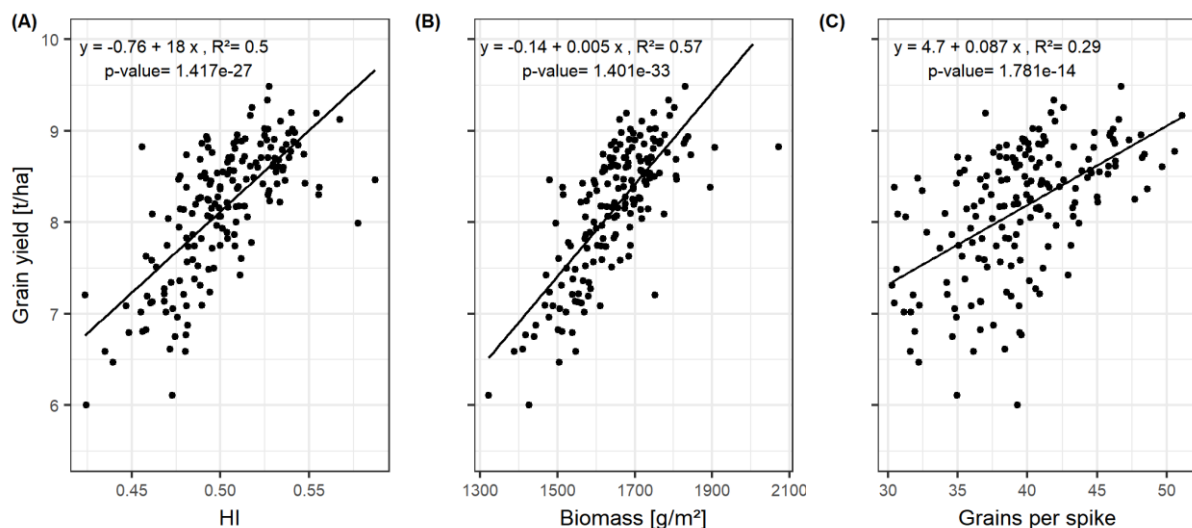


Figure 3.2: Relationships between grain yield and (A) harvest index (HI); (B) biomass; and (C) grains per spike. Each point represents the mean values of a cultivar in three growing seasons. In total, 174 cultivars representing the breeding history were used.

Linear relationships between the yield components and the source characteristics indicate that grain number per spike was mainly influenced by the photosynthetic capacity around anthesis. The SPAD values explained 21% of the variation of grain number per spike when averaged over the three seasons (Fig 3.3 A).

Grain number per spike was significantly related to GCD (Fig. 3.3 B, Fig. S3.4). The influence of grains per spike on grain yield is therefore in parts indirectly mediated by the canopy duration, which explains 34% of the variation in grain yield (Fig. 3.3 C). For a subset of 20 cultivars, the grain filling duration (temperature sum of BBCH59 subtracted from temperature sum of BBCH87) showed on average a significant correlation with GCD with $R^2=0.60$ (Fig. S3.5). This tight relationship indicates a physiological link between GCD and the grain filling duration. Surprisingly, insignificant correlation between GCD and TGW rejected our hypothesis and suggested that the influence of canopy duration and yield formation was already determined at the beginning of the grain filling phase. The source activity around anthesis affects the grain number which then decides on the durability of the source to fill the grains.

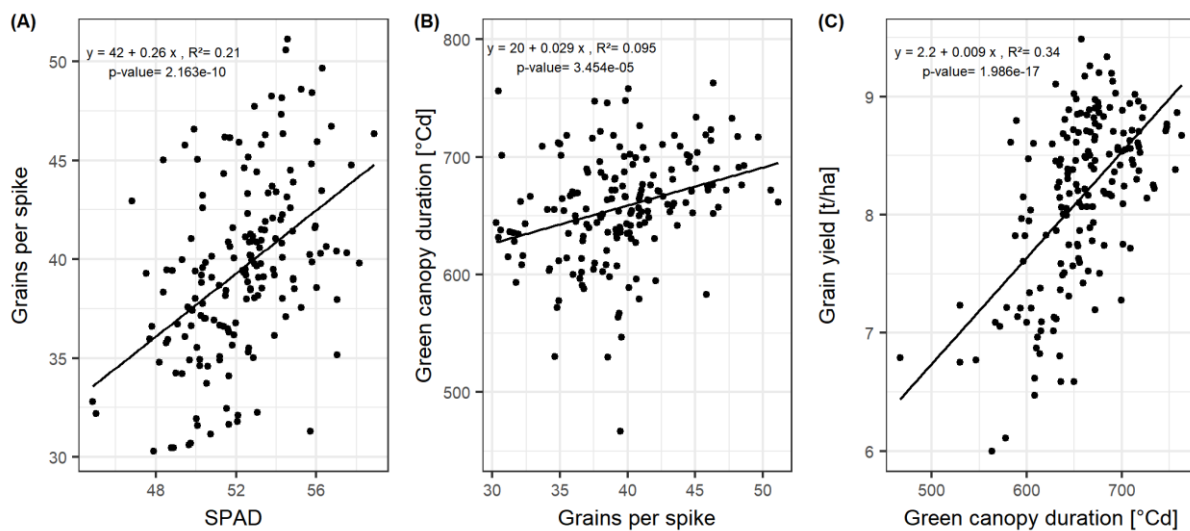


Figure 3.3: Relationships between (A) grains per spike and SPAD; (B) green canopy duration and grain per spike; and (C) grain yield and green canopy duration. Each point represents the mean values of a cultivar in three growing seasons. In total, 174 cultivars representing the breeding history were used.

Breeding progress was most pronounced in grains per spike and green canopy duration

The absolute breeding progress in yield between 1970 and 2010 was clearly linear and was nearly twice as high in 2015 than in 2016 and 2017 (Fig. 3.4). On average, the grain yield in 2015 was 7.55 t/ha for the cultivars released in the 1970s, increased annually by 59 kg/ha and reached 9.85 t/ha for cultivars released in 2010, indicating a relative breeding progress of 31.3 % in grain yield between 1970 and 2010 (Fig. 3.4 A). The corresponding values for 2016 and 2017 were 22.6 % and 21.3 %, respectively (Fig. 3.4 B and 3.4 C).

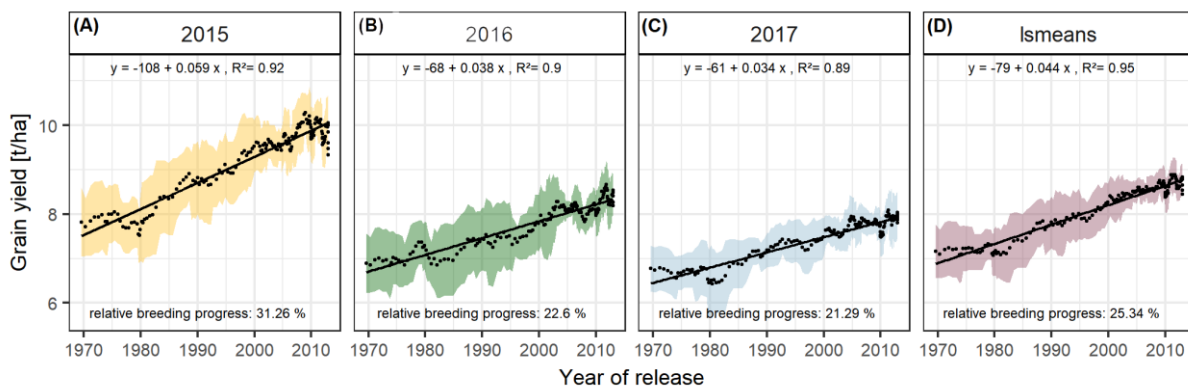


Figure 3. 4: Sliding window plots showing breeding progress in grain yield per season (A-C) and on average (D). Each dot represents a mean value of a group of 10 cultivars and the colored area represents their standard deviations. The slopes of the linear regression lines (black line) are referred to as absolute breeding progress and the relative breeding progress is the ratio between the values in 2010 and 1970.

Grain yield can be expressed as the product of biomass and harvest index (HI). The relative breeding progress in yield from 1970 to 2010 may be considered as the result of changes in biomass and HI:

$$\frac{Yield_{2010}}{Yield_{1970}} = \frac{Biomass_{2010}}{Biomass_{1970}} \times \frac{HI_{2010}}{HI_{1970}}$$

With approx. 12 % the relative breeding progress in biomass was similar in all three experimental years (Fig. 3.5 E – H), while the relative breeding progress in HI in 2015 was 15.98 %, about 6 % higher than the progress measured in 2016 and 2017 (Fig. 3.5 A - D). This indicates that, in comparison with 2016 and 2017, the larger differences in yield between old and new cultivars grown in 2015 were due to their differences in HI. This agrees with the fact that in 2015 the correlation of yield with HI was higher than with biomass. In contrast, biomass showed the highest correlation with yield among all yield components in 2016, 2017 and on average (Fig. 3.2 and S3.4).

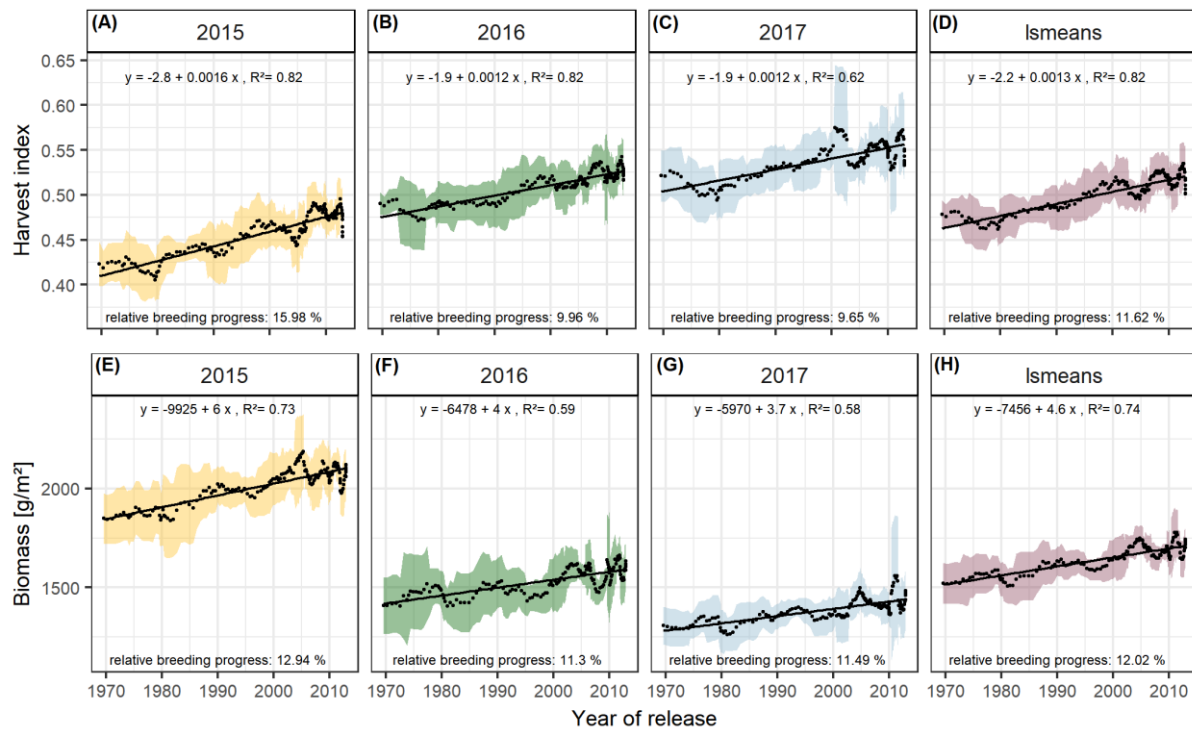


Figure 3. 6: Sliding window plots showing breeding progress of harvest index (A-D) and biomass (E-H). For detail, see the caption of Fig. 3.4.

Dissecting the breeding progress into that of the yield components, it is remarkable that the relative breeding progress of TGW was generally low and only conspicuous in 2015, showing an increase of 10% from 1970 to 2010 (Table 3.1). Accordingly, the correlations between TGW and grain yield, HI and the year of release were also higher in 2015 (Fig. S4 B). A slightly higher relative breeding progress in 2015 was also observed for all tested source parameters. However, the progress of grain number was lower than in the other years and spikes per m² even showed a negative genetic trend in 2015, indicating that the modern cultivars developed 1.6 spikes per m² less than the old cultivars. Despite having a lower spike number in 2015, the modern cultivars still developed higher yields than the older cultivars due to a 22.7% increase in grains per spike (Fig. 3.6).

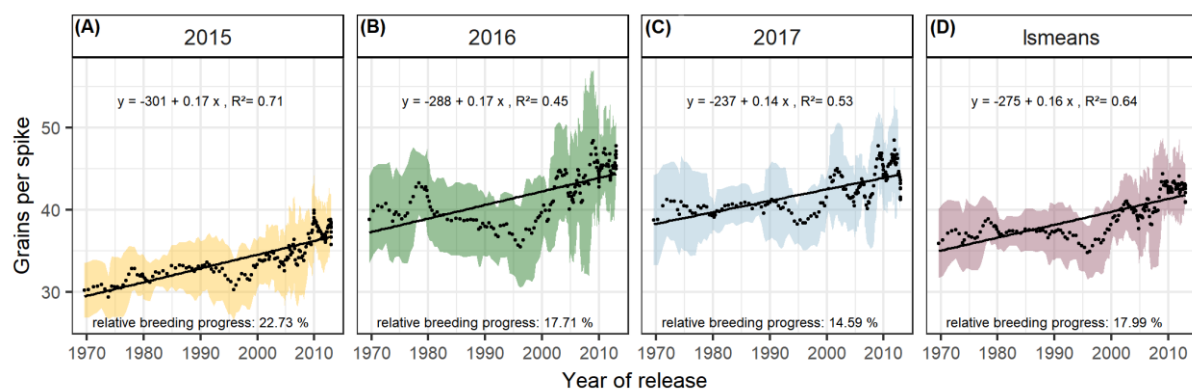


Figure 3. 5: Sliding window plots showing breeding progress of grain per spike. For detail, see the caption of Fig. 3.4.

Table 3.1: Breeding progress of the main yield and stay green parameters dissected into the development within each growing season separately and calculated for all seasons together (overall). Absolute and relative breeding progress was derived from sliding window means. Units for absolute breeding progresses are: grain yield: t ha⁻¹; harvest index (HI): unitless; biomass: g m⁻²; straw: t ha⁻¹; thousand grain weight (TGW): g; grain m⁻²; spikes m⁻²; grain spike⁻¹; maximal leaf area index (LAI_{max}): unitless; green canopy duration (GCD): °Cd; leaf area duration (LAD); and SPAD (unitless). Relative breeding progress is expressed in percent (%).

	2015			2016			2017			Overall		
	absolute	R ²	relative	absolute	R ²	relative	absolute	R ²	relative	absolute	R ²	relative
Grain yield	0.06	0.92	31.26	0.04	0.90	22.60	0.03	0.89	21.29	0.04	0.95	25.34
HI	0.0016	0.82	15.98	0.0012	0.82	9.96	0.0012	0.62	9.65	0.0013	0.82	11.62
Biomass	5.98	0.73	12.94	4.01	0.59	11.30	3.68	0.58	11.49	4.55	0.74	12.02
Straw	-1.34	0.09	-4.12	0.77	0.04	3.59		n.s.			n.s.	
TGW	0.10	0.54	9.86		n.s.		0.06	0.43	5.50	0.05	0.32	4.83
Grains/m²	75.70	0.40	12.51	122.46	0.52	26.66	81.72	0.58	16.67	93.29	0.76	18.00
Spikes/m²	-1.49	0.16	-7.26	0.89	0.15	7.15		n.s.			n.s.	
Grains/spike	0.17	0.71	22.73	0.17	0.45	17.71	0.14	0.53	14.59	0.16	0.64	17.99
LAI_{max}		n.s.		0.02	0.45	11.36	-0.01	0.27	-3.69	0.00	0.20	2.64
LAD	27.20	0.79	22.55	15.16	0.50	16.36	8.38	0.36	10.98	16.92	0.74	17.52
GCD	3.17	0.84	21.26	0.81	0.44	4.63	2.07	0.57	16.47	2.02	0.79	13.46
SPAD				0.07	0.50	5.77	0.11	0.59	8.42	0.09	0.62	7.11

Among all yield components, grains per spike had the highest relevance for breeding progress. This was indicated by the highest correlations with the year of release within the seasons and on average (Fig. S3.4) and high relative breeding progress (Table 3.1).

The significant Pearson correlations of sink and source parameters and the year of release averaged over all seasons cover a range from $r = 0.78$ for grain yield to $r = 0.17$ for TGW. With that, GCD ranked among the highest values ($r = 0.52$) and is improved by breeding with a relative breeding progress of 13% (Fig. S3.4A, Table 3.1). A significant breeding progress was also observed for the photosynthetic activity during anthesis (SPAD) (Fig. 3.7 A – C).

Breeding progress in LAI_{max} was inconsistent between years (Fig. S3.4, Table 3.1), significant only in 2016 (11.4%) and 2017 (-3.7%). Furthermore, in all seasons the absolute breeding progress in LAI_{max} was marginal, indicating that the breeding progress in source capacity was in general not achieved by the increasing canopy size. By contrast, with 17.5% the relative average breeding progress for leaf area duration was the second-highest breeding progress value after grain yield and grain number increase (LAD, Table 3.1). Notwithstanding, the correlation of the year of release and GCD was significant in all seasons and comparable with that for grains per spike ($r = 0.52$, $r = 0.48$, respectively, Fig. S3.4A). The absolute breeding progress of GCD was about 2 °Cd per year of release (Table 3.1). Thus, modern cultivars stay about 7 days with a mean temperature of 15 °C longer green than old cultivars.

Although GCD explained the variations in yield to the same extent as grains per spike, breeding progress in GCD showed four times differences between years (Fig. 3.7 D – G) whereas the breeding progress in grains per spike was independent of the year (about 0.17 grains per year of release, or 6.4 grains per spike from 1970 to 2010, Table 3.1). This implies a higher environmental dependency of canopy duration.

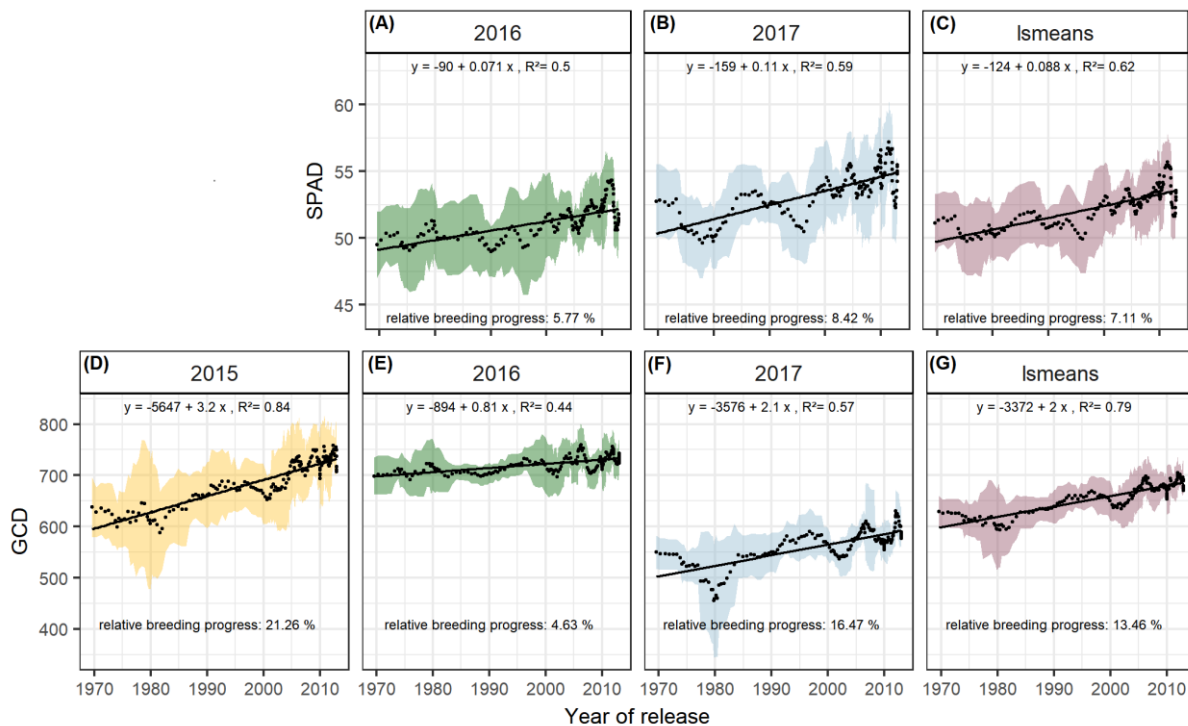


Figure 3.7: Sliding window plots showing breeding progress of SPAD (A-C) and green canopy duration (D-G). For detail, see the caption of Fig. 3.4.

Significant marker-trait associations for GCD and biomass

Based on the Bonferroni threshold with $p < 0.05$ ($-\log_{10}(p) = 5.96$), one significant marker was detected for biomass on chromosome 3A (1.93 Mbp) and considering the FDR < 0.1 , one additional significant association appears on chromosome 6A for GCD (441.4 Mbp) (Fig. S3.6 and Fig. 3.8). To investigate these signals, the linkage disequilibrium (LD) pattern of all marker-trait associations among the 100 highest $-\log(p\text{-values})$ for each analysed trait were investigated. Chromosomes 3A and 6A showed relevant patterns (Fig. 3.8).

Besides the significant marker around 2 Mbp for biomass on chromosome **3A**, a collection of marker-trait-associations for grain yield and biomass were detected around 500 Mbp with high LD values. Remarkably, several marker-trait associations for grain yield and GCD colocalised at 20 Mbp and showed high LD values.

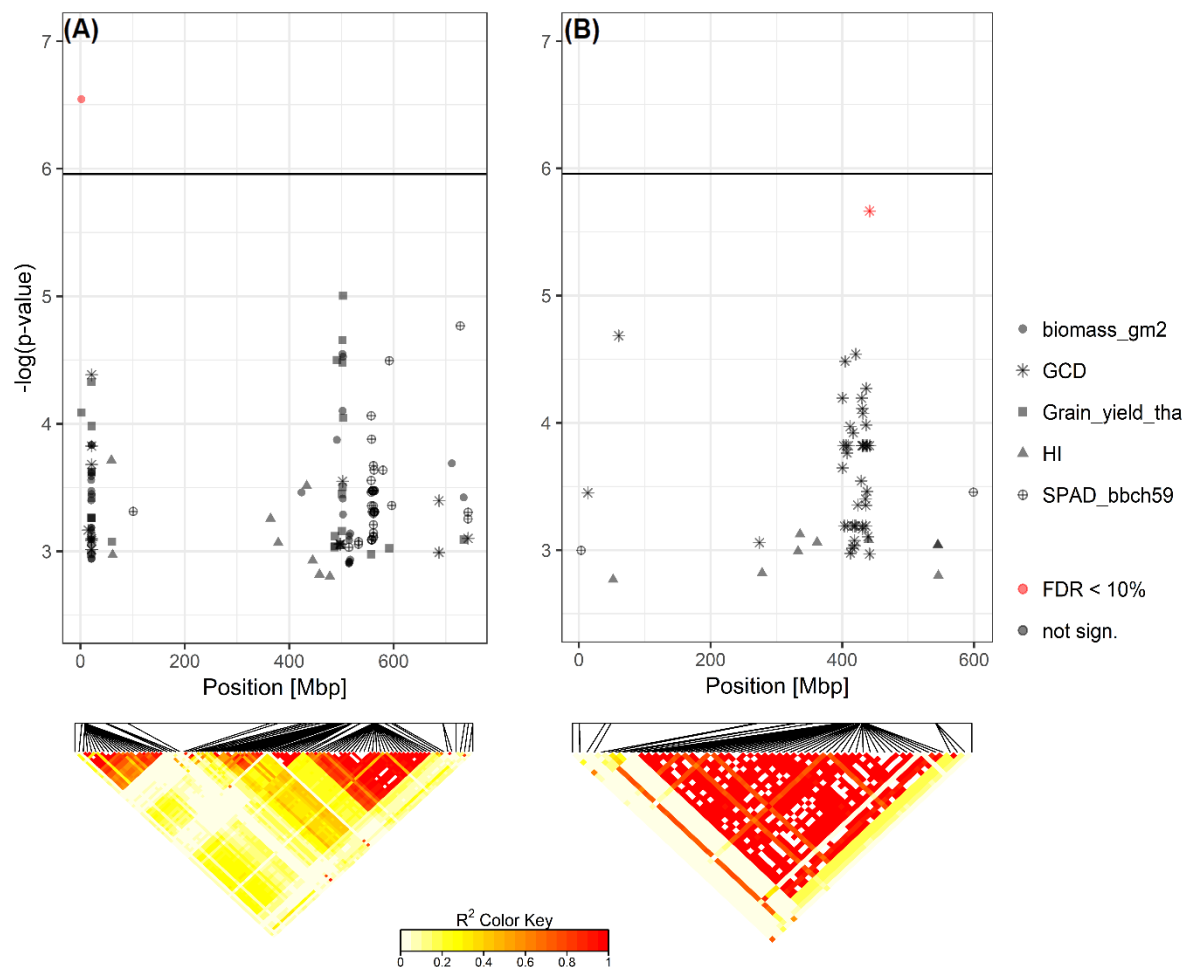


Figure 3.8: Heat maps of pairwise LD of the SNP-markers with significant marker-trait-associations for (A) biomass on chromosome 3A and (B) green canopy duration (GCD) on chromosome 6A . SNP-markers among the top 100 $-\log(p\text{-value})$ for each analyzed trait on these chromosomes are also shown.

Furthermore, a block of SNP-markers in high LD was observed 560 Mbp which were associated with SPAD at heading stage and at the same time grain yield or biomass (Fig. 3.8 A). On chromosome 6A we detected a block of SNP markers between 400 and 442 Mbp associated with GCD which were all in high LD ($r^2=0.84$ for SNP markers between 400 and 442 Mbp). Each of the minor alleles of the GCD associated markers on chromosome 6A had a negative effect on canopy longevity, and the explained phenotypic variance reached up to 22.5% (data not shown). Interestingly, neighbouring SNP markers associated with HI or SPAD, were not genetically linked to the GCD markers on this chromosome (Fig. 3.8 B). However, the effect of the associated SNP markers between 400 and 442 Mbp was not additive, as indicated in Figure 3.9. The mean value for cultivars carrying all 42 minor GCD alleles was not lower than the mean GCD values for cultivars carrying the minor GCD allele with the highest $\log(p\text{-value})$.

Furthermore, it could be shown that cultivars with no minor GCD allele were rather recently released and the cultivars carrying all minor GCD alleles with negative effects were on average older. This indicates a shift of the frequency of the GCD reducing alleles in that region during breeding history.

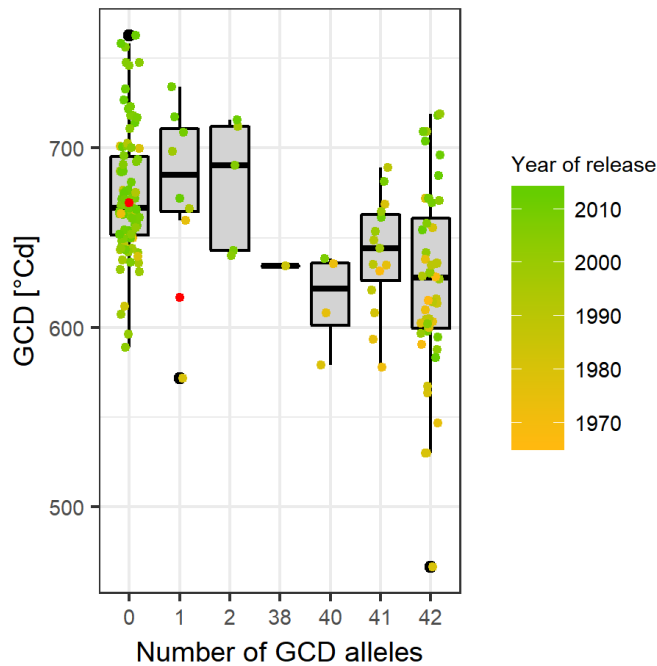


Figure 3.9: Green canopy duration (GCD) of cultivars in relation to their number of GCD alleles in the selected region between 400 and 441 Mbp on chromosome 6A. Point colors representing the year of release and grey points are the cultivars with unknown year of release. Red points indicate the mean GCD for cultivars carrying the major allele ($x=0$) or the minor allele ($x=1$).

DISCUSSION

Significant breeding progress in biomass, HI, grains per spike, SPAD and GCD

The present investigations revealed biomass, HI, grains per spike, SPAD values around anthesis and GCD as the most relevant traits for progress in German winter wheat breeding in the past five decades. The results are consistent with the findings showing an increased number of grains per spike in modern German cultivars (Würschum *et al.*, 2018). Several other studies also identified grains per spike as the trait with the closest relationship to yield progress in other regional cultivar collections (Brancourt-Hulmel *et al.*, 2003; Acreche *et al.*, 2008; Foulkes *et al.*, 2009; Sanchez-Garcia *et al.*, 2013). This implies that breeding progress has been achieved predominantly by increasing sink size. An important role of sink size was also suggested by studies indicating that HI (Brancourt-Hulmel *et al.*, 2003; Lo Valvo *et al.*, 2018) or TGW (Sadras and Lawson, 2011; Tian *et al.*, 2011; Aisawi *et al.*, 2015) were the main factors of yield increase. However, source characteristics like photosynthetic capacity or canopy longevity, the stay green traits, have also been associated with breeding progress (Fischer *et al.*, 1998; De Vita *et al.*, 2007; Tian *et al.*, 2011; Sanchez-Garcia *et al.*, 2015). The identification of different causal agents for yield progress can on the one hand be assigned to the origin of the cultivars in focus. The geographic pattern in genetic diversity has been demonstrated using 407 cultivars with European origin (Würschum *et al.*, 2018). Among the set of varieties, patterns of allele frequencies matched with the geographical origin of the cultivars. On the other hand, the investigation of the breeding progress is largely dependent on the variance of the cultivars' year of release in the collection. The studies, elaborating HI as most relevant for breeding progress included cultivars from prior to the Green Revolution (Brancourt-Hulmel *et al.*, 2003; Lo Valvo *et al.*, 2018).

Interestingly, the breeding progress in the present materials accelerated around 1996 especially for grains per spike and the SPAD values (Fig. 3.6 A - D and 3.7 A - C). Segmented regressions for grains per spike suggested breakpoints in 2003, 1996, 1996 and 1997 for the seasons 2015, 2016, 2017 and on average, respectively (data not shown). Breeding progress in the first phase was insignificant (or even negative) and steeply increased in the second phase. The slope of the sliding window plots after the breakpoint is more than double (on average: 0.4, $r^2=0.68$). This indicates that breeding progress in the number of grains per spike started from the middle of 1990s. Nonetheless, the goodness of fit (r^2 of the regression) improves only slightly with the segmented regression (data not shown). Possible candidates introducing the beneficial genetic materials are two cultivars outnumbering their contemporaries in grains per spike, *Flair* and *Dekan*, released in 1996 and 1999, respectively. The stepper increase could as well be attributed to a drop of the trait expression before the breakpoint.

Two cultivars with conspicuous constant low number of grains per spike were *Asketis* and *Aristos*, released 1997 and 1998, respectively. Interestingly, the steeper increase or drop in grains per spike, was not translated into the total grain yield. For *Asketis* and *Aristos* in fact a constantly higher TGW was observed in comparison to other cultivars released in 1997 and 1998, compensating for the reduced number of grains. For SPAD, the parallel development with grains per spike was apparent but the segmented regression did not better explain the breeding progress than the linear regression.

GCD and grain yield: correlation does not imply causation

An extended duration of the green leaf area was assumed to boost grain filling and therefore thousand grain weight (Foulkes *et al.*, 2009), but no relationship was observed between the TGW and the source components. So, our hypothesis was rejected. GCD and LAD did not correlate with TGW, but with biomass, HI, grains per m² and total grain yield. An alternative hypothesis could be that, prior to grain filling, at the time point when the number of grains is fixed, the potential longevity of the green canopy is also predetermined. To fill a higher number of grains, the available photosynthetic tissue had to be adjusted either in size, specific activity or duration. Apparently, an extended canopy life was the most appropriate adjustment in the selection process of German winter wheat breeding. Therefore, the effect of grains per spike on total grain yield was in parts mediated by the extended canopy longevity. Similarly, in the study of Liang *et al.*, 2018, the degree of senescence during grain filling was also negatively correlated to yield but not to thousand grain weight. The authors revealed that the photosynthesis at these stages is determined by the size of the carbon sink which is genetically predefined. The suggestion for wheat breeders was subsequently to select for higher grain number, which is likely to come along with a prolongation of the ability to fill the grains (Liang *et al.*, 2018). But besides leaf longevity, also the photosynthetic capacity is relevant for grain yield as shown here with the results of the SPAD measurements. Growth conditions around anthesis, the stage at which the final number of fertile florets is set, could directly be linked to the number of seeds and therefore grain yield.

Relevance of GCD for breeding

Grain number per spike is in detail determined by the number of spikelets per spike and the number of grains per spikelet, namely spikelet fertility. In-depth analyses of the spike and grain traits identified the spikelet fertility as the key driver of grain yield progress in wheat (Würschum *et al.*, 2018). It was further suggested that the trait was unintentionally selected during breeding progress of German winter wheat and therefore holds a high potential if breeders start to actively select (Würschum *et al.*, 2018). Our study presents GCD as a hidden mediator of yield potential.

It seems that canopy longevity was unintentionally increased by selection processes during the last 50 years of breeding history and therefore holds potential for further progress by targeted selection. Furthermore, GCD can be assessed easily and is suitable for large scale phenotyping.

To develop higher yielding varieties, selecting parental lines based on physiological characteristics for complementary crosses is one promising strategy. Additionally, it has been suggested to set a focus during the selection cycles on the yield components, because of higher heritabilities in comparison to yield itself (Falconer and Mackay, 2009; Schulthess *et al.*, 2017). Plant breeders might use the information about the drivers of the historical breeding progress as one criterion in their strategy to obtain further improved wheat varieties.

The persistence of the green canopy together with the photosynthetic capacity have been suggested as target traits in the process of improving the radiation use efficiency (RUE) by applying high-throughput phenotyping techniques. Aerial imaging is proposed as a promising strategy to estimate the canopy photosynthesis and thereby light utilisation on a spatial and temporal scale by multispectral-sensing. The advancement of these techniques will, together with genomics, facilitate a more efficient selection of source parameters and thereby accelerate progress in the final yield (Furbank *et al.*, 2019).

Genetic associations of GCD

Previous studies on the genetics of stay-green traits in winter wheat were exclusively designed to investigate genetic variation with experiments under different drought and heat stress conditions. A prolongation of the available photosynthetic tissue is known to facilitate yield formation under post-anthesis abiotic stress conditions without detrimental impact under non-stress conditions (Verma *et al.*, 2004; Vijayalakshmi *et al.*, 2010; Kumar *et al.*, 2010; Christopher *et al.*, 2014; Pinto *et al.*, 2016; Shi *et al.*, 2017; Christopher *et al.*, 2018). The present study, however, shows that GCD even has positive effects on yield under rainfed conditions and optimal crop management.

QTLs of GCD explained up to 22% of the phenotypic variance and at only one single location the SNP markers exceeded the significance threshold (chromosome 6A). Nevertheless, this dataset showed the progress of GCD during breeding history genetically, in parallel to previous findings demonstrating a shift in haplotype blocks with detrimental effects on stay-green through breeding (Voss-Fels *et al.*, 2019). The confirmation of the trait association with this genomic region proves the potential of the novel haplotype-based approach, where complete chromosomal segments instead of single markers are applied for the association analyses. The expected colocalization of significant association with source and sink traits could not be confirmed in the present study. SNP markers, significantly associated to sink or source traits, were not linked, indicated by a low LD.

To confirm the co-evolution genetically, the LD was expected to increase within the genomic regions of interest with the year of release. However, the average LD decrease instead. For the region on chromosome 6A (400 – 442 Mbp), the LD decreased from $r^2= 0.79$ within a cultivar group released before 1970 to $r^2= 0.68$ within a cultivar group released after 2010. The selection pressure against early senescing phenotypes possibly has favoured recombination in this particular region. Interestingly, within the other conspicuous regions on chromosome 3A, the LD did not change and also the complete LD per chromosome calculated based on all SNP markers on each chromosome did rather decrease with the year of release for nearly all chromosomes (except 1D, 3D and 4D) and was on average low (0.10 for cultivars release before 1970 and 0.07 for cultivars released after 2010).

To our knowledge, there are only two chromosomes, on which no one ever detected a significant marker trait association with a stay-green trait in wheat: 5D and 6D. All other 19 chromosomes have been mentioned to carry some genetic regions relevant for the stay-green trait expression but unfortunately, there is no chromosome, which was conspicuous in all genomic marker association reports. This indicates the great complexity of the trait. Regions on chromosomes 1B and 3B are most prominent as in summary four further groups of researchers detected relevant signals (Vijayalakshmi *et al.*, 2010; Kumar *et al.*, 2010; Naruoka *et al.*, 2012; Pinto *et al.*, 2016; Shi *et al.*, 2017; Christopher *et al.*, 2018). Contrary to the present work, the previous studies used solely mapping populations, consisting of double haploids (Verma *et al.*, 2004; Shi *et al.*, 2017; Christopher *et al.*, 2018) or recombinant inbred lines (Vijayalakshmi *et al.*, 2010; Kumar *et al.*, 2010; Naruoka *et al.*, 2012; Pinto *et al.*, 2016) which were all obtained from crosses of cultivars contrasting in the stay-green and senescence traits. The stay-green phenotypes were examined in many cases via measurements of the normalised difference vegetation index but also visual scorings or measurements of the chlorophyll content with the SPAD-502 meter are common. Most of the investigators fitted sigmoid curves to the data but with slightly different formulae so that and the estimated parameters were different. Either the integral, time points or durations were used for marker trait associations. Nevertheless, the studies hold potential to be of great use for marker assisted breeding, when the genetic map positions get synchronised on the physical reference map, as most previous studies published the genetic QTL position. Additionally, further work is needed to investigate possible underlying candidate genes and the allele frequency changes to further resolve patterns of selection and linkage. Nevertheless, the necessity to understand the genetic bases of source related traits was again emphasised in recent investigations on the sink strength, as the increase in spikelets per spike can only be translated into considerable higher yield, when the source is adapted concomitantly (Kuzay *et al.*, 2019).

CONCLUSION

The present study identified the photosynthetic activity around anthesis and the longevity of the green canopy as the relevant source traits ensuring the supply to the increased number of sink organs in the course of wheat breeding. The linkage between duration and capacity of the source and grain number suggests a predetermined longevity of green leaf area around anthesis when the grain number is fixed. Our results suggest placing emphasis on a balanced improvement of floret fertility and canopy longevity during the development of wheat cultivars. Furthermore, combining and selecting the most promising components of sink and source traits may further increase grain yield. The genome wide association study underpinned the association of breeding progress in canopy longevity. Further analyses of allele frequencies and associations with known genes involved in plant development will reveal in depth insights in the interdependencies of the yield relevant traits and whether the theory of unintentional selection can be confirmed.

CHAPTER 4

Genetic structures of physiological parameters relevant for yield formation and breeding progress in Germany

Carolin Lichthardt¹, Tsu-Wei Chen¹, Andreas Stahl², Kai P. Voss-Fels^{2,3}, HueyTyng Lee², Hartmut Stützel³

¹ Institute of Horticultural Production Systems, Leibniz University Hannover, Hannover, Germany

² Department of Plant Breeding, IFZ Research Centre for Biosystems, Land Use and Nutrition, Justus Liebig University, Giessen, Germany

³ Queensland Alliance for Agriculture and Food Innovation, The University of Queensland, St Lucia, Queensland, Australia

ABSTRACT

Physiological breeding is a promising strategy for the improvement of winter wheat. However, to completely understand the network of physiological traits relevant for yield formation and to ensure their applicability, it is also of crucial importance to investigate the genetic basis of these parameters.

A genome-wide association study (GWAS) was applied to a panel of 213 cultivars consisting of a set of lines representing the breeding progress of the last 50 years supplemented by a diversity set. The wheat lines were evaluated for 20 traits over 3 years of field trials under optimal conditions. The assessed traits are characterising the canopy architecture and function. Associations were estimated for each single marker of the 50,098 high-quality, polymorphic SNPs and additionally for chromosomal segments (haplotypes) which were designed based on the LD of neighbouring SNPs.

In total 213 highly significant associations were observed for single marker effects of which some were overlapping with high haplotype variances. Especially a region spanning over 40 Mbp on chromosome 6A was of great interest, as it associates with canopy height and also parameters describing the canopy architecture, persistence and thereby light interception. The results present important findings and can be applied in the network of genomic, phenomics and crop modelling to predict the performance of a specific ideotype.

Introduction

Intense phenotyping is of substantial importance in the context of physiological breeding and in combination with genomics and crop modelling, a prediction of the performance of ideotypes becomes achievable (Furbank *et al.*, 2019). Concrete quantitative trait loci (QTL) for physiological traits, the genotypic data, can be applied to improve functional plant models (Yin *et al.*, 2004). From the characteristics of a specific genotype in a categorised environment, the performance of the crop under environmental stress can be estimated (Hammer *et al.*, 2006; Chenu *et al.*, 2009).

The identification of significant genotype – phenotype associations for the relevant physiological traits is the first step to make this procedure possible. Furthermore, colocalizations of genotype – phenotype associations of different physiological traits could provide important findings regarding associations between traits (e.g. a co-evolution). A link can on the one hand be expected if traits physiologically depend on each other, like sink and source traits. On the other hand, an association could also be detected, if antagonists are genetically linked and detrimental characteristics of breeding lines are unintentionally selected e.g. the negative effect of the dwarf gene *Rht-D1b* on flowering traits relevant for hybrid seed production (Boeven *et al.*, 2016). We assume that such interdependencies are visible on the genome and relevant loci are inherited together

We applied a genome wide association study (GWAS) to detect single marker – trait associations and supplemented the analyses with the investigations of the variances of local genomic estimated breeding values (local GEBVs) calculated for haploblocks. The collection of the 213 winter wheat cultivars (described in detail in chapter 2 and 3 and in Voss-Fels *et al.*, 2019) allow to related selection processes during the last 50 years of breeding to developments on the genome scale, because the collection included a subset of cultivars representing the breeding progress.

Material and methods

Plant material and experimental conditions

The analyses were performed with 213 winter wheat lines, of which 185 lines were released in Europe between 1966 and 2013 and were selected based on their relevance in the German wheat market. The 28 additional lines were randomly selected diverse breeding lines (not released in Germany) from the German gene bank (Table S2.1). Field experiments were conducted in 2015, 2016 and 2017 at the research station in Ruthe near Hannover in Northwest Germany. Please find detailed descriptions of the experimental conditions in chapter 2 and 3.

Parameters for genetic association

The genome-wide association was performed based on 20 traits, among which 14 parameters represent source related traits and physiological canopy characteristics (Table 4.1, described in detail in chapter 1, summarised in Table 2.1) and 6 parameters comprised yield and yield components.

Table 4.1: List of the 20 traits used for the genetic associations.

Symbol	Parameter
BBCH59	Heading date
GCD	Green canopy duration
\widehat{gLAI}_{int}	Green LAI integral
\widehat{gLAI}_{dur}	Green LAI duration
\widehat{gLAI}_{mean}	Mean GLAI
\widehat{gLAI}_{BBCH59}	Green LAI at BBCH59
SPAD _{BBCH59}	SPAD close to BBCH59
\widehat{gl}_{int}	Relative light interception integral
\widehat{gl}_{dur}	Duration of relative light interception
\widehat{gl}_{mean}	Mean relative light interception
iPAR _{gf}	Intercepted radiation
RUE _{gf}	Radiation use efficiency
k	Extinction coefficient
height	Canopy height
	Biomass
	Grain yield
HI	Harvest index
	Spike number
	Grains per spike
TGW	Thousand grain weight

A mixed model representing the experimental design was applied to estimate the adjusted means (best linear unbiased estimators, BLUE) across the three experimental seasons and two field replications. We applied the following statistical model:

$$P_{ijkl} = \mu + c_i + y_j + cy_{ij} + YR_{jk} + YRG_{jkl} + e_{ijkl} \quad (1)$$

where P_{ijkl} was the phenotypic observation of the i^{th} cultivar (i = cultivar number 1 – 213, factorial) in the j^{th} year (j = 2015, 2016 and 2017, factorial) in the k^{th} complete replication and l^{th} incomplete sub-group (l = early and short; early and long late and short; late and short). The model was used to estimate adjusted means for each cultivar with lower case letters indicating fixed factors (cultivar and year) and capital letters indicating random effects (replication, and group). The observation was dissected into the general mean, μ , the genetic effect of the i^{th} cultivar, c_i , the effect of the j^{th} year, y_j , the interaction between the cultivar and the year, cy_{ij} , the interaction of the year and the replication YR_{jk} , the interaction of the year, replication and sub-group, YRG_{jkl} and the residual e_{ijkl} . The model was fit to the data with the lmer function of the lme4 package in the R environment (Bates *et al.*, 2015).

Genotyping

DNA samples extracted from leaves were genotyped with the 15K Illumina Infinium iSelect genotyping array with 13,006 single nucleotide polymorphism (SNP) - markers and with the 135K Affymetrix TGWEXCAP Array carrying a total of 136,780 SNP markers (TraitGenetics, Gatersleben, Germany). To anchor the SNP markers to physical positions, both SNP subsets were aligned to the *T.aestivum* genome (IWGSC release iwgsc_refseqv1.0 assembly soft-masked version (IWGSC, 2018) using BLASTN 2.2.31 (Camacho *et al.*, 2009). Markers were excluded if their SNP probe sequence could not be aligned with high stringency to a unique physical position on the reference sequence (E-value $\leq 10^{-5}$). The results were filtered with the following criteria 1) uniquely mapped 2) no gap, and 3) minimum 1 base mismatch. By that we obtained a total of 5,486 anchored SNP markers and 92,464 anchored SNP markers from the 15K SNP chip and the 135K SNP chip, respectively.

Because the SNP markers were mapped on the same reference genome, we were able to merge the two data sets. After quality control by filtering monomorphic markers with > 10% missing values or a minor allele frequency < 5%, a complete selection of 50,098 high-quality, polymorphic SNPs remained in the data set for further analyses.

Genome wide association with single markers

The allelic associations of single SNP markers were calculated for genotypic trait values (BLUE) with the polygenic function in the R package genABEL by implementing the population structure (detailed description in chapter 3) and the genome-wide kinship matrix (Aulchenko et al., 2007). The Bonferroni method (threshold= $-\log_{10}\left(\frac{0.05}{\text{number of SNP markers}}\right)$) and the false discovery rate (FDR 10%) were considered as thresholds for significant marker-trait-associations.

Genome wide association with chromosomal segments

Genome-wide SNP markers were additionally assigned to blocks (haplotypes) by grouping them based on the linkage disequilibrium (LD). The minimum LD for SNP markers to be assigned to the same block was $r^2= 0.7$ and SNPs that were not in high LD with any other marker were assigned to an individual block. Within a block, the marker effects were summed and the variances were estimated for each haplotypes.

For a detailed description of this novel method please see Voss-Fels *et al.*, 2019.

In this study, we investigated potential overlapping of significant single marker associations and high-ranking variances of haplotype – trait – associations.

Results

Single marker – trait association

The associations of marker or haploblocks and traits were calculated using BLUE values calculated over three growing seasons and two replications each. For the associations of single markers and traits, the significant threshold of 6.00085 for the $-\log(p\text{-values})$ and $FDR < 10\%$ was defined. In total 213 associations distributed over all 21 chromosomes met either one of the criteria and were therefore considered as significant (Table S4.1). Chromosomes 3A, 4B, and 6A were most prominent with 22, 22 and 21 associations, respectively. Most associations were detected for the parameter canopy height but also for heading date, many associations were detected on nearly all chromosomes (Table 4.2).

Table 4.2: Summary of significant marker-trait associations, in parentheses: number of associations per chromosome.

Trait	Number of significant marker – trait associations	Chromosomes
BBCH59	33	1B (3), 2A (1), 2B (2), 2D (1), 3A (1), 3B (1), 3D (3), 4A (2), 4B (2), 5B (1), 5D (6), 6A (5), 6B (2), 6D (1), 7B (1), 7D (1)
GCD	1	6A
\hat{g}_{int}	13	3A (6), 4B (7)
\hat{g}_{dur}	1	4B
\hat{g}_{mean}	10	3A (3), 4A (2), 4B (4), 5A (1)
iPAR _{gf}	9	3A (3), 4B (6)
RUE _{gf}	4	5B (1), 5D (3)
Height	136	1A (7), 1B (4), 1D (7), 2A (8), 2B (11), 2D (6), 3A (8), 3B (15), 3D (2), 4B (1), 4D (7), 5A (2), 5B (17), 5D (5), 6A (15), 6B (2), 6D (2), 7A (6), 7B (10), 7D (1) all chromosomes except 4A
Total Biomass	1	3A
Grain yield	4	4D
TGW	1	4B

Multi-trait associations (more than one marker – trait association for the same SNP marker) were detected for three SNP markers on chromosome 3A, for six markers on chromosome 4B and one marker on chromosome 4D (Table 4.3).

Table 4.3: Multi-trait associations of single marker effects.

Chr	Position [Mbp]	Trait	log(p-value)	FDR	Minor allele effect
3A	21.37711	iPAR _{gf}	5.517	2.4%	-10.431
		\hat{g}_{int}	5.271	5.4%	-19.008
3A	21.37866	\hat{g}_{int}	4.936	7.3%	-18.446
		iPAR _{gf}	5.341	2.5%	-10.308
3A	21.40877	\hat{g}_{int}	5.007	7%	-19.247
		iPAR _{gf}	5.363	2.5%	-10.706
4B	654.44033	\hat{g}_{mean}	6.249	2.8%	-0.017
		iPAR _{gf}	6.141	1.6%	-13.528
		\hat{g}_{int}	5.778	2.8%	-24.379
4B	654.73540	\hat{g}_{mean}	5.22	6%	-0.017
		iPAR _{gf}	5.648	2.3%	-13.945
		\hat{g}_{int}	4.83	8.2%	-23.779
4B	654.89793	iPAR _{gf}	5.483	2.4%	-12.858
		\hat{g}_{mean}	5.118	6.4%	-0.015
		\hat{g}_{int}	5.162	5.8%	-23.199
4B	655.41128	iPAR _{gf}	5.647	2.3%	-12.36
		\hat{g}_{mean}	5.605	4.4%	-0.015
		\hat{g}_{int}	5.357	5.4%	-22.402
4B	656.16086	iPAR _{gf}	6.025	1.6%	-12.298
		\hat{g}_{int}	5.969	2.7%	-22.855
4B	656.28706	\hat{g}_{dur}	6.053	4.4%	-21.17
		\hat{g}_{int}	7.189	0.3%	-25.295
		iPAR _{gf}	7.105	0.4%	-13.476
4D	18.78107	Height	5.945	2.8%	0.281
		Grain yield	5.616	0.3%	-2.854

These results indicate that the parameters relative light interception integral, duration and the mean are affected by the same alleles as the absolute light interception. Hotspots for the light interception can be found on chromosome 3A and 4B, as the diagnostic SNP markers are clustered within 0.03 Mbp and 1.85 Mbp, respectively. It is conspicuous, that the minor allele effect is negative for all the traits listed here except height, indicating that the minor allele had detrimental effects and as the traits were improved with breeding (see chapter 1 and chapter 2), the selection acted against the minor allele. Co-localisations of marker-trait associations of different traits (markers less than 1 Mbp apart) were detected for BBCH59 and height on chromosome 2A, 5B and 6A, but no expected co-localisation of sink and source traits was observed. However, the value of a co-localisations of marker-trait associations depends on the linkage disequilibrium between the markers. Therefore, the associations were additionally calculated for haplotypes (blocks of markers in high LD).

Haplotype – trait association

A total number of 20 174 blocks were constructed with a maximum number of 188 SNP markers assigned to one block (chromosome 5B, 497.003841 - 518.958307 Mbp). However, more than 80%, 16 782 blocks, contained only one or two SNP markers. Indicating that the majority of the SNP markers were in low LD (< 0.7) with their neighbouring markers in this population of wheat lines.

The applied method was inherited from a classical genomic prediction method and the initial step to estimate the association of haplotypes and traits is the estimation of local genomic estimated breeding values (GEBVs). Different combinations of the SNP marker alleles within a block form the haplotypes for each block. The effect of each marker in a block on a trait is summed up per haplotype and thereby a combined effect of the interacting alleles on a trait was estimated. The variance among these haplotype effects per block, the local GEBV variance, can therefore be interpreted as the strength of the haplotype effect on the trait.

We considered the top 10 local GEBV variances as relevant associations for further investigations. The complete list of the top 10 associations can be found in table S4.2. Interestingly, multi-trait associations were detected for 35 blocks with high variance (among top 10) in two or more traits (table 4.4).

Table 4.4: Multi-trait associations of local GEBV variances.

Chr	Block	Start [Mbp]	End [Mbp]	Traits
2A	b003531	73.16408	75.653161	HI, TGW, Grains per spike, Height
2A	b003615	192.193574	214.450827	TGW, Spike number
2A	b003637	313.300127	384.680041	TGW, Spike number, Grains per spike
2A	b003700	520.562826	530.221481	Grains per spike, RUEgf
2A	b003701	530.745151	549.136394	Grain yield, HI, TGW, Grains per spike, BBCH59, GCD, gLAI_dur, SPAD_BBCH59, gl_mean, RUEgf, Height
2A	b003707	554.509185	562.104411	TGW, Grains per spike, gLAI_int, gLAI_mean, gLAI_BBCH59
2A	b003708	562.455937	582.640558	TGW, Grains per spike, BBCH59, GCD
3A	b007063	557.257246	566.868118	Grain yield, HI, SPAD_BBCH59, gl_mean
3B	b007962	103.034742	114.10418	Spike number, BBCH59
4A	b009735	101.510451	120.605007	Grain yield, Biomass, Height
4B	b010704	59.234305	66.811857	Grain yield, Biomass, gLAI_int, SPAD_BBCH59, RUEgf
4B	b010740	95.85825	106.824437	Grain yield, Biomass, Grains per spike, gLAI_mean, gLAI_BBCH59, RUEgf, Height
4B	b010843	409.345161	420.093011	gLAI_mean, gLAI_BBCH59, gl_int, gl_mean, iPAR, RUEgf
5A	b011539	46.674914	51.604533	Grain yield, Spike number

5A	b011540	51.676254	67.320171	Biomass, Spike number, gLAI_int, gLAI_mean, gLAI_BBCH59, RUEgf
5A	b011553	98.037448	109.943112	HI, BBCH59, gLAI_BBCH59
5A	b011928	503.796316	510.162213	Spike number, Height
5A	b012501	702.873159	706.442737	HI, Spike number, BBCH59, GCD, gLAI_dur, gl_int, gl_dur, gl_mean, iPAR
5B	b012901	383.035659	394.023386	gLAI_dur, gl_int, gl_dur, gl_mean, iPAR
5B	b013045	497.003841	518.958307	Grain yield, Biomass, Spike number, Grains per spike, GCD, gLAI_dur, gl_dur, RUEgf, k, Height
5D	b013977	43.409508	46.318871	Grain yield, HI, SPAD_BBCH59, RUEgf, Height
6A	b014704	29.229698	33.538666	Biomass, BBCH59
6A	b014797	65.855849	72.844592	HI, Spike number, BBCH59, k
6A	b014823	92.347663	99.40941	GCD, gLAI_int, gLAI_dur, SPAD_BBCH59, gl_dur, k, Height
6A	b014828	102.15334	115.462302	Biomass, GCD, gLAI_int, gLAI_dur, gl_int, gl_dur, iPAR, RUEgf, k
6A	b014914	400.248016	417.39771	GCD, gLAI_dur, gl_int, gl_dur, iPAR, k, Height
6A	b014917	417.638448	441.806842	Grain yield, Biomass, HI, TGW, BBCH59, GCD, gLAI_int, gLAI_dur, gLAI_mean, gLAI_BBCH59, gl_int, gl_dur, iPAR, k, Height
6B	b016267	634.315361	640.129615	gLAI_int, gLAI_mean, gLAI_BBCH59, gl_int, gl_mean, iPAR, k
7A	b017655	129.867965	148.012193	Biomass, TGW, SPAD_BBCH59
7A	b017697	224.314704	238.829041	HI, TGW, BBCH59, gLAI_int, gLAI_mean, gLAI_BBCH59, gl_mean, k
7A	b017759	485.610481	497.740992	TGW, Spike number
7A	b018188	663.958958	669.029287	Grain yield, Biomass, GCD, gLAI_dur, SPAD_BBCH59, gl_int, gl_dur, gl_mean, iPAR
7A	b018219	672.258666	674.020659	gl_mean, iPAR
7B	b018804	181.036029	199.180188	gLAI_mean, gLAI_BBCH59, gl_int, gl_dur, k
7B	b018915	552.780293	564.173696	GCD, gLAI_int, gLAI_mean, gLAI_BBCH59, gl_int, gl_dur, iPAR

Here, we also detect overlapping associations of sink and source traits, e.g. for RUEgf and grains per spike on chromosome 2A. However, only few of them (b014823, b014914 and b014917 on chromosome 6A) additionally overlap with significant association of single marker effects estimated in the GWAS. Interestingly, the variance of the local GEBVs of light interception parameters was not among the top 10 for the genomic region in chromosome 4B, where the cluster of single marker – trait associations was observed. Obviously, the relevant SNP markers were not in high LD.

For the conspicuous regions on chromosome 6A, additional plots were prepared to visualise the overlapping associations of the two methods (Fig. 4.1). The two neighbouring blocks between 400.2 and 441.8 Mbp show high variances for local GEBVs of numerous traits. Interestingly, the region seems to have relevance for canopy height, canopy architecture (k), canopy duration (GCD) and light interception and not radiation utilisation (RUE) and the local GEBV variances of that block for yield, biomass, HI and the yield component TGW ranked among the top 10. This indicates, that potential underlying genes have an influence on physiological parameters affecting light interception and thereby yield components.

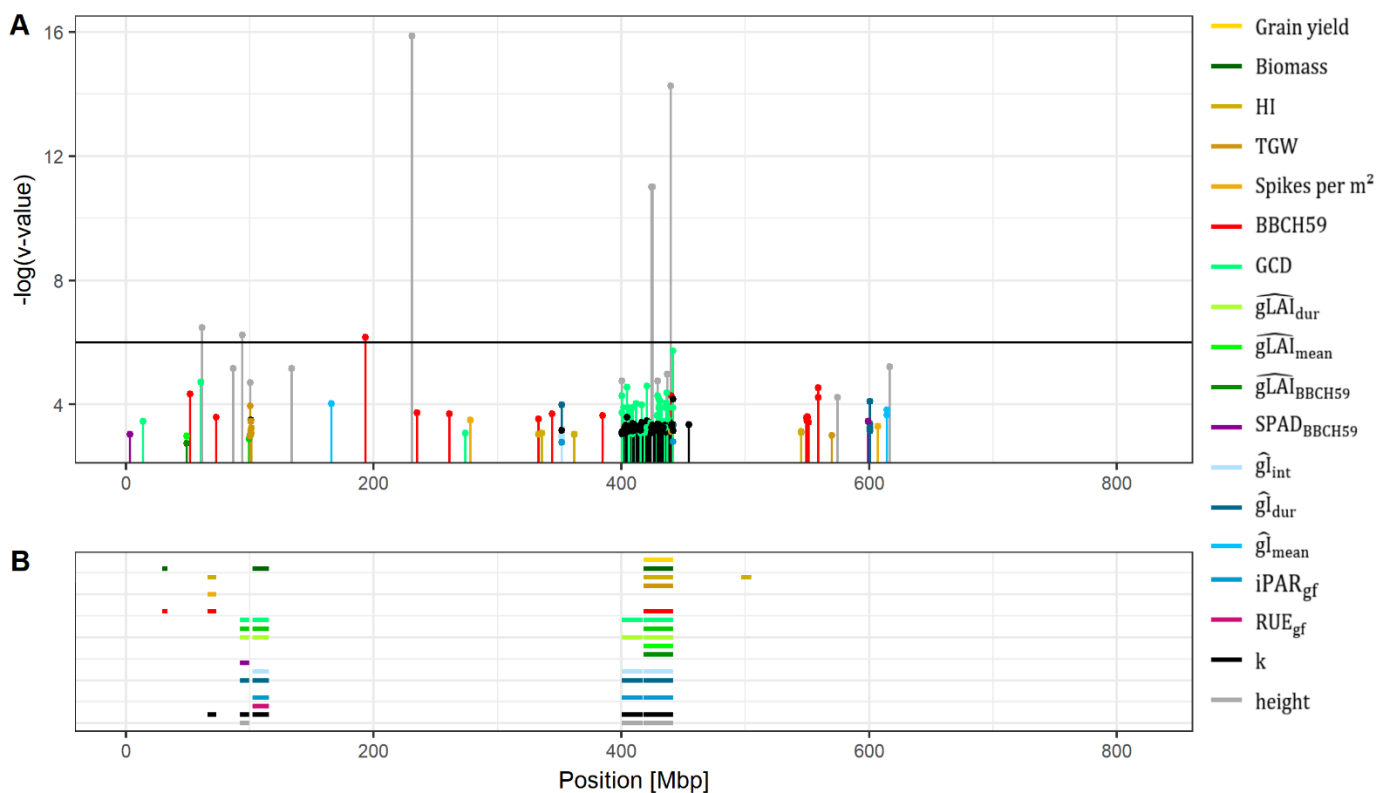


Figure 4.1: Single marker – trait associations on chromosome 6A (A) and overlapping LD blocks (B). A bar indicates that for the trait the local GEBV variance is among the top 10.

Discussion and conclusion

For physiological breeding, the detailed investigation of the genetic constitution is of great importance. On the one hand, physiological dependencies can be examined and on the other hand the gained knowledge has the potential to guide ideotype development (Furbank *et al.*, 2019). Within the present study we identified a high number of significant associations of single markers. However, of the 213 significant associations, only 45 exceeded the Bonferroni threshold of which 34 associations were for the canopy height. In wheat, the canopy height and its genetic basis in terms of dwarfing (*Rht*-) genes and QTL for plant height, is a widely studied parameter as the reduction of height is associated with an increase in yield (Tian *et al.*, 2017; Würschum *et al.*, 2018). Two homoeoloci *Rht-B1* and *Rht-D1* are extensively used in wheat breeding and have been assigned to the chromosomes 4B and 4D. Also here, we find associations on those two chromosomes for canopy height. More interestingly, the associations with canopy height with the highest significance were detected on chromosome 6A between 400 and 450 Mbp, a region which has just recently been assigned to a novel *Rht* – gene, *Rht24*. Our findings prove the relevance of chromosome 6A for height reduction in winter wheat, as we identified the same relevant genetic regions as previously published (Würschum *et al.*, 2018, compare figure S2). Additionally, we were able to show here, that the specific locus between 400 and 441 Mbp on chromosome 6A not only had a relevance for canopy height but also canopy architecture and persistence and therefore light interception. Further in-depth investigations are necessary to unravel possible known genes in that target region.

The present study further identified regions on chromosome 3A and 4B as relevant for light interception. Interestingly, highly significant single-marker associations were detected for several neighbouring SNP markers, but the analyses of the haplotype associations did not show high local GEBV variances for that specific region. As the effect of the minor alleles was generally negative, a selection against the minor alleles was presumed and thereby a possible reduction in the LD, which would explain the absence of the LD block. A detailed investigation of the LD pattern in that region would underpin that assumption. However, also an overall investigation of the LD among the investigated markers might improve the applied method of haplotype associations. The relatively low number of blocks with three or more markers (only 20%) indicates, that the threshold $LD > 0.7$ for markers to be assigned to a group might be too high for this population of wheat lines. Additionally, the investigations of shifts in the allele frequencies during breeding history with a sliding window approach would shed light in the parallel development of the physiological constitution of the cultivars and the genetic setup.

CHAPTER 5

Discussion and future recommendations

Wir würden unser Wissen nicht für Stückwerk erklären, wenn wir nicht einen Begriff von einem Ganzen hätten.

Johann Wolfgang von Goethe (1749 – 1832)

Discussion and future recommendations

The progress in yield and the development of high-yielding and resilient new cultivars is of great importance (Ray et al. 2013). Breeding progress has to be shifted to the next level, from an annual gain of less than 1% to an increase of 2.4% per year to meet the future global demands of the growing population (Hawkesford et al. 2013; Ray et al. 2013). Physiological breeding has been proposed as one promising strategy to facilitate the steep progress and at the same time secure a suitability of cultivars to future climatic conditions (Furbank et al. 2019). The physiological perspective on yield formation enables a target-oriented breeding of lines suitable to specific growing conditions (Reynolds et al., 2017).

The previous chapters present valuable results and insights into the initial steps of physiological breeding by analysing interdependencies and the breeding progress of canopy related physiological traits. Chapter 2 and 3 identified concrete physiological traits relevant for yield formation by focusing on especially the light interception and utilization (chapter 2) or the interdependencies between sinks and sources of yield (chapter 3). To my knowledge, this is the first study, naming concrete causal agents relevant for light interception and utilization in the grain filling phase of wheat. The results indicate that the SPAD measurements and the green canopy duration are the source parameters most relevant for yield formation. Furthermore, the data suggests that the concrete interface of the assimilate-producing parameters and the yield components can be assigned to the growth phase relevant for grain number per spike and a parallel breeding progress of the pair of sinks and sources was discovered. The genetic analyses revealed significant associations of the physiological traits relevant for yield formation. The region on the genome, where we identified a significant association with canopy duration also showed relevance for plant, canopy architecture and light interception.

The present study provides valuable results facilitating a mechanistic approach of breeding for which physiological traits play an important role (Furbank et al. 2019). Considering the trait network relevant for the production of total biomass, especially light interception and utilization, the results suggest that an extended persistence of the canopy and the photosynthetic constitution around anthesis have a positive effect. A strategic combination of certain traits leads to an accumulation of complementary alleles (Reynolds et al., 2017) and we suggest that the canopy duration and the photosynthetic constitution around anthesis should gain relevance in the selection process.

The usability of especially the SPAD meter and alternative measurements of the leaf reflectance properties are discussed in detail in chapter 2. Besides an efficient light utilization, a high SPAD value (and thereby photosynthetic activity) certainly indicates an efficient nitrogen utilization (Sinclair et al. 2019). However, genetic differences in uptake and utilization of nitrogen could have an effect on the greenness of leaves and their persistence during grain filling (Noulas et al. 2018; Nguyen et al. 2016). This means that when selecting for high SPAD values around anthesis and an extended canopy duration, one would actually select for an increased nitrogen use efficiency (Sinclair und Jamieson 2006). In the field trial underlying this thesis, the plots were treated with optimal nitrogen supply, so no limitation can be expected. Future investigations regarding this topic should inspect the carbon and nitrogen fluxes to completely understand the dependencies. Analysing for instances water soluble carbohydrates and nitrogen in the stem would additionally provide in depth insight into the sink–source dependency.

The detailed analyses of the results separately for each of the experimental seasons demonstrate the great plasticity of the wheat cultivars in their ability to react to environmental conditions. Thereby, also the canopy architecture parameters assessed by the extinction coefficient appeared as relevant for light interception. The canopy architecture solely showed relevance for yield formation in one of the seasons and only little relevance was assigned to it in the overall network of the parameters analysed in the structural equation model. However, we expected a greater differentiation of the architectural parameter and thereby a greater importance for light interception, biomass production and yield as for instances recently proven by Richards et al. 2019. The measurements of light interception and leaf area index to calculate the extinction coefficient as the measure for the canopy architecture might not be as suitable as expected. The low heritability indicates a poor quality, whereas a visual scoring of the canopy architecture showed a heritability of around 90% in Richards et al. 2019. Besides the measurement technique, another impairing factor was the too little variation within the assessed population of wheat cultivars as the comparable study investigated a segregating breeding population. For future investigations, visual scoring should at least supplement the measurements of the light extinction coefficient. Another possibility to overcome the high environmental variance of the extinction coefficient is to expand the structural equation modelling. The mathematical approach could be further improved by introducing environmental conditions as exogenous variables into the model or by adding latent variables to specify an individual error (Lamb et al. 2011).

Genome wide association studies revealed numerous significant associations of traits with single markers or blocks of markers. Overlapping associations on chromosome 6A for canopy duration, plant height, the extinction coefficient and yield highlighted a valuable locus for future breeding. Especially for hybrid breeding, new sources of plant height reduction are of great interest, as the commonly used dwarf gene have negative effects on the anther extrusion (Boeven et al. 2016).

The final aim of the thesis is to identify physiological breeding innovations suitable to facilitate the future development of high yielding and resilient cultivars. It has been suggested that the combination of physiological breeding and crop modelling has a great potential (Furbank et al. 2019; Wang et al. 2019). However, the present findings need to be optimized to use them directly for that purpose. First of all, modelling is usually based on the complete growth phase (Wang et al. 2019), however, in this study only the grain filling phase was investigated. Thus, it is challenging to accurately predict growth and development before anthesis. Furthermore, environmental-independent data is needed for the implementation of genetic information in a modelling approach to predict the performance of a hypothetical genotype in a hypothetical environment (Wang et al. 2019, Cooper et al. 2016). The data could be produced by testing the genotypes under controlled conditions, to quantify the effect of a QTL in dependency of specific environmental characteristics. Generally, the targeted development of new cultivars in terms of ideotypes for specific environment must be a great success as it has been shown in retrospective, that the regional adaptation can be mirrored on the genome scale and in the physiological relevance for yield (Würschum et al. 2018).

In conclusion, the present study presents a complex evaluation of innovations in breeding winter wheat and the greenness of the canopy around anthesis and the persistence of the canopy were identified as valuable traits within the interdependencies between the canopy structure and yield. Genetic regions relevant for the breeding innovations have been identified. The results present important findings which can be applied in the network of genomic, phenomics and crop modelling. A co-evolution of source and sink strength during the breeding history contribute to the yield formation of the modern cultivars. As the investigated parameters can be estimated by remote sensing using for instance reflectance data from aerial imaging or multispectral sensors, the investigations provide a new avenue for the application of high-throughput phenotyping within breeding. For future breeding we suggest to choose parental lines with high grain numbers per spike on the sink side, and high photosynthetic activity around anthesis and canopy duration on the source side, and to place emphasis on these traits throughout selection. If at the same time breeder care for the degree of genetic variation in the germplasm, the physiological plasticity should be ensured and therefore facilitate stability in yield.

SUPPLEMENTARY MATERIAL

Table S2.1: Complete list of cultivars, Bh= breeding history collection, Div= diversity collection, Hyb= hybrid cultivar, org= cultivars with recommendation for use in organic farming, europ.reg= cultivars registered in other European countries, *= lines in the genome wide association study. The double bar indicates the distinction between cultivars used for breeding history analyses in chapter 2 and the diversity set.

Cultivar name	Year of reg.	Breeder	Quality class	Country of registration	sub-group (field)	sub-set (analyses)	
Diplomat	1966	Firlbeck	A	DE	late, tall	Bh	*
Pantus	1966	Streng	A	DE	late, short	Bh	*
Admiral	1968	Firlbeck	A	DE	late, tall	Bh	*
Caribo	1968	Heidenreich und Eger	B	DE	late, tall	Bh	*
Progress	1969	Hege, H.-U.	A	DE	late, short	Bh	*
Kranich	1969	Lochow-Petkus	A	DE	late, short	Bh	*
Joss	1972	Breustedt	C	DE	late, short	Bh	*
Topfit	1972	Strube, Dr. H.	B	DE	late, tall	Bh	*
Benno	1973	Bauer, G.	E	DE	late, tall	Bh	*
Kormoran	1973	Lochow-Petkus	A	DE	late, tall	Bh	*
Saturn	1973	MPI	C	DE	late, short	Bh	*
Disponent	1975	Bayrische Saatzuchtgesellschaft	A	DE	late, tall	Bh	*
Monopol	1975	Firlbeck	E	DE	late, tall	Bh	*
Nimbus	1975	Firlbeck	B	DE	early, short	Bh	*
Vuka	1975	Franck	A	DE	late, tall	Bh	*
Carimulti	1975	Heidenreich und Eger	C	DE	late, tall	Bh	*
Carisuper	1975	Heidenreich und Eger	A	DE	late, tall	Bh	*
Maris Huntsman	1975	Nordsaat Saatzucht	A	DE	late, short	Bh	*
Götz	1978	Bayrische Saatzuchtgesellschaft	B	DE	late, short	Bh	*
Kobold	1978	Firlbeck	B	DE	late, tall	Bh	*
Aquila	1979	Nickerson	C	UK, IT	late, tall	Bh	*
Tabor	1979	Strube, Dr. H.	A	DE	late, short	Bh	*
Camp Remy	1980	Unisigma	B	DE	early, short	Bh	*
Severin	1980	Bauer, G.	E	DE	late, short	Bh	*
Urban	1980	Bauer, G.	E	DE	late, short	Bh	*
Kronjuwel	1980	Bayrische Saatzuchtgesellschaft	B	DE	late, short	Bh	*
Rektor	1980	Firlbeck	E	DE	late, tall	Bh	*
Basalt	1980	Hege, H.-U.	B	DE	late, tall	Bh	*
Kanzler	1980	Saatzucht Engelen Büchling e.K.	B	DE	late, tall	Bh	*
Oberst	1980	Saatzucht Engelen Büchling e.K.	A	DE	late, tall	Bh	*
Granada	1980	Saatzucht Schweiger GbR	B	DE	late, short	Bh	*
Sperber	1982	Lochow-Petkus	A	DE	late, short	Bh	*
Kraka	1982	Petersen, A.S.	A	DE	late, tall	Bh	*
Ares	1983	Strube, Dr. H.	B	DE	late, tall	Bh	*
Apollo	1984	Saatzucht Josef Breun	C	DE	late, tall	Bh	*
Knirps	1985	Semundo	B	DE	late, tall	Bh	*
Sorbas	1985	Strube, Dr. H.	B	DE	late, short	Bh	*
Herzog	1986	Saatzucht Josef Breun	A	DE	late, short	Bh	*
Alidos	1987	Saatzucht Hadmersleben	E	DE	late, tall	Bh	*
Obelisk	1987	Strube, Dr. H.	B	NL, DE	late, short	Bh	*
Orestis	1988	Strube, Dr. H.	B	DE	late, short	Bh	*
Greif	1989	Lochow-Petkus	B	DE	late, short	Bh	*
Zentos	1989	Saatzucht Hadmersleben	E	DE	late, tall	Bh	*
Astron	1989	Strube, Dr. H.	A	DE	late, tall	Bh	*
Kontrast	1990	Saatzucht Hadmersleben	A	DE	early, short	Bh	*
Contra	1990	Saatzucht Josef Breun	C	DE	late, short	Bh	*
Toronto	1990	Strengs Erben	A	DE	late, short	Bh	*
Konsul	1990	SW Seeds	B	DE	late, tall	Bh	*
Ibis	1991	Lochow-Petkus	A	DE	late, tall	Bh	*
Tarso	1992	Saatzucht Hadmersleben	A	DE	late, short	Bh	*
Aron	1992	Semundo	E	DE	late, tall	Bh	*
Ritmo	1993	Cebeco	B	DE	late, short	Bh	*
Tambor	1993	Semundo	A	DE	late, tall	Bh	*
Piko	1994	Nordsaat Saatzucht	B	DE	early, short	Bh	*
Transit	1994	Saatzucht Josef Breun	A	DE	late, short	Bh	*

Pegassos	1994	Strube, Dr. H.	A	AT, CH, DE, LT, PL, SI, SK	early, short	Bh	*
Isengrain	1996	Florimond-Desprez	B	FR, SI, ES	early, short	Bh	*
Flair	1996	Saatzucht Schweiger GbR	B	DE	late, short	Bh	*
Apache	1997	Nickerson	A	CZ	early, short	Bh	*
Aristos	1997	Strube, Dr. H.	A	DE	late, tall	Bh	*
Ludwig	1998	Franck	A	DE	late, tall	Bh	*
Cardos	1998	Saatzucht Hadmersleben	A	DE	early, short	Bh	*
Asketis	1998	Strube, Dr. H.	A	DE	late, tall	Bh	*
Dekan	1999	Lochow-Petkus	B	DE	late, short	Bh	*
Drifter	1999	Nickerson	B	DE	late, short	Bh	*
Skater	2000	Limagrain GmbH	B	DE	late, short	Bh	*
Biscay	2000	Lochow-Petkus	C	DE	late, short	Bh	*
Magnus	2000	Saatzucht Engelen Büchling e.K.	A	DE	late, tall	Bh	*
Altos	2000	Syngenta Seeds GmbH	E	DE	late, short	Bh	*
Terrier	2001	Nickerson	B	DE	late, short	Bh	*
Sokrates	2001	Saatzucht Engelen Büchling e.K.	A	DE	late, tall	Bh	*
Winnetou	2002	Firlbeck	C	DE	late, short	Bh	*
Cubus	2002	Lochow-Petkus	A	DE	late, short	Bh	*
Tommi	2002	Nordsaat Saatzeit	A	DE	late, short	Bh	*
Ellvis	2002	Saatzeit Josef Breun	A	DE	late, short	Bh	*
Enorm	2002	Saatzeit Schweiger GbR	E	DE	late, short	Bh	*
SW Topper	2002	SW Seeds	E	DE	late, short	Bh	*
Akteur	2003	DSV	E	DE	late, tall	Bh	*
Limes	2003	Innoseeds	B	DE	late, short	Bh	*
Paroli	2004	DSV	A	DE	late, short	Bh	*
Türkis	2004	SW Seeds	A	DE	late, short	Bh	*
Magister	2005	Bauer, G.	E	DE	late, short	Bh	*
Chevalier	2005	DSV	A	AT, CZ, LT, LU	late, short	Bh	*
Anthus	2005	KWS Lochow GmbH	B	DE	late, short	Bh	*
Tuareg	2005	Nordsaat Saatzeit	A	DE	late, short	Bh	*
Schamane	2005	Saatzeit Engelen Büchling e.K.	A	DE	late, short	Bh	*
Impression	2005	Saatzeit Schweiger GbR	A	DE	late, short	Bh	*
Brillant	2005	SW Seeds	A	DE	late, short	Bh	*
Torrild	2005	W. von Borries-Eckendorf	A	DE	late, short	Bh	*
Carenius	2006	Dieckmann	B	DE	late, short	Bh	*
Potenzial	2006	DSV	A	DE	late, short	Bh	*
Skalmeje	2006	KWS Lochow GmbH	C	DE	late, short	Bh	*
Mulan	2006	Nordsaat Saatzeit	B	DE	late, short	Bh	*
Premio	2006	RAGT	B	FR	early, short	Bh	*
Manager	2006	Saatzeit Schweiger GbR	B	DE	late, short	Bh	*
Lucius	2006	Secobra Recherches	A	DE	late, short	Bh	*
Zobel	2006	Syngenta Seeds GmbH	A	DE	late, short	Bh	*
Skagen	2006	W. von Borries-Eckendorf	E	DE	late, short	Bh	*
Jenga	2007	Ackermann Saatzeit	A	DE	late, short	Bh	*
Boregar	2007	RAGT	A	FR	early, short	Bh	*
Esket	2007	RAGT	A	DE	late, short	Bh	*
Inspiration	2007	Saatzeit Josef Breun	B	DE	late, short	Bh	*
Fedor	2007	W. von Borries-Eckendorf	A	DE	late, short	Bh	*
Profilus	2008	RAGT	A	DE	late, short	Bh	*
JB Asano	2008	Saatzeit Josef Breun	A	DE	late, short	Bh	*
Jafet	2008	Sandra Senghaas-Kirschenlohr	E	DE	late, short	Bh	*
Tabasco	2008	W. von Borries-Eckendorf	C	DE	late, short	Bh	*
Zappa	2009	Ackermann Saatzeit	C	DE	late, short	Bh	*
Primus	2009	DSV	B	DE	late, short	Bh	*
Kredo	2009	Nordsaat Saatzeit	B	DE	late, short	Bh	*
Global	2009	RAGT	B	DE, AT	late, short	Bh	*
Event	2009	Saatzeit Josef Breun	E	DE	late, short	Bh	*
Arktis	2010	DSV	E	DE	late, short	Bh	*
Matrix	2010	DSV	B	DE	late, short	Bh	*
Muskat	2010	DSV	C	DE	early, short	Bh	*
KWS Pius	2010	KWS Lochow GmbH	A	DE	late, short	Bh	*
Edgar	2010	Limagrain GmbH	B	DE	late, short	Bh	*

Kalahari	2010	Limagrain GmbH	B	DE, BE	late, short	Bh	*
Linus	2010	RAGT	A	DE	late, short	Bh	*
Oxal	2010	RAGT	B	DE	late, short	Bh	*
Orcas	2010	Secobra Recherches	B	DE	early, short	Bh	*
Alves	2010	SW Seeds	A	DE	late, tall	Bh	*
KWS Santiago	2011	KWS Lochow GmbH	C	UK	late, short	Bh	*
Colonia	2011	Limagrain GmbH	B	DE, BE, HU	late, short	Bh	*
Intro	2011	RAGT	B	DE, FR DE, FR	late, short	Bh	*
Kometus	2011	Saatzucht Schweiger GbR	A	DE	late, short	Bh	*
Nelson	2011	Saatzucht Schweiger GbR	E	DE	late, short	Bh	*
Xanthippe	2011	Sejet Planteforaedling I/S	C	DE	late, short	Bh	*
Glaucus	2011	Strube, Dr. H.	A	DE	late, short	Bh	*
Tobak	2011	W. von Borries-Eckendorf	B	DE	late, short	Bh	*
Joker	2012	DSV	A	DE	late, short	Bh	*
Patras	2012	DSV	A	DE	late, short	Bh	*
KWS Ferrum	2012	KWS Lochow GmbH	B	DE	early, short	Bh	*
Atomic	2012	Limagrain GmbH	A	DE	late, short	Bh	*
Capone	2012	Limagrain GmbH	A	DE	late, short	Bh	*
Forum	2012	Nordsaat Saatzucht	A	DE, EE, PL, SE	late, short	Bh	*
Mentor	2012	RAGT	B	DE	late, short	Bh	*
WW 4180	2012	Saatzucht Josef Breun	NA	DE	early, short	Bh	*
Bombus	2012	Secobra Recherches	C	DE	late, short	Bh	*
Estivus	2012	Strube, Dr. H.	A	DE	late, short	Bh	*
SY Ferry	2012	Syngenta Seeds GmbH	B	DE	late, short	Bh	*
Boxer	2013	Ackermann Saatzucht	C	DE	late, tall	Bh	*
KWS Cobalt	2013	KWS Lochow GmbH	A	DE	late, short	Bh	*
Kurt	2013	Limagrain GmbH	B	DE	late, short	Bh	*
Anapolis	2013	Nordsaat Saatzucht	C	DE	late, short	Bh	*
Rebell	2013	RAGT	A	DE	late, short	Bh	*
Avenir	2013	Saatzucht Josef Breun	A	DE	late, short	Bh	*
Gourmet	2013	Secobra Recherches	E	DE	late, short	Bh	*
Landsknecht	2013	Secobra Recherches	C	DE	late, short	Bh	*
Memory	2013	Secobra Recherches	B	DE	late, short	Bh	*
Apertus	2013	Strube, Dr. H.	A	DE	late, short	Bh	*
Rumor	2013	Strube, Dr. H.	B	DE	early, short	Bh	*
Desamo	2013	Syngenta Seeds GmbH	B	DE	late, short	Bh	*
Gordian	2013	Syngenta Seeds GmbH	B	DE	late, short	Bh	*
Edward	2013	W. von Borries-Eckendorf	B	DE	late, short	Bh	*
Hybred	2003	Nordsaat Saatzucht	B	DE, FR	early, short	Bh ^{Hyb}	
Hystar	2007	Saaten Union Recherche	B	FR	early, short	Bh ^{Hyb}	
Hyland	2009	Nordsaat Saatzucht	B	DE, HU	early, short	Bh ^{Hyb}	
Hybery	2010	Saaten Union Recherche	B	FR	early, short	Bh ^{Hyb}	
Hylux	2012	Saaten Union	B	FR	early, short	Bh ^{Hyb}	
Bussard	1990	Lochow-Petkus	E	DE	late, tall	Bh ^{Org}	*
Batis	1994	Strube, Dr. H.	A	DE	late, tall	Bh ^{Org}	*
Tiger	2001	Franck	A	DE	late, tall	Bh ^{Org}	*
Hermann	2004	Nickerson	C	DE	late, short	Bh ^{Org}	*
Kerubino	2004	Saatzucht Schmid Landau	E	DE	late, short	Bh ^{Org}	*
Akratos	2004	Strube, Dr. H.	A	DE	late, tall	Bh ^{Org}	*
Discus	2007	Pflanzenzucht SaKa GmbH&Co.KG	A	DE	late, short	Bh ^{Org}	*
Famulus	2010	DSV	E	DE	late, short	Bh ^{Org}	*
Florian	2010	Nordsaat Saatzucht	E	DE	late, short	Bh ^{Org}	*
Genius	2010	Nordsaat Saatzucht	E	DE	late, short	Bh ^{Org}	*
Meister	2010	RAGT	A	DE	late, short	Bh ^{Org}	*
Elixer	2012	W. von Borries-Eckendorf	C	DE	late, short	Bh ^{Org}	*
Pionier	2013	DSV	A	DE	late, short	Bh ^{Org}	*
KWS Milaneco	2013	KWS Lochow GmbH	E	DE	late, tall	Bh ^{Org}	*
NaturaStar	2002	Saatzucht Schweiger GbR	A	DE	late, tall	Bh ^{Org}	*
Aszita	2005	Kunz und Schmidt	B	DE	late, tall	Bh ^{Org}	*
Butaro	2009	Landbauschule Dottenfelderhof e.V.	E	DE	late, tall	Bh ^{Org}	*
Soissons	1987	Florimond-Desprez	NA	BE, ES, FR, IE, IT, SI	early, short	Div ^{europ.reg.}	*
Tremie	1991	Serasem	NA	ES, FR, IT	early, short	Div ^{europ.reg.}	*

Gaicho	1993	USDA-ARS, Oklahoma AES	NA	US	late, short	Div ^{europ.reg.}	*
Sponsor	1994	Unisigma	NA	FR, IE	late, short	Div ^{europ.reg.}	*
Ivanka	1998	Inst. of Field and Veg. Crops, Novi Sad	NA	CS	early, short	Div ^{europ.reg.}	*
Claire	1999	Nickerson	C	IE, UK	late, short	Div ^{europ.reg.}	*
Caphorn	2000	RAGT	NA	FR	early, short	Div ^{europ.reg.}	*
Solstice	2001	Limagrain GmbH	NA	UK	late, short	Div ^{europ.reg.}	*
Cordiale	2003	KWS UK	NA	UK	early, short	Div ^{europ.reg.}	*
Robigus	2004	KWS UK	B	UK	late, short	Div ^{europ.reg.}	*
Einstein	2004	Nickerson	B	UK	late, short	Div ^{europ.reg.}	*
Alixan	2005	Limagrain GmbH	A	FR	early, short	Div ^{europ.reg.}	*
Arlequin	2007	Limagrain GmbH	NA	FR	early, short	Div ^{europ.reg.}	*
Oakley	2008	KWS UK	C	UK, BE	late, short	Div ^{europ.reg.}	*
Phoenix	NA	WWAI	NA	AU; US	early, tall	Div	*
Helios	NA	Arizona Plant Breeders	NA	US	late, short	Div	*
Mex. 3	NA	BAZ	NA	MX	early, short	Div	*
Cajeme 71	NA	CIMMYT	NA	MX	early, short	Div	*
Mex. 17 bb	NA	CIMMYT	NA	MX	early, short	Div	*
BCD 1302/83	NA	Goertzen Seed Research	NA	MD	early, short	Div	*
Sonalika	NA	Indian Agricultural Research Institute	NA	IN	early, short	Div	*
Lambriego Inia	NA	INIA	NA	Chile	early, short	Div	*
Siete Cerros	NA	INIA	NA	MX	early, short	Div	*
Triple dirk \S\''''	NA	INIA	NA	AU	early, short	Div	*
Pobeda	NA	Inst. of Field and Veg. Crops, Novi Sad	NA	SR	early, short	Div	*
Reناسansa	NA	Inst. of Field and Veg. Crops, Novi Sad	NA	SR	early, short	Div	*
Centurk	NA	Nebraska Agr. Exp. Station	NA	US	early, tall	Div	*
Avalon	NA	Plant Breeding Int. Cambridge	NA	UK	early, short	Div	*
Highbury	NA	Plant Breeding Int. Cambridge	A	UK	early, short	Div	*
Brigand	NA	Plant Breeding Int. Cambridge	NA	UK	late, short	Div	*
TJB 990-15	NA	Plant Breeding Int. Cambridge	NA	UK	late, short	Div	*
Benni mult.	NA	Purdue University	NA	US	early, tall	Div	*
Hope	NA	S.Dakota Agr. Exp. Station	NA	US	early, tall	Div	*
SUR99820	NA	Saaten Union Recherche	NA	FR	early, short	Div	*
Capelle Desprez	NA	SAS Florimond Desprez	C	FR; CH; UK	late, tall	Div	*
Durin	NA	NA	NA	FR	late, short	Div	*
Florida	NA	NA	NA	US	early, short	Div	*
INTRO 615	NA	NA	NA	US	early, short	Div	*
Mironovska 808	NA	NA	NA	UA	early, tall	Div	*
NS 22/92	NA	NA	NA	SR	early, tall	Div	*
NS 46/90	NA	NA	NA	SR	early, short	Div	*
NS 66/92	NA	NA	NA	SR	early, short	Div	*
Vel	NA	NA	NA	US	early, tall	Div	*

Table S2.2: Nitrogen content of the soil in [kg/ha] and amount of fertilized Nitrogen in the last row for every season. Three applications: at vegetation start, at stem elongation and around booting.

	2015	2016	2017
before sowing (0-60 cm depth)	149.9	18.1	22.8
at vegetation start (0-90 cm depth)¹	70.8	29.3	43.1
after harvest (0-90 cm depth)	86.6	34.2	28.9
	150	190	180

Fertilization in three applications

Table S2.3: Duration and Environmental conditions during the main phenological phases: from sowing to heading date and from heading date to maturity. Mean values calculated based on all cultivars for heading date and based on a subset of 23 cultivars for maturity (BBCH87, "hard-dough"). In brackets average daily value for that period.

	Season	From sowing to mean heading	From mean heading to mean maturity
Days	2015	221	46
	2016	217	40
	2017	213	36
Temperature sum	2015	1448.82	804.20 (17.48)
	2016	1615.17	720.64 (18.02)
	2017	1426.01	662.26 (18.40)
Precipitation sum	2015	122.65	106.60 (2.32)
	2016	282.49	75.68 (1.89)
	2017	237.53	64.31 (1.79)
Radiation sum	2015	1637.77	886.97 (19.28)
	2016	1665.54	792.81 (19.82)
	2017	1603.27	674.84 (18.75)

¹ measured in April, after the first fertilisation

Table S3.2: Summary of the plant protection measures.

	Growth stage	Spraying agents		
		2015	2016	2017
Herbicide	BBCH 21/25	1,2 l/ha Axial	1,2 l/ha Axial	1,2 l/ha Axial
	BBCH 25/29	70 g/ha Biathlon4D	70 g/ha Biathlon4D	70 g/ha Biathlon4D
		1 l/ha Dash	1 l/ha Dash	
		20 g/ha Dirigent SX	20 g/ha Dirigent SX	
Fungicide	BBCH 31/37	2 l/ha Capalo	2 l/ha Capalo	1,6 l Capalo
	BBCH 49/55	1,1 l/ha Adexar	1,1 l/ha Adexar	2 l/ha Adexar
		1,1 l/ha Diamant	1,1 l/ha Diamant	
	BBCH59/61	1 l/ha Prosaro	1 l/ha Prosaro	1 l/ha Prosaro
Growth regulator	BBCH 25/29	1,2 l/ha Stabilan 720		
	BBCH 31	0,5 l/ha Stabilan 720	0,5 l/ha Stabilan 720	1,5 l/ha Medax Top
		0,5 l/ha Medax Top	0,5 l/ha Medax Top	
Insecticide		0,2 l/ha Sumicidin	0,2 l/ha Sumicidin	0,2 l/ha Sumicidin
			0,075 l/ha Karate Zeon	

Table S3.3: P-values from the ANOVA results for the yield and senescence parameters. No interaction effect for BBCH59 because of only one value per year, p-value for the factor year was calculated with cultivar as random factor. In all other calculations cultivar, year and the interaction were set as fixed in the linear mixed model.

	p-value for Factor effect		
	Cultivar	Year	Interaction
Seed yield	< 0.001	< 0.01	< 0.001
Biomass²	< 0.001	< 0.01	n.s.
Harvest Index	< 0.001	< 0.01	n.s.
TKW	< 0.001	n.s.	< 0.001
Spikes per m²	< 0.001	< 0.01	n.s.
Grains per ear	< 0.001	< 0.05	< 0.001
Grains per m²	< 0.001	n.s.	n.s.
BBCH59	< 0.001	< 0.001	-
LAI_{max}	< 0.001	< 0.05	< 0.001
SPAD³	< 0.001	n.s.	< 0.05
GLA₅₀	< 0.001	< 0.01	< 0.001
LAD	< 0.001	< 0.05	< 0.001
GCD	< 0.001	< 0.05	< 0.001

² Calculated from Harvest Index und final plot yield³ only for 2016 and 2017

Table S3.4: Weather conditions during the experimental periods in comparison with the 30 years mean values from the DWD (DE's National Meteorological Service) for the relevant region.

	Sowing date	Avg. heading date (BBCH 59)		Precipitation sum (March - July) [mm]	Avg. Temp. (Oct - July) [°C]
		days after sowing	Tsum [°Cd]		
2015	28 th Oct 2014	221	1461	201.8	11.92
2016	27 th Oct 2015	217	1618	235.7	12.73
2017	2 nd Nov 2016	213	1436	325.7	13.42
30year mean from DWD				296.3	11.6

Table S3.5: Broad-sense heritability (last column "Overall") and repeatability calculated within each year, Within each year the repeatability was calculated accordingly but without the cultivar – season interaction $\sigma_{c\gamma}^2$ and the residual variance σ_e^2 divided by two instead.

	2015	2016	2017	Overall
Seed yield	0.78	0.68	0.76	0.74
Grains per spike	0.76	0.64	0.66	0.75
BBCH 59	-	-	-	0.87
LAI_{max}	0.57	0.51	0.36	0.50
SPAD	-	0.65	0.56	0.66
LAD	0.71	0.59	0.62	0.51
GCD	0.75	0.75	0.79	0.57

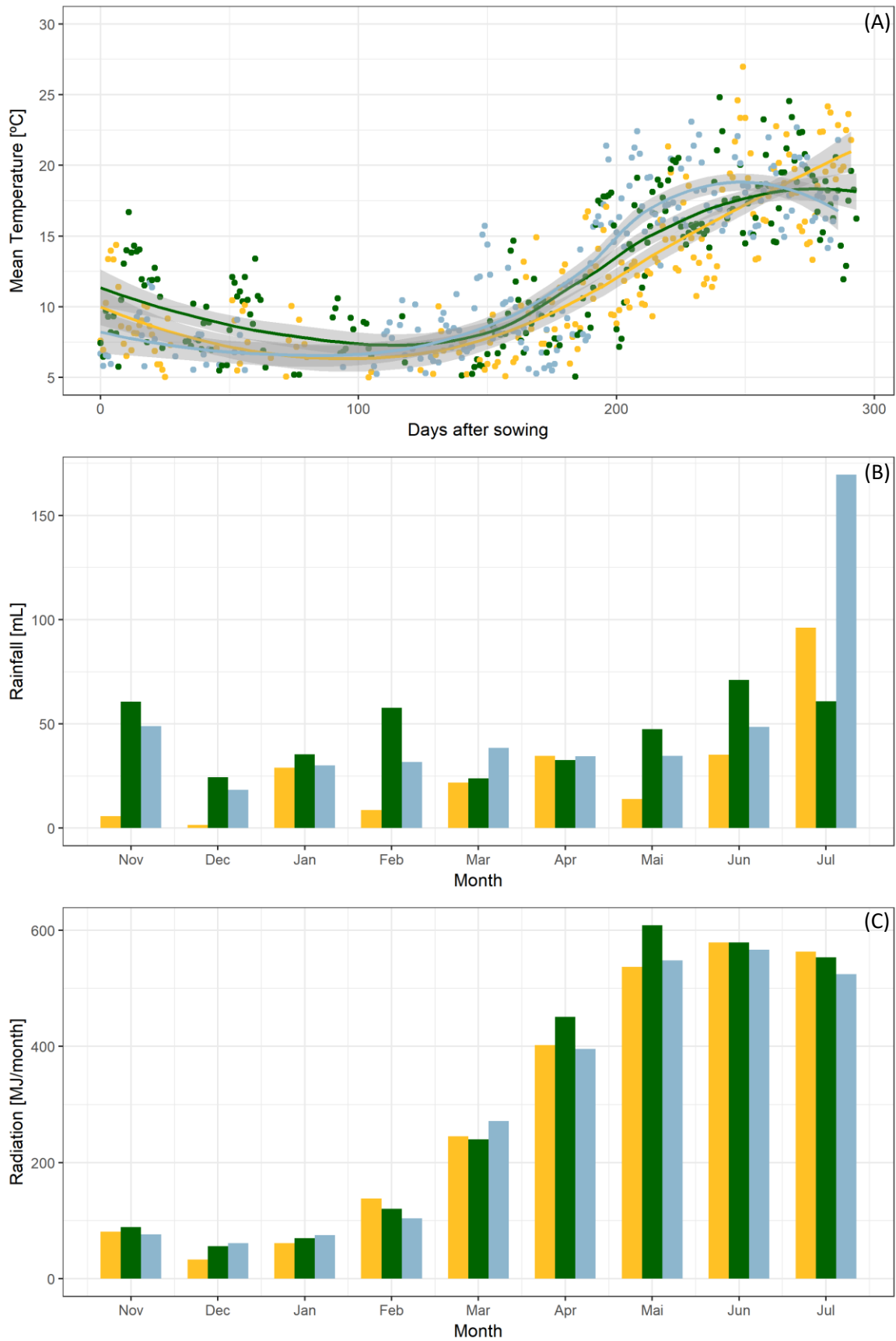


Figure S2.1: Mean temperature during the growing seasons (A); Monthly sums of precipitation (B); Monthly sums of radiation (C), yellow= 2015, green= 2016, blue= 2017.

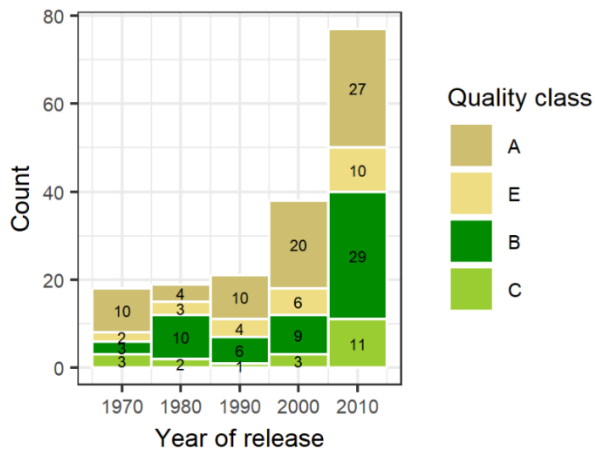


Figure S3.1: Proportion of cultivars per decade and quality class within the cultivar collection representing the breeding history of German winter wheat, oldest cultivar from 1966 and youngest from 2013, in total 174 cultivars including 5 hybrids.

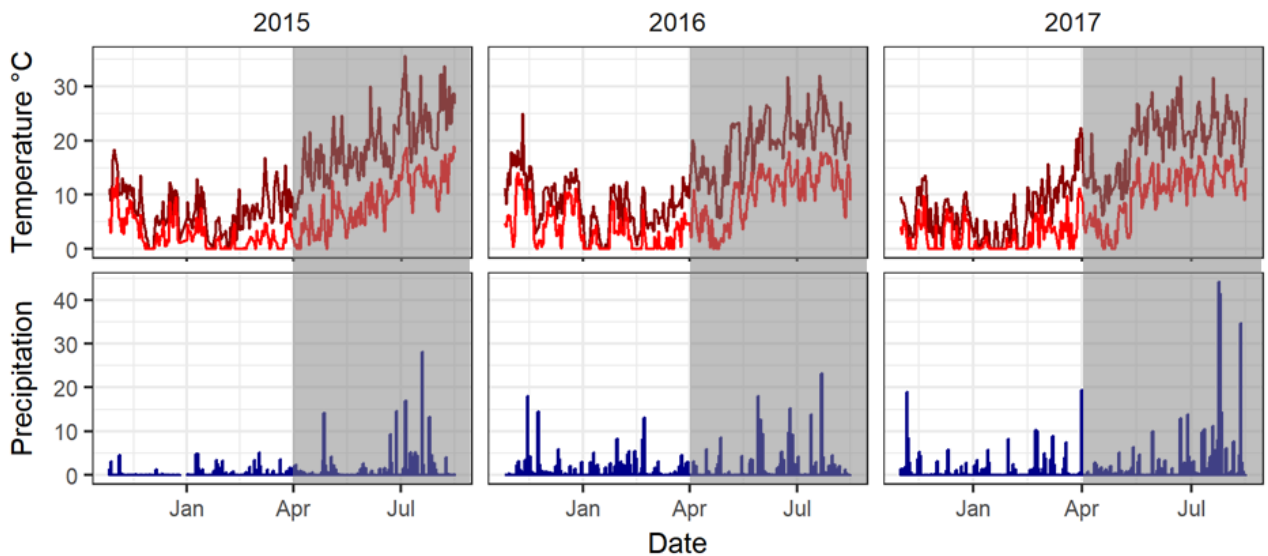


Figure S3.2: Summary of minimum (above 0°C) and maximum temperature and daily precipitation sum during the experimental periods, grey area: approximately generative phase.

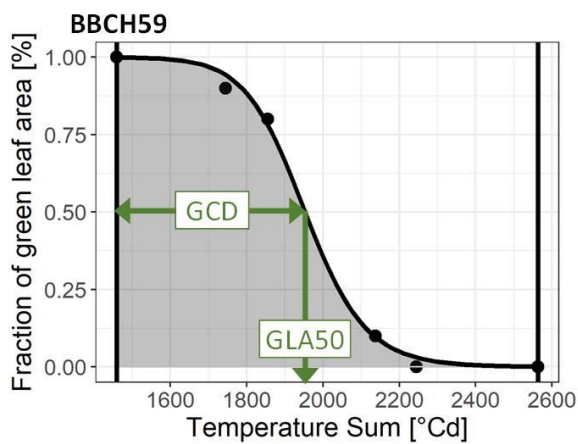


Figure S3.3: Explanation graph for parameters describing the senescence pattern. The black dots are visually scored green leaf area (%). A logistic power function (black line) with two parameters was fitted to the data. For each cultivar, integral of green canopy area (grey area) was calculated between its heading (BBCH59) and harvest date in each season. GLA50 is the temperature sum when 50% green was reached and green canopy duration (GCD) is the temperature sum from heading to GLA50.

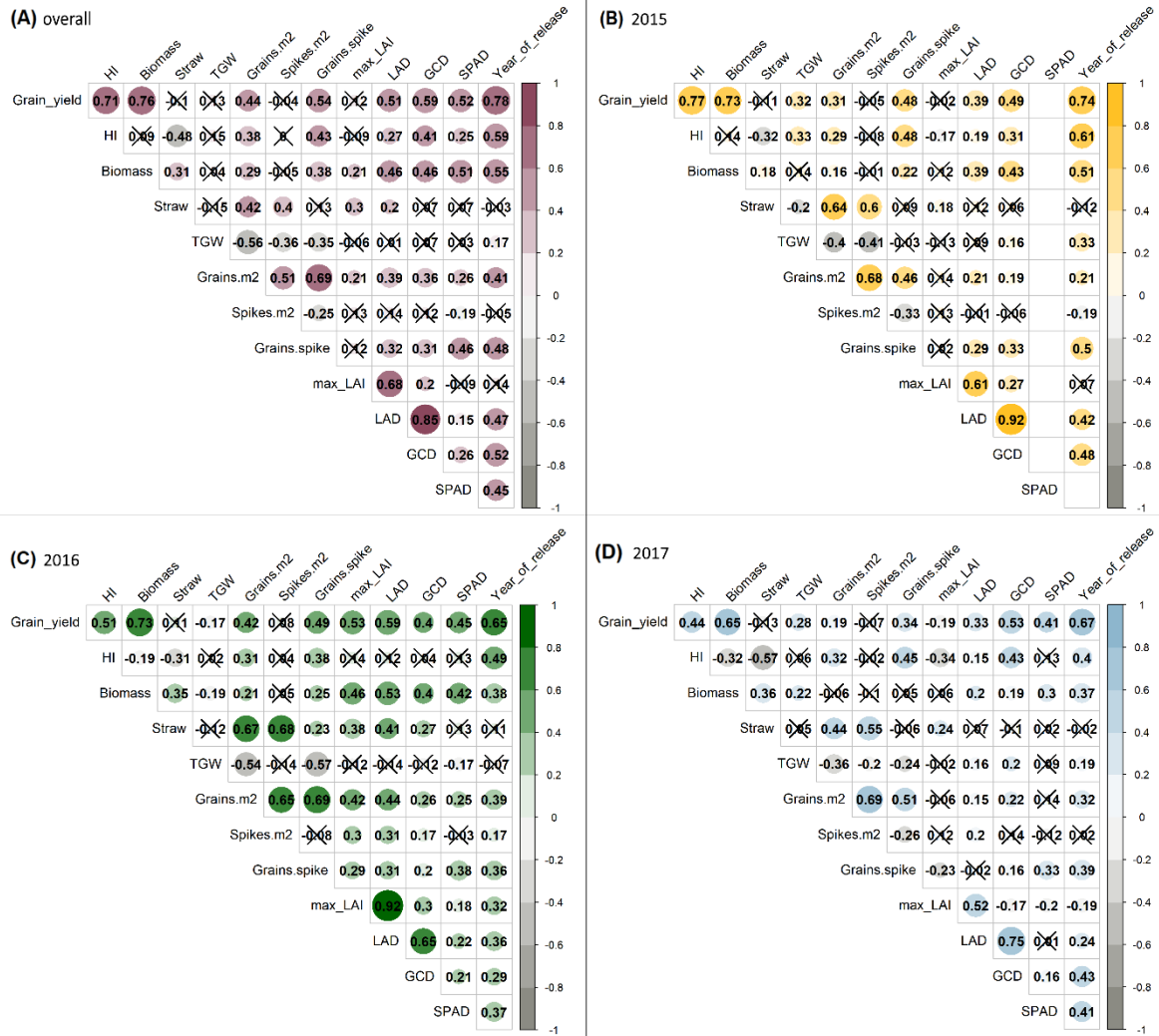


Fig. S3.4: Pearson correlations of yield and stay green parameters, A: means for cultivars over all three seasons and two replications each, B: means for cultivars within 2015, C: means for cultivars within 2016, D: means for cultivars within 2017, crossed values were not significant.

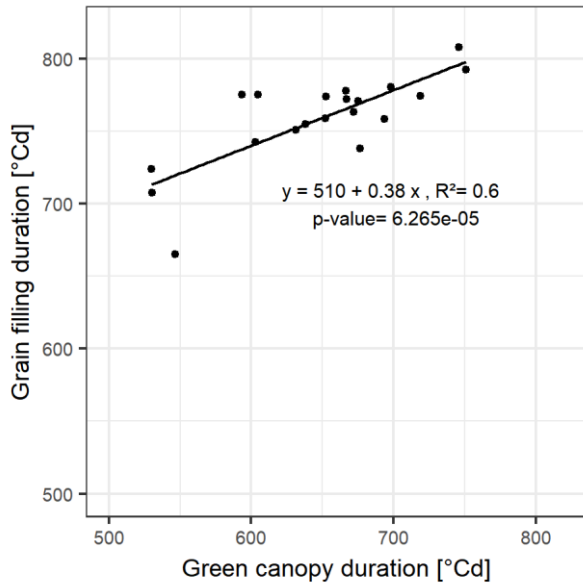


Fig. S3.5: Linear relationship between the grain filling duration (temperature sum of BBCH87 – temperature sum of BBCH59) and the green canopy duration for a subset of 20 cultivars. Each dot represents a mean value of three seasons and 2 replications (n=6).

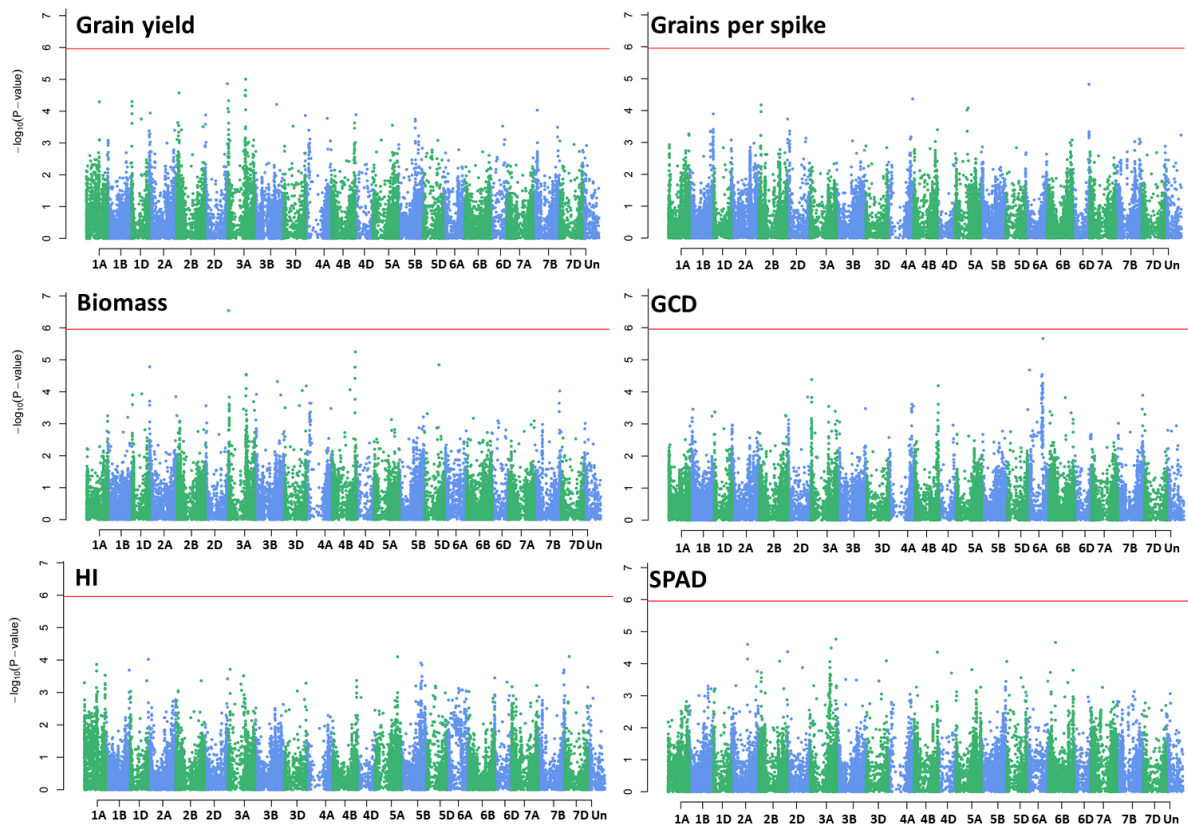


Fig. S3.6: Manhattan plots for genome wide marker - trait associations. P-values shown on a $-\log_{10}(p\text{-value})$ scale and the red line indicates the significance threshold (Bonferroni, 0.05).

Table S4.1: Complete list of significant (either false discovery rate (FDR) <10% or **log(p-value) < 6.00085** (in bold letters)) marker – trait associations. Marker names starting with AX-... originate from the 135K chip, all others from the 15K chip (Chr= chromosome, effB= effect of the minor allele, se_effB= standard error of the minor allele effect).

Chr	Position		A	B	effB	se_effB	Trait	log(p)	FDR
	[Mbp]	Marker name							
1A	1.208304	tplb0028p02_562	C	T	2.131	0.534	height	4.181	3.3%
1A	7.185981	RAC875_c30657_82	A	G	2.734	0.442	height	9.193	0.0%
1A	7.292664	BS00073243_51	T	C	2.032	0.523	height	3.987	4.8%
1A	37.508433	AX-110977774	A	G	-1.997	0.504	height	4.126	3.6%
1A	490.419496	AX-110913638	G	A	2.216	0.549	height	4.269	2.9%
1A	559.048071	AX-158605784	G	A	3.605	0.682	height	6.908	0.0%
1A	577.841067	wsnp_Ex_c9343_15514687	G	T	2.234	0.519	height	4.782	1.3%
1B	17.68609	AX-89493320	A	G	1.689	0.463	height	3.583	9.7%
1B	442.177567	AX-158545043	C	T	-25.034	6.167	BBCH59	4.308	9.2%
1B	566.391418	AX-158521220	G	T	1.783	0.453	height	4.079	4.0%
1B	569.977781	AX-158560970	T	C	-32.016	7.204	BBCH59	5.055	4.0%
1B	648.454022	BS00043666_51	A	G	1.739	0.474	height	3.616	9.1%
1B	665.424002	AX-158601991	C	T	2.176	0.528	height	4.428	2.2%
1B	677.913176	AX-158595694	C	T	-28.662	5.951	BBCH59	5.835	1.1%
1D	0.209474	AX-158595990	T	G	3.719	0.955	height	4.003	4.6%
1D	0.216962	wsnp_Ex_c41048_47969948	G	A	4.561	0.979	height	5.495	0.4%
1D	0.217173	AX-109955585	T	C	3.555	0.961	height	3.664	8.4%
1D	0.217204	AX-111029556	G	A	3.722	0.972	height	3.894	5.7%
1D	3.429078	AX-158571818	C	T	2.799	0.699	height	4.205	3.2%
1D	55.671046	BS00031658_51	T	C	3.180	0.529	height	8.744	0.0%
1D	56.751122	BS00051826_51	C	T	3.428	0.543	height	9.549	0.0%
2A	1.361437	AX-158573231	C	T	-3.454	0.775	height	5.081	0.7%
2A	159.8762	GENE-1028_694	C	T	3.319	0.578	height	8.030	0.0%
2A	764.81898	AX-158572320	C	T	1.661	0.446	height	3.706	7.9%
2A	149.231071	AX-110916855	C	T	3.183	0.598	height	6.994	0.0%
2A	157.933779	BS00089457_51	A	G	3.359	0.574	height	8.313	0.0%
2A	507.430979	AX-158561824	T	G	-2.988	0.645	height	5.448	0.4%
2A	636.910044	BS00063518_51	A	G	2.607	0.562	height	5.458	0.4%
2A	744.076371	AX-158608838	T	C	-31.220	6.321	BBCH59	6.104	1.1%
2A	745.023598	AX-158545965	T	C	-2.082	0.567	height	3.618	9.1%
2B	62.202282	AX-158575116	C	T	15.963	3.995	BBCH59	4.191	9.8%
2B	710.28387	AX-111453747	G	A	-3.764	0.900	height	4.536	1.7%
2B	89.314082	AX-158610368	C	T	1.997	0.547	height	3.579	9.7%
2B	91.836638	Excalibur_rep_c68899_1400	A	G	-29.985	5.639	BBCH59	6.977	0.5%
2B	636.112718	AX-158538091	C	T	1.868	0.485	height	3.926	5.4%
2B	644.147921	AX-158547164	A	G	2.964	0.595	height	6.198	0.1%
2B	646.211395	AX-89608149	C	T	2.899	0.600	height	5.860	0.2%
2B	680.203593	AX-158540945	T	C	2.503	0.626	height	4.197	3.2%
2B	683.134889	AX-158574321	G	A	2.202	0.540	height	4.343	2.6%
2B	698.207385	AX-110984191	A	G	-2.689	0.698	height	3.936	5.3%
2B	734.933659	AX-158573970	T	C	-3.298	0.757	height	4.877	1.1%
2B	747.821575	BS00009060_51	A	C	2.310	0.568	height	4.326	2.6%
2B	750.013149	BS00030361_51	C	T	2.605	0.567	height	5.357	0.4%
2D	16.12992	AX-158576111	A	C	-30.742	6.771	BBCH59	5.250	3.5%
2D	9.402187	AX-158576368	C	T	2.041	0.496	height	4.421	2.2%

Chr	Position		A	B	effB	se_effB	Trait	log(p)	FDR
	[Mbp]	Marker name							
2D	116.803262	AX-158522586	C	T	2.212	0.524	height	4.622	1.5%
2D	587.291496	AX-158597620	A	G	-2.369	0.582	height	4.328	2.6%
2D	590.337285	AX-158521935	T	C	-4.152	1.027	height	4.274	2.9%
2D	637.639555	AX-158547601	C	T	-2.261	0.494	height	5.326	0.5%
2D	638.777522	AX-158575974	T	C	-1.937	0.502	height	3.948	5.2%
3A	1.925915	AX-89761988	C	T	-74.558	14.646	biomass	6.448	1.8%
3A	59.43283	AX-158577612	G	T	4.669	1.084	height	4.785	1.3%
3A	8.866733	RFL_Contig1488_671	C	T	2.388	0.501	height	5.737	0.2%
3A	21.377111	AX-158524093	A	G	-10.431	2.235	iPAR	5.517	2.4%
3A	21.377111	AX-158524093	A	G	-19.008	4.177	gl_int	5.271	5.4%
3A	21.378662	AX-109871577	C	T	-10.308	2.249	iPAR	5.341	2.5%
3A	21.378662	AX-109871577	C	T	-18.446	4.206	gl_int	4.936	7.3%
3A	21.408769	AX-158524116	G	A	-10.706	2.330	iPAR	5.363	2.5%
3A	21.408769	AX-158524116	G	A	-19.247	4.354	gl_int	5.007	7.0%
3A	444.721312	IAAV4343	A	G	2.097	0.564	height	3.699	7.9%
3A	445.265353	AX-111073136	A	G	2.256	0.604	height	3.729	7.7%
3A	496.990926	AX-158576725	G	A	-19.635	4.637	gl_int	4.640	8.8%
3A	498.235988	AX-109485322	G	A	-19.635	4.637	gl_int	4.640	8.8%
3A	502.165507	AX-158612328	T	C	-21.007	4.884	gl_int	4.769	8.5%
3A	515.246917	AX-158523075	C	T	2.845	0.594	height	5.783	0.2%
3A	700.809163	BS00097265_51	T	C	2.750	0.478	height	8.051	0.0%
3A	705.251089	AX-158523671	G	A	1.912	0.483	height	4.114	3.7%
3A	710.829414	AX-158523081	A	G	4.143	0.968	height	4.728	1.3%
3A	734.001451	AX-110447070	A	G	-0.016	0.004	gl_mean	4.792	9.0%
3A	734.001559	AX-158523434	T	C	-0.016	0.004	gl_mean	5.008	7.0%
3A	734.008866	AX-158523433	C	T	-0.018	0.004	gl_mean	5.582	4.4%
3A	742.228859	AX-158523283	C	A	-34.311	7.117	BBCH59	5.845	1.1%
3B	18.55901	IACX6214	G	A	-1.765	0.463	height	3.854	6.1%
3B	2.032293	AX-158562921	A	G	2.730	0.504	height	7.221	0.0%
3B	23.78218	Tdurum_contig43252_1762	T	G	3.556	0.506	height	11.683	0.0%
3B	232.63614	wsnp_Ex_c257_491667	C	T	6.219	0.697	height	18.342	0.0%
3B	232.63629	BS00106922_51	G	A	6.342	0.704	height	18.660	0.0%
3B	39.907114	RFL_Contig1456_842	G	A	3.580	0.583	height	9.072	0.0%
3B	68.464256	BS00102622_51	G	T	3.637	0.583	height	9.358	0.0%
3B	457.023204	AX-158541662	G	A	2.312	0.550	height	4.582	1.6%
3B	570.259045	AX-158578000	C	T	2.537	0.583	height	4.867	1.1%
3B	575.256555	AX-94451121	G	A	2.530	0.612	height	4.446	2.1%
3B	585.686397	AX-112290121	G	A	1.971	0.528	height	3.727	7.7%
3B	602.362074	AX-89595105	G	A	3.918	0.603	height	10.083	0.0%
3B	617.683148	wsnp_JD_c5643_6802211	A	G	2.610	0.526	height	6.159	0.1%
3B	722.366477	AX-158538426	T	C	-2.446	0.579	height	4.626	1.5%
3B	726.150416	AX-158579060	C	T	-35.101	7.305	BBCH59	5.811	1.1%
3B	758.347768	AX-158578744	T	C	1.972	0.538	height	3.612	9.1%
3D	505.98392	AX-158615240	T	C	-26.743	5.998	BBCH59	5.083	4.0%
3D	355.627267	AX-158580226	G	A	4.044	1.055	height	3.898	5.7%
3D	426.078176	AX-158615732	G	A	-30.506	7.161	BBCH59	4.690	6.0%
3D	433.541443	AX-158580163	C	T	-24.165	5.976	BBCH59	4.278	9.2%

Chr	Position		A	B	effB	se_effB	Trait	log(p)	FDR
	[Mbp]	Marker name							
3D	592.875873	AX-158615374	C	T	1.930	0.510	height	3.810	6.7%
4A	666.483291	AX-158549864	C	T	-31.402	6.455	BBCH59	5.941	1.1%
4A	705.508068	AX-158598696	G	A	-0.013	0.003	gl_mean	4.953	7.0%
4A	707.037698	AX-108861756	C	T	-0.013	0.003	gl_mean	4.717	9.6%
4A	709.869816	AX-158564187	C	T	-28.551	6.942	BBCH59	4.408	8.9%
4B	2.684569	AX-158564639	C	T	2.526	0.539	height	5.553	0.3%
4B	32.807946	AX-158538723	C	A	2.160	0.441	TGW	6.025	4.7%
4B	652.85529	AX-158582146	C	A	-24.138	5.947	BBCH59	4.306	9.2%
4B	498.588993	AX-158582589	A	G	-32.761	7.634	BBCH59	4.751	5.6%
4B	654.440332	AX-108751780	A	G	-0.017	0.003	gl_mean	6.249	2.8%
4B	654.440332	AX-108751780	A	G	-13.528	2.730	iPAR	6.141	1.6%
4B	654.440332	AX-108751780	A	G	-24.379	5.090	gl_int	5.778	2.8%
4B	654.735395	AX-110977556	G	A	-13.945	2.949	iPAR	5.648	2.3%
4B	654.735395	AX-110977556	G	A	-0.017	0.004	gl_mean	5.220	6.0%
4B	654.735395	AX-110977556	G	A	-23.779	5.489	gl_int	4.830	8.2%
4B	654.897925	AX-110574351	C	T	-12.858	2.764	iPAR	5.483	2.4%
4B	654.897925	AX-110574351	C	T	-23.199	5.159	gl_int	5.162	5.8%
4B	654.897925	AX-110574351	C	T	-0.015	0.003	gl_mean	5.118	6.4%
4B	655.411283	AX-111555251	T	C	-12.360	2.614	iPAR	5.647	2.3%
4B	655.411283	AX-111555251	T	C	-0.015	0.003	gl_mean	5.605	4.4%
4B	655.411283	AX-111555251	T	C	-22.402	4.879	gl_int	5.357	5.4%
4B	656.160859	AX-108970403	C	T	-12.298	2.508	iPAR	6.025	1.6%
4B	656.160859	AX-108970403	C	T	-22.855	4.686	gl_int	5.969	2.7%
4B	656.163137	BS00023204_51	C	T	-19.061	4.493	gl_int	4.656	8.8%
4B	656.287059	AX-111093604	T	C	-25.295	4.680	gl_int	7.189	0.3%
4B	656.287059	AX-111093604	T	C	-13.476	2.509	iPAR	7.105	0.4%
4B	656.287059	AX-111093604	T	C	-21.170	4.307	gl_dur	6.053	4.4%
4D	12.534569	AX-158619793	C	A	-2.468	0.633	height	4.014	4.6%
4D	12.773259	Kukri_rep_c68594_530	A	G	-2.618	0.609	height	4.762	1.3%
4D	14.572749	AX-111523860	A	G	-2.507	0.592	height	4.643	1.5%
4D	18.781069	TG0011b	G	T	0.281	0.058	Grain yield	5.945	2.8%
4D	18.781069	TG0011b	G	T	0.281	0.058	Grain yield	5.945	2.8%
4D	18.781069	TG0011a	G	T	0.281	0.058	Grain yield	5.945	2.8%
4D	18.781069	TG0011a	G	T	0.281	0.058	Grain yield	5.945	2.8%
4D	18.781069	TG0011a	G	T	-2.854	0.605	height	5.616	0.3%
4D	18.781069	TG0011a	G	T	-2.854	0.605	height	5.616	0.3%
4D	18.781069	TG0011b	G	T	-2.854	0.605	height	5.616	0.3%
4D	18.781069	TG0011b	G	T	-2.854	0.605	height	5.616	0.3%
5A	499.009785	AX-158584906	G	A	1.698	0.454	height	3.731	7.7%
5A	610.463847	AX-158550645	A	G	-0.019	0.004	gl_mean	5.428	4.7%
5A	641.119796	AX-158537196	G	A	1.979	0.496	height	4.173	3.3%
5B	31.148205	AX-158586383	C	T	2.502	0.556	height	5.168	0.6%
5B	239.391214	AX-110576540	A	G	3.966	0.667	height	8.567	0.0%
5B	243.436218	AX-158621152	G	T	-0.115	0.026	RUeGf	5.131	9.3%
5B	316.706975	AX-158599726	G	A	5.195	0.738	height	11.725	0.0%
5B	323.894417	AX-158586194	G	A	2.984	0.613	height	5.939	0.2%
5B	485.904236	AX-89388932	T	C	5.110	1.198	height	4.700	1.3%

Chr	Position		A	B	effB	se_effB	Trait	log(p)	FDR
	[Mbp]	Marker name							
5B	486.082233	AX-158525583	T	C	4.921	1.226	height	4.222	3.1%
5B	486.693512	AX-158525581	G	T	5.054	1.198	height	4.607	1.5%
5B	487.223196	AX-86179003	G	A	5.054	1.198	height	4.607	1.5%
5B	487.223574	AX-158533925	A	G	5.054	1.198	height	4.607	1.5%
5B	490.745865	AX-108799004	T	C	5.344	1.224	height	4.897	1.1%
5B	490.760257	AX-110491411	G	A	5.342	1.225	height	4.888	1.1%
5B	529.609324	AX-158542872	C	T	2.458	0.608	height	4.281	2.9%
5B	557.803114	AX-110558109	G	C	2.560	0.509	height	6.308	0.1%
5B	559.995543	AX-109990794	G	A	2.046	0.537	height	3.860	6.1%
5B	595.638134	BS00071206_51	G	A	2.228	0.515	height	4.817	1.2%
5B	647.940863	Tdurum_contig97407_196	T	C	3.521	0.589	height	8.634	0.0%
5B	671.238689	BS00099986_51	C	T	1.956	0.532	height	3.625	9.1%
5B	671.300753	AX-158525839	T	C	-23.948	5.926	BBCH59	4.275	9.2%
5D	384.1431	AX-108780655	C	T	2.017	0.509	height	4.136	3.6%
5D	5.488532	AX-158519550	T	G	-26.117	5.843	BBCH59	5.106	4.0%
5D	56.46567	AX-158552008	C	T	1.922	0.481	height	4.196	3.2%
5D	242.12225	AX-110923577	A	G	0.095	0.021	RUEgf	5.452	5.9%
5D	366.91634	AX-158587450	A	G	-23.197	5.762	BBCH59	4.246	9.5%
5D	80.436274	AX-158537246	A	G	-31.385	7.316	BBCH59	4.748	5.6%
5D	251.306856	AX-158587248	T	C	0.096	0.020	RUEgf	5.949	3.6%
5D	255.561722	AX-108737396	G	T	0.095	0.020	RUEgf	5.839	3.6%
5D	411.170267	AX-158622308	T	C	-33.061	7.951	BBCH59	4.494	7.7%
5D	430.064365	AX-158587458	C	T	4.176	0.749	height	7.605	0.0%
5D	431.198991	AX-158586734	G	A	3.377	0.615	height	7.406	0.0%
5D	446.742163	AX-158622377	A	G	-8.769	2.357	height	3.702	7.9%
5D	530.441579	AX-158551729	C	T	-15.695	3.837	BBCH59	4.366	9.2%
5D	530.645753	AX-94992245	G	A	-17.796	4.444	BBCH59	4.208	9.7%
6A	424.0938	BS00078715_51	T	C	4.993	0.734	height	10.999	0.0%
6A	51.923266	AX-158527586	T	C	10.164	2.497	BBCH59	4.328	9.2%
6A	559.00937	AX-158623518	A	C	-20.228	4.834	BBCH59	4.544	7.2%
6A	61.383565	AX-158534782	A	G	-4.009	0.786	height	6.468	0.1%
6A	86.627353	AX-158552300	C	T	2.302	0.512	height	5.166	0.6%
6A	94.065806	AX-158624004	C	T	-3.844	0.770	height	6.231	0.1%
6A	100.257462	AX-158588223	C	A	2.150	0.504	height	4.704	1.3%
6A	133.762811	AX-158588213	G	A	3.095	0.688	height	5.158	0.6%
6A	148.532157	AX-158600364	G	A	2.729	0.735	height	3.690	8.0%
6A	193.177421	AX-111560362	A	G	-26.063	5.246	BBCH59	6.169	1.1%
6A	230.706136	BS00043716_51	T	C	5.081	0.615	height	15.864	0.0%
6A	400.248301	AX-158587882	G	A	2.913	0.678	height	4.759	1.3%
6A	425.277806	BS00086046_51	A	G	4.993	0.734	height	10.999	0.0%
6A	429.385874	AX-110477615	A	G	2.913	0.678	height	4.759	1.3%
6A	436.860896	AX-158552120	C	T	3.097	0.703	height	4.971	0.9%
6A	439.668875	Excalibur_c49239_97	A	G	4.755	0.609	height	14.255	0.0%
6A	440.255656	AX-95631833	G	A	-24.357	6.019	BBCH59	4.285	9.2%
6A	441.443362	AX-108851909	G	A	-22.568	4.732	GCD	5.733	9.3%
6A	559.007142	AX-158587822	C	T	-18.461	4.601	BBCH59	4.221	9.7%
6A	574.479841	IAAV151	C	T	-2.062	0.514	height	4.225	3.1%

Chr	Position		A	B	effB	se_effB	Trait	log(p)	FDR
	[Mbp]	Marker name							
6A	616.760666	Ra_c7741_1403	T	C	2.298	0.508	height	5.209	0.6%
6B	54.21737	AX-158529761	T	G	-28.083	6.357	BBCH59	5.001	4.2%
6B	201.442326	AX-108741810	C	A	3.975	0.809	height	6.054	0.1%
6B	461.265426	AX-158539333	A	C	-25.090	5.968	BBCH59	4.582	7.0%
6B	469.768864	AX-111545010	T	G	1.586	0.421	height	3.789	7.0%
6D	2.981513	AX-158536394	G	A	2.953	0.567	height	6.725	0.0%
6D	16.963907	AX-158531543	G	A	2.351	0.493	height	5.728	0.2%
6D	464.761165	AX-158530749	G	A	-28.116	6.694	BBCH59	4.574	7.0%
7A	41.959616	BS00023055_51	G	A	2.164	0.503	height	4.772	1.3%
7A	41.963528	AX-158539553	C	T	2.194	0.516	height	4.673	1.4%
7A	266.637086	AX-158567196	C	T	2.364	0.527	height	5.132	0.7%
7A	493.702281	AX-158543700	C	T	2.081	0.566	height	3.628	9.1%
7A	621.322209	AX-158556274	A	G	2.455	0.520	height	5.628	0.3%
7A	682.005138	AX-109435946	C	T	2.275	0.531	height	4.736	1.3%
7B	595.170195	AX-109331686	G	A	4.638	0.635	height	12.554	0.0%
7B	644.192702	AX-158559899	C	T	-8.769	2.357	height	3.702	7.9%
7B	648.924055	BS00067530_51	G	A	-2.439	0.571	height	4.707	1.3%
7B	706.697294	AX-158592201	C	T	4.904	1.320	height	3.694	8.0%
7B	708.558531	BS00049730_51	T	C	2.296	0.497	height	5.411	0.4%
7B	708.566285	AX-158567617	T	G	2.348	0.509	height	5.404	0.4%
7B	731.441933	AX-158567844	C	T	1.615	0.429	height	3.782	7.0%
7B	731.443505	AX-158539585	G	A	2.878	0.566	height	6.438	0.1%
7B	742.260629	AX-158592674	C	T	2.979	0.524	height	7.871	0.0%
7B	749.413941	AX-158601377	G	A	-12.051	2.808	BBCH59	4.752	5.6%
7B	750.592615	AX-158539569	C	T	-2.529	0.600	height	4.609	1.5%
7D	14.426956	Ex_c25027_535	T	C	1.769	0.486	height	3.570	9.9%
7D	51.522626	AX-158555158	A	G	-27.473	6.364	BBCH59	4.800	5.6%

Table S4.2: Top 10 local GEBV variances for each analysed trait sorted by chromosome (Chr) and the position of the block.

Chr	Block	Start [Mbp]	End [Mbp]	Trait	Local GEBV variance	Rank
1A	b000471	370.105557	376.505348	Grains per spike	0.0028	6
2A	b003531	73.16408	75.653161	HI	0.000000068	2
2A	b003531	73.16408	75.653161	TGW	0.0018	5
2A	b003531	73.16408	75.653161	Grains per spike	0.0027	4
2A	b003531	73.16408	75.653161	height	0.0055	4
2A	b003615	192.193574	214.450827	TGW	0.0017	4
2A	b003615	192.193574	214.450827	Spike number	0.033	1
2A	b003637	313.300127	384.680041	TGW	0.0039	9
2A	b003637	313.300127	384.680041	Spike number	0.070	7
2A	b003637	313.300127	384.680041	Grains per spike	0.0030	7
2A	b003700	520.562826	530.221481	Grains per spike	0.0028	5
2A	b003700	520.562826	530.221481	RUEgf	0.0000036	2
2A	b003701	530.745151	549.136394	Grain yield	0.000248	9
2A	b003701	530.745151	549.136394	HI	0.000000216	10
2A	b003701	530.745151	549.136394	TGW	0.0060	10
2A	b003701	530.745151	549.136394	Grains per spike	0.0313	10
2A	b003701	530.745151	549.136394	BBCH59	0.31	9
2A	b003701	530.745151	549.136394	GCD	0.26	2
2A	b003701	530.745151	549.136394	gLAI_dur	0.018	4
2A	b003701	530.745151	549.136394	SPAD_BBCH59	0.00073	6
2A	b003701	530.745151	549.136394	gl_mean	0.000000059	9
2A	b003701	530.745151	549.136394	RUEgf	0.0000134	9
2A	b003701	530.745151	549.136394	height	0.0046	1
2A	b003707	554.509185	562.104411	TGW	0.0024	7
2A	b003707	554.509185	562.104411	Grains per spike	0.0034	8
2A	b003707	554.509185	562.104411	gLAI_int	5.11	7
2A	b003707	554.509185	562.104411	gLAI_mean	0.0000069	8
2A	b003707	554.509185	562.104411	gLAI_BBCH59	0.0000064	6
2A	b003708	562.455937	582.640558	TGW	0.0016	3
2A	b003708	562.455937	582.640558	Grains per spike	0.0105	9
2A	b003708	562.455937	582.640558	BBCH67	0.21	8
2A	b003708	562.455937	582.640558	GCD	0.36	4
2A	b003797	674.509882	677.043207	Grains per spike	0.0015	1
2D	b006018	62.980802	70.796805	k	0.0000000087	2
3A	b007000	529.216222	533.625984	gl_mean	0.000000023	5
3A	b007063	557.257246	566.868118	Grain yield	0.000071	3
3A	b007063	557.257246	566.868118	HI	0.000000064	1
3A	b007063	557.257246	566.868118	SPAD_BBCH59	0.00109	9
3A	b007063	557.257246	566.868118	gl_mean	0.000000049	8
3B	b007962	103.034742	114.10418	Spike number	0.051	5
3B	b007962	103.034742	114.10418	BBCH64	0.14	3
3B	b008704	705.817298	712.802819	gLAI_mean	0.0000046	2
4A	b009735	101.510451	120.605007	Grain yield	0.000072	4
4A	b009735	101.510451	120.605007	Biomass	2.20	5
4A	b009735	101.510451	120.605007	height	0.0047	2
4B	b010704	59.234305	66.811857	Grain yield	0.000068	2
4B	b010704	59.234305	66.811857	Biomass	2.40	6

Chr	Block	Start [Mbp]	End [Mbp]	Trait	Local GEBV variance	Rank
4B	b010704	59.234305	66.811857	gLAI_int	4.64	6
4B	b010704	59.234305	66.811857	SPAD_BBCH59	0.00064	5
4B	b010704	59.234305	66.811857	RUEgf	0.0000039	4
4B	b010740	95.85825	106.824437	Grain yield	0.000122	7
4B	b010740	95.85825	106.824437	Biomass	2.17	4
4B	b010740	95.85825	106.824437	Grains per spike	0.0024	3
4B	b010740	95.85825	106.824437	gLAI_mean	0.0000063	6
4B	b010740	95.85825	106.824437	gLAI_BBCH59	0.0000066	7
4B	b010740	95.85825	106.824437	RUEgf	0.0000072	7
4B	b010740	95.85825	106.824437	height	0.0127	8
4B	b010843	409.345161	420.093011	gLAI_mean	0.0000067	7
4B	b010843	409.345161	420.093011	gLAI_BBCH59	0.0000075	8
4B	b010843	409.345161	420.093011	gl_int	0.09	6
4B	b010843	409.345161	420.093011	gl_mean	0.000000061	10
4B	b010843	409.345161	420.093011	iPAR	0.026	4
4B	b010843	409.345161	420.093011	RUEgf	0.0000040	6
4B	b010915	535.248651	546.263435	gLAI_dur	0.025	5
5A	b011539	46.674914	51.604533	Grain yield	0.000088	6
5A	b011539	46.674914	51.604533	Spike number	0.078	9
5A	b011540	51.676254	67.320171	Biomass	1.55	1
5A	b011540	51.676254	67.320171	Spike number	0.048	4
5A	b011540	51.676254	67.320171	gLAI_int	4.47	4
5A	b011540	51.676254	67.320171	gLAI_mean	0.0000053	5
5A	b011540	51.676254	67.320171	gLAI_BBCH59	0.0000053	3
5A	b011540	51.676254	67.320171	RUEgf	0.0000039	5
5A	b011553	98.037448	109.943112	HI	0.000000089	4
5A	b011553	98.037448	109.943112	BBCH60	0.15	5
5A	b011553	98.037448	109.943112	gLAI_BBCH59	0.0000053	2
5A	b011555	109.962879	126.695733	RUEgf	0.0000039	3
5A	b011928	503.796316	510.162213	Spike number	0.072	8
5A	b011928	503.796316	510.162213	height	0.0095	7
5A	b012501	702.873159	706.442737	HI	0.000000091	5
5A	b012501	702.873159	706.442737	Spike number	0.056	6
5A	b012501	702.873159	706.442737	BBCH65	0.31	10
5A	b012501	702.873159	706.442737	GCD	0.26	3
5A	b012501	702.873159	706.442737	gLAI_dur	0.016	2
5A	b012501	702.873159	706.442737	gl_int	0.07	3
5A	b012501	702.873159	706.442737	gl_dur	0.037	2
5A	b012501	702.873159	706.442737	gl_mean	0.000000020	3
5A	b012501	702.873159	706.442737	iPAR	0.028	6
5B	b012901	383.035659	394.023386	gLAI_dur	0.013	1
5B	b012901	383.035659	394.023386	gl_int	0.11	9
5B	b012901	383.035659	394.023386	gl_dur	0.056	5
5B	b012901	383.035659	394.023386	gl_mean	0.000000019	2
5B	b012901	383.035659	394.023386	iPAR	0.047	9
5B	b013045	497.003841	518.958307	Grain yield	0.000305	10
5B	b013045	497.003841	518.958307	Biomass	10.69	10
5B	b013045	497.003841	518.958307	Spike number	0.133	10

Chr	Block	Start [Mbp]	End [Mbp]	Trait	Local GEBV variance	Rank
5B	b013045	497.003841	518.958307	Grains per spike	0.0021	2
5B	b013045	497.003841	518.958307	GCD	0.22	1
5B	b013045	497.003841	518.958307	gLAI_dur	0.038	7
5B	b013045	497.003841	518.958307	gl_dur	0.031	1
5B	b013045	497.003841	518.958307	RUEgf	0.0000158	10
5B	b013045	497.003841	518.958307	k	0.0000000687	9
5B	b013045	497.003841	518.958307	height	0.0258	9
5D	b013977	43.409508	46.318871	Grain yield	0.000065	1
5D	b013977	43.409508	46.318871	HI	0.000000095	7
5D	b013977	43.409508	46.318871	SPAD_BBCH59	0.00042	1
5D	b013977	43.409508	46.318871	RUEgf	0.0000085	8
5D	b013977	43.409508	46.318871	height	0.0049	3
6A	b014704	29.229698	33.538666	Biomass	2.89	7
6A	b014704	29.229698	33.538666	BBCH68	0.11	1
6A	b014797	65.855849	72.844592	HI	0.000000088	3
6A	b014797	65.855849	72.844592	Spike number	0.047	3
6A	b014797	65.855849	72.844592	BBCH61	0.18	7
6A	b014797	65.855849	72.844592	k	0.0000000064	1
6A	b014823	92.347663	99.40941	GCD	0.45	7
6A	b014823	92.347663	99.40941	gLAI_int	6.37	8
6A	b014823	92.347663	99.40941	gLAI_dur	0.045	9
6A	b014823	92.347663	99.40941	SPAD_BBCH59	0.00057	4
6A	b014823	92.347663	99.40941	gl_dur	0.047	3
6A	b014823	92.347663	99.40941	k	0.0000000226	5
6A	b014823	92.347663	99.40941	height	0.0092	6
6A	b014828	102.15334	115.462302	Biomass	4.43	9
6A	b014828	102.15334	115.462302	GCD	1.00	9
6A	b014828	102.15334	115.462302	gLAI_int	6.99	9
6A	b014828	102.15334	115.462302	gLAI_dur	0.042	8
6A	b014828	102.15334	115.462302	gl_int	0.09	5
6A	b014828	102.15334	115.462302	gl_dur	0.072	9
6A	b014828	102.15334	115.462302	iPAR	0.024	3
6A	b014828	102.15334	115.462302	RUEgf	0.0000035	1
6A	b014828	102.15334	115.462302	k	0.0000000334	8
6A	b014914	400.248016	417.39771	GCD	0.66	8
6A	b014914	400.248016	417.39771	gLAI_dur	0.017	3
6A	b014914	400.248016	417.39771	gl_int	0.08	4
6A	b014914	400.248016	417.39771	gl_dur	0.061	8
6A	b014914	400.248016	417.39771	iPAR	0.026	5
6A	b014914	400.248016	417.39771	k	0.0000000232	6
6A	b014914	400.248016	417.39771	height	0.0076	5
6A	b014917	417.638448	441.806842	Grain yield	0.000208	8
6A	b014917	417.638448	441.806842	Biomass	3.27	8
6A	b014917	417.638448	441.806842	HI	0.000000173	9
6A	b014917	417.638448	441.806842	TGW	0.0037	8
6A	b014917	417.638448	441.806842	BBCH62	0.17	6
6A	b014917	417.638448	441.806842	GCD	2.78	10
6A	b014917	417.638448	441.806842	gLAI_int	13.06	10

Chr	Block	Start [Mbp]	End [Mbp]	Trait	Local GEBV variance	Rank
6A	b014917	417.638448	441.806842	gLAI_dur	0.072	10
6A	b014917	417.638448	441.806842	gLAI_mean	0.0000051	3
6A	b014917	417.638448	441.806842	gLAI_BBCH59	0.0000063	5
6A	b014917	417.638448	441.806842	gl_int	0.31	10
6A	b014917	417.638448	441.806842	gl_dur	0.254	10
6A	b014917	417.638448	441.806842	iPAR	0.109	10
6A	b014917	417.638448	441.806842	k	0.0000001005	10
6A	b014917	417.638448	441.806842	height	0.0320	10
6A	b014950	496.62401	504.889552	HI	0.000000091	6
6B	b015671	96.633181	113.453272	gLAI_int	4.25	3
6B	b016267	634.315361	640.129615	gLAI_int	4.48	5
6B	b016267	634.315361	640.129615	gLAI_mean	0.0000053	4
6B	b016267	634.315361	640.129615	gLAI_BBCH59	0.0000054	4
6B	b016267	634.315361	640.129615	gl_int	0.07	2
6B	b016267	634.315361	640.129615	gl_mean	0.000000022	4
6B	b016267	634.315361	640.129615	iPAR	0.022	2
6B	b016267	634.315361	640.129615	k	0.0000000117	4
7A	b017655	129.867965	148.012193	Biomass	1.63	2
7A	b017655	129.867965	148.012193	TGW	0.0018	6
7A	b017655	129.867965	148.012193	SPAD_BBCH59	0.00077	7
7A	b017659	155.600083	172.224313	SPAD_BBCH59	0.00081	8
7A	b017697	224.314704	238.829041	HI	0.000000140	8
7A	b017697	224.314704	238.829041	TGW	0.0013	1
7A	b017697	224.314704	238.829041	BBCH63	0.14	4
7A	b017697	224.314704	238.829041	gLAI_int	3.81	2
7A	b017697	224.314704	238.829041	gLAI_mean	0.0000142	10
7A	b017697	224.314704	238.829041	gLAI_BBCH59	0.0000161	10
7A	b017697	224.314704	238.829041	gl_mean	0.000000017	1
7A	b017697	224.314704	238.829041	k	0.0000000283	7
7A	b017709	263.732902	275.962713	SPAD_BBCH59	0.00051	3
7A	b017759	485.610481	497.740992	TGW	0.0014	2
7A	b017759	485.610481	497.740992	Spike number	0.036	2
7A	b018188	663.958958	669.029287	Grain yield	0.000081	5
7A	b018188	663.958958	669.029287	Biomass	1.91	3
7A	b018188	663.958958	669.029287	GCD	0.40	6
7A	b018188	663.958958	669.029287	gLAI_dur	0.026	6
7A	b018188	663.958958	669.029287	SPAD_BBCH59	0.00120	10
7A	b018188	663.958958	669.029287	gl_int	0.11	8
7A	b018188	663.958958	669.029287	gl_dur	0.059	6
7A	b018188	663.958958	669.029287	gl_mean	0.000000024	6
7A	b018188	663.958958	669.029287	iPAR	0.033	7
7A	b018219	672.258666	674.020659	gl_mean	0.000000026	7
7A	b018219	672.258666	674.020659	iPAR	0.013	1
7B	b018789	124.239206	133.496311	BBCH66	0.11	2
7B	b018804	181.036029	199.180188	gLAI_mean	0.0000110	9
7B	b018804	181.036029	199.180188	gLAI_BBCH59	0.0000118	9
7B	b018804	181.036029	199.180188	gl_int	0.05	1
7B	b018804	181.036029	199.180188	gl_dur	0.047	4

Chr	Block	Start [Mbp]	End [Mbp]	Trait	Local GEBV variance	Rank
7B	b018804	181.036029	199.180188	k	0.0000000098	3
7B	b018915	552.780293	564.173696	GCD	0.36	5
7B	b018915	552.780293	564.173696	gLAI_int	3.68	1
7B	b018915	552.780293	564.173696	gLAI_mean	0.0000046	1
7B	b018915	552.780293	564.173696	gLAI_BBCH59	0.0000051	1
7B	b018915	552.780293	564.173696	gl_int	0.09	7
7B	b018915	552.780293	564.173696	gl_dur	0.060	7
7B	b018915	552.780293	564.173696	iPAR	0.033	8
7D	b020083	603.724494	607.295832	SPAD_BBCH59	0.00043	2

REFERENCES

- Acreche MM, Briceño-Félix G, Sánchez JAM, Slafer GA. 2008.** Physiological bases of genetic gains in Mediterranean bread wheat yield in Spain. *European Journal of Agronomy* **28**: 162-170.
- Aisawi KAB, Reynolds MP, Singh RP, Foulkes MJ. 2015.** The physiological basis of the genetic progress in yield potential of CIMMYT spring wheat cultivars from 1966 to 2009. *Crop Science* **55**: 1749-1764.
- Alonso MP, Abbate PE, Mirabella NE, Aramburu Merlos F, Panelo JS, Pontaroli AC. 2018.** Analysis of sink/source relations in bread wheat recombinant inbred lines and commercial cultivars under a high yield potential environment. *European Journal of Agronomy* **93**: 82-87.
- Asseng S, Martre P, Ewert F, Dreccer MF, Beres BL, Reynolds MP, Braun HJ, Langridge P, Le Gouis J, Salse J *et al.* 2019.** Model-driven multidisciplinary global research to meet future needs: the case for “improving radiation use efficiency to increase yield”. *Crop Science* **59**: 843.
- Aulchenko YS, Koning D-J de, Haley C. 2007.** Genomewide rapid association using mixed model and regression. A fast and simple method for genomewide pedigree-based quantitative trait loci association analysis. *Genetics* **177**: 577-585.
- Austin RB, Bingham J, Blackwell RD, Evans LT, Ford MA, Morgan CL, Taylor M. 1980.** Genetic improvements in winter wheat yields since 1900 and associated physiological changes. *Journal of Agricultural Science* **94**: 675-689.
- Balfourier F, Bouchet S, Robert S, Oliveira R de, Rimbert H, Kitt J, Choulet F, Paux E. 2019.** Worldwide phylogeography and history of wheat genetic diversity. *Science Advances* **5**: eaav0536.
- Bancal P. 2008.** Positive contribution of stem growth to grain number per spike in wheat. *Field Crops Research* **105**: 27-39.
- Bannari A, Khurshid KS, Staenz K, Schwarz JW. 2007.** A comparison of hyperspectral chlorophyll indices for wheat crop chlorophyll content estimation using laboratory reflectance measurements. *IEEE Transactions on Geoscience and Remote Sensing* **45**: 3063-3074.
- Bates D, Mächler M, Bolker B, Walker S. 2015.** Fitting linear mixed-effects models using lme4. *Journal of Statistical Software* **67**: 1-48.
- BMEL. 2019.** *Buchführungsergebnisse Landwirtschaft. Wirtschaftliche Lage landwirtschaftlicher Haupterwerbsbetriebe - mehrjähriger Zeitvergleich 2001/02 bis 2016/17.* [WWW document] URL www.bmel-statistik.de.
- Boeven PHG, Longin CFH, Leiser WL, Kollers S, Ebmeyer E, Würschum T. 2016.** Genetic architecture of male floral traits required for hybrid wheat breeding. *Theoretical and Applied Genetics* **129**: 2343-2357.

-
- Borlaug NE. 2007.** Sixty-two years of fighting hunger: personal recollections. *Euphytica* **157**: 287-297.
- Brancourt-Hulmel M, Doussinault G, Lecomte C, Bérard P, Le Buanec B, Trottet M. 2003.** Genetic improvement of agronomic traits of winter wheat cultivars released in France from 1946 to 1992. *Crop Science* **43**: 37-45.
- Cabrera-Bosquet L, Fournier C, Bricet N, Welcker C, Suard B, Tardieu F. 2016.** High-throughput estimation of incident light, light interception and radiation-use efficiency of thousands of plants in a phenotyping platform. *New Phytologist* **212**: 269-281.
- Calderini DF, Dreccer MF, Slafer GA. 1997.** Consequences of breeding on biomass, radiation interception and radiation-use efficiency in wheat. *Field Crops Research* **52**: 271-281.
- Camacho C, Coulouris G, Avagyan V, Ma N, Papadopoulos J, Bealer K, Madden TL. 2009.** BLAST+: architecture and applications. *BMC Bioinformatics* **10**: 421.
- Cavanagh CR, Chao S, Wang S, Huang BE, Stephen S, Kiani S, Forrest K, Saintenac C, Brown-Guedira GL, Akhunova A et al. 2013.** Genome-wide comparative diversity uncovers multiple targets of selection for improvement in hexaploid wheat landraces and cultivars. *Proceedings of the National Academy of Sciences of the United States of America* **110**: 8057-8062.
- Chenu K, Chapman SC, Tardieu F, McLean G, Welcker C, Hammer GL. 2009.** Simulating the yield impacts of organ-level quantitative trait loci associated with drought response in maize: a "gene-to-phenotype" modeling approach. *Genetics* **183**: 1507-1523.
- Christopher JT, Veyradier M, Borrell AK, Harvey G, Fletcher S, Chenu K. 2014.** Phenotyping novel stay-green traits to capture genetic variation in senescence dynamics. *Functional Plant Biology* **41**: 1035-1048.
- Christopher M, Chenu K, Jennings R, Fletcher S, Butler D, Borrell AK, Christopher J. 2018.** QTL for stay-green traits in wheat in well-watered and water-limited environments. *Field Crops Research* **217**: 32-44.
- Cooper M, Technow F, Messina C, Gho C, Totir LR. 2016.** Use of crop growth models with whole-genome prediction: application to a maize multi-environment trial. *Crop Science* **56**: 2141-2156.
- De Vita P, Nicosia OLD, Nigro F, Platani C, Riefolo C, Di Fonzo N, Cattivelli L. 2007.** Breeding progress in morpho-physiological, agronomical and qualitative traits of durum wheat cultivars released in Italy during the 20th century. *European Journal of Agronomy* **26**: 39-53.
- Dubcovsky J, Dvorak J. 2007.** Genome plasticity a key factor in the success of polyploid wheat under domestication. *Science* **316**: 1862-1866.
- Evenson RE, Gollin D. 2003.** Assessing the impact of the Green Revolution, 1960 to 2000. *Science* **300**: 758-762.
- Falconer DS, Mackay TFC. 2009.** Introduction to quantitative genetics. Harlow: Pearson Prentice Hall.
- FAO. 2019.** FAOSTAT. [WWW document] URL <http://www.fao.org/faostat/en/#data/QC>.
-

-
- Feuillet C, Langridge P, Waugh R. 2008.** Cereal breeding takes a walk on the wild side. *Trends in Genetics* **24**: 24-32.
- Fischer RA. 2011.** Wheat physiology: a review of recent developments. *Crop and Pasture Science* **62**: 95-114.
- Fischer RA, Rees D, Sayre KD, Lu Z-M, Condon AG, Saavedra AL. 1998.** Wheat yield progress associated with higher stomatal conductance and photosynthetic rate, and cooler canopies. *Crop Science* **38**: 1467-1475.
- Foulkes MJ, Hawkesford MJ, Barraclough PB, Holdsworth MJ, Kerr S, Kightley S, Shewry PR. 2009.** Identifying traits to improve the nitrogen economy of wheat: Recent advances and future prospects. *Field Crops Research* **114**: 329-342.
- Foulkes MJ, Reynolds MP, Sylvester-Bradley R. 2009.** Chapter 15. Genetic improvement of grain crops: yield potential. In: Sadras VO, Calderini DF, eds. *Crop physiology. Applications for genetic improvement and agronomy*. Elsevier Science, 355-385.
- Furbank RT, Jimenez-Berni JA, George-Jaeggli B, Potgieter AB, Deery DM. 2019.** Field crop phenomics: enabling breeding for radiation use efficiency and biomass in cereal crops. *New Phytologist* **223**: 1714-1727.
- Ganal MW, Plieske J, Hohmeyer A, Polley A, Röder MS. 2019.** High-throughput genotyping for cereal research and breeding. In: Miedaner T, Korzun V, eds. *Applications of genetic and genomic research in cereals*. Elsevier, 3-17.
- Gitelson AA, Gamon JA. 2015.** The need for a common basis for defining light-use efficiency: Implications for productivity estimation. *Remote Sensing of Environment* **156**: 196-201.
- Gready JE, Dwyer SA, Evans JR, eds. 2013.** Applying photosynthesis research to improvement of food crops. Proceedings of a workshop held at the Australian National University. Canberra, ACT, Australia, 2-4 September 2009. Canberra.
- Gregersen PL, Culetic A, Boschian L, Krupinska K. 2013.** Plant senescence and crop productivity. *Plant Molecular Biology* **82**: 603-622.
- Guo Z, Chen D, Röder MS, Ganal MW, Schnurbusch T. 2018.** Genetic dissection of pre-anthesis sub-phase durations during the reproductive spike development of wheat. *Plant Journal*: 909-918.
- Guo Z, Chen D, Schnurbusch T. 2015.** Variance components, heritability and correlation analysis of anther and ovary size during the floral development of bread wheat. *Journal of Experimental Botany* **66**: 3099-3111.
- Guo Z, Schnurbusch T. 2015.** Variation of floret fertility in hexaploid wheat revealed by tiller removal. *Journal of Experimental Botany* **66**: 5945-5958.
- Guo Z, Zhao Y, Röder MS, Reif JC, Ganal MW, Chen D, Schnurbusch T. 2018.** Manipulation and prediction of spike morphology traits for the improvement of grain yield in wheat. *Scientific Reports* **8**: 1-10.

-
- Hammer GL, Cooper M, Tardieu F, Welch S, Walsh B, van Eeuwijk FA, Chapman SC, Podlich D. 2006.** Models for navigating biological complexity in breeding improved crop plants. *Trends in Plant Science* **11**: 587-593.
- Hawkesford MJ, Araus J-L, Park R, Calderini D, Miralles DJ, Shen T, Zhang J, Parry MAJ. 2013.** Prospects of doubling global wheat yields. *Food and Energy Security* **2**: 34-48.
- Hickey LT, N Hafeez A, Robinson H, Jackson SA, Leal-Bertioli SCM, Tester M, Gao C, Godwin ID, Hayes BJ, Wulff BBH. 2019.** Breeding crops to feed 10 billion. *Nature Biotechnology* **37**: 744-754.
- Impens I, Lemeur R. 1969.** Extinction of net radiation in different crop canopies. *Archiv für Meteorologie, Geophysik und Bioklimatologie* **17**: 403-412.
- IWGSC. 2018.** Shifting the limits in wheat research and breeding using a fully annotated reference genome. *Science* **361**: 7191.
- Jagadish KSV, Kavi Kishor PB, Bahuguna RN, Wirén N von, Sreenivasulu N. 2015.** Staying alive or going to die during terminal senescence-an enigma surrounding yield stability. *Frontiers in Plant Science* **6**: 1070.
- Jombart T. 2008.** adegenet. A R package for the multivariate analysis of genetic markers. *Bioinformatics* **24**: 1403-1405.
- Juliana P, Montesinos-López OA, Crossa J, Mondal S, González Pérez L, Poland J, Huerta-Espino J, Crespo-Herrera L, Govindan V, Dreisigacker S *et al.* 2019.** Integrating genomic-enabled prediction and high-throughput phenotyping in breeding for climate-resilient bread wheat. *Theoretical and Applied Genetics* **132**: 177-194.
- Knopf C, Becker H, Ebmeyer E, Korzun V. 2008.** Occurrence of three dwarfing Rht genes in German winter wheat varieties. *Cereal Research Communications* **36**: 553-560.
- Kobayashi H, Ryu Y, Baldocchi DD, Welles JM, Norman JM. 2013.** On the correct estimation of gap fraction. How to remove scattered radiation in gap fraction measurements? *Agricultural and Forest Meteorology* **174-175**: 170-183.
- Kumar U, Joshi AK, Kumari M, Paliwal R, Kumar S, Röder MS. 2010.** Identification of QTLs for stay green trait in wheat (*Triticum aestivum* L.) in the 'Chirya 3' × 'Sonalika' population. *Euphytica* **174**: 437-445.

-
- Kuzay S, Xu Y, Zhang J, Katz A, Pearce S, Su Z, Fraser M, Anderson JA, Brown-Guedira GL, DeWitt N. 2019.** Identification of a candidate gene for a QTL for spikelet number per spike on wheat chromosome arm 7AL by high-resolution genetic mapping. *Theoretical and Applied Genetics* **132**: 2689-2705
- Lamb E, Shirliffe S, May W. 2011.** Structural equation modeling in the plant sciences: An example using yield components in oat. *Canadian Journal of Plant Science* **91**: 603-619.
- Langridge P. 2018.** Innovation in Breeding and Biotechnology. Chapter 8. In: World Scientific Publishing Co. Pte. Ltd., ed. *Agriculture & food systems to 2050. Global Trends, Challenges and Opportunities*. World Scientific, 245-284.
- Lawlor DW, Paul MJ. 2014.** Source/sink interactions underpin crop yield. The case for trehalose 6-phosphate/SnRK1 in improvement of wheat. *Frontiers in Plant Science* **5**: 418.
- Lenth RV. 2016.** Least-Squares Means. The R Package lsmeans. *Journal of Statistical Software* **69**.
- Lesk C, Rowhani P, Ramankutty N. 2016.** Influence of extreme weather disasters on global crop production. *Nature* **529**: 84-87.
- Liang X, Liu Y, Chen J, Adams C. 2018.** Late-season photosynthetic rate and senescence were associated with grain yield in winter wheat of diverse origins. *Journal of Agronomy and Crop Science* **204**: 1-12.
- Lichthardt C, Chen T-W, Stahl A, Stützel H. 2020.** Co-evolution of sink and source in the recent breeding history of winter wheat in Germany. *Frontiers in Plant Science* **10**: 1771.
- Lo Valvo PJ, Miralles DJ, Serrago RA. 2018.** Genetic progress in Argentine bread wheat varieties released between 1918 and 2011. Changes in physiological and numerical yield components. *Field Crops Research* **221**: 314-321.
- Lüttringhaus S, Noleppa S, Gornott C, Lotze-Campen H. 2019.** Climate change impacts on European crop production. A literature review. Berlin, Germany.
- Meier U. 2018.** Growth stages of mono- and dicotyledonous plants. BBCH Monograph. Open Agrar Repository.
- Miedaner T, Korzun V, eds. 2019.** Applications of genetic and genomic research in cereals. Elsevier.
- Mir RR, Reynolds MP, Pinto F, Khan MA, Bhat MA. 2019.** High-throughput phenotyping for crop improvement in the genomics era. *Plant Science* **282**: 60-72.
- Molero G, Joynson R, Pinera-Chavez FJ, Gardiner L-J, Rivera-Amado C, Hall A, Reynolds MP. 2019.** Elucidating the genetic basis of biomass accumulation and radiation use efficiency in spring wheat and its role in yield potential. *Plant Biotechnology Journal* **17**: 1276-1288.
- Monsi M, Saeki T. 2005.** On the factor light in plant communities and its importance for matter production. 1953. *Annals of Botany* **95**: 549-567.

-
- Nagaraja Rao CR. 1984.** Photosynthetically active components of global solar radiation: Measurements and model computations. *Archiv für Meteorologie, Geophysik und Bioklimatologie* **34**: 353-364.
- Naruoka Y, Sherman JD, Lanning SP, Blake NK, Martin JM, Talbert LE. 2012.** Genetic analysis of green leaf duration in spring wheat. *Crop Science* **52**: 99-109.
- Nguyen GN, Panozzo J, Spangenberg G, Kant S. 2016.** Phenotyping approaches to evaluate nitrogen-use efficiency related traits of diverse wheat varieties under field conditions. *Crop and Pasture Science* **67**: 1139-1148.
- Noulas C, Herrera JM, Tziouvalekas M, Qin R. 2018.** Agronomic assessment of nitrogen use efficiency in spring wheat and interrelations with leaf greenness under field conditions. *Communications in Soil Science and Plant Analysis* **49**: 763-781.
- Peng S, Khush GS, Virk P, Tang Q, Zou Y. 2008.** Progress in ideotype breeding to increase rice yield potential. *Field Crops Research* **108**: 32-38.
- Pingali PL. 2012.** Green Revolution: impacts, limits, and the path ahead. *Proceedings of the National Academy of Sciences of the United States of America* **109**: 12302-12308.
- Pinto RS, Lopes MS, Collins NC, Reynolds MP. 2016.** Modelling and genetic dissection of staygreen under heat stress. *Theoretical and Applied Genetics* **129**: 2055-2074.
- R Core Team. 2019.** R: A Language and Environment for Statistical Computing. Vienna, Austria: R Core Team.
- Rasheed A, Xia X. 2019.** From markers to genome-based breeding in wheat. *Theoretical and Applied Genetics* **132**: 767-784.
- Ray DK, Mueller ND, West PC, Foley JA. 2013.** Yield trends are insufficient to double global crop production by 2050. *PLoS One* **8**: e66428.
- Reynolds MP. 2012.** Introduction. In: Reynolds MP, Pask AJD, Mullan DM, eds. *Physiological breeding I: interdisciplinary approaches to improve crop adaptation*. CIMMYT, 2-4.
- Reynolds MP, Bonnett D, Chapman SC, Furbank RT, Manès Y, Mather DE, Parry MAJ. 2011.** Raising yield potential of wheat. I. Overview of a consortium approach and breeding strategies. *Journal of Experimental Botany* **62**: 439-452.
- Reynolds MP, Condon AG, Parry MAJ, Furbank RT. 2013.** Status of photosynthetic and associated research in wheat and prospects for increasing photosynthetic efficiency and yield potential. In: Gready JE, Dwyer SA, Evans JR, eds. *Applying photosynthesis research to improvement of food crops. Proceedings of a workshop held at the Australian National University. Canberra, ACT, Australia, 2–4 September 2009*. Canberra: 43-50.

-
- Reynolds MP, Foulkes MJ, Furbank RT, Griffiths S, King J, Murchie E, Parry MAJ, Slafer GA. 2012.** Achieving yield gains in wheat. *Plant, Cell & Environment* **35**: 1799-1823.
- Reynolds MP, Foulkes MJ, Furbank RT, Parry MAJ. 2012.** Chapter 4: Opportunities to improve genetic wheat yield potential. In: Reynolds MP, Pask AJD, Mullan DM, eds. *Physiological breeding I: interdisciplinary approaches to improve crop adaptation*. CIMMYT, 43-50.
- Reynolds MP, Foulkes MJ, Slafer GA, Berry P, Parry MAJ, Snape JW, Angus WJ. 2009.** Raising yield potential in wheat. *Journal of Experimental Botany* **60**: 1899-1918.
- Reynolds MP, Langridge P. 2016.** Physiological breeding. *Current Opinion in Plant Biology* **31**: 162-171.
- Reynolds MP, Manes Y, Izanloo A, Langridge P. 2009.** Phenotyping approaches for physiological breeding and gene discovery in wheat. *Annals of Applied Biology* **155**: 309-320.
- Reynolds MP, Pask AJD, Hoppitt WJE, Sonder K, Sukumaran S, Molero G, Pierre CS, Payne T, Singh RP, Braun HJ et al. 2017.** Strategic crossing of biomass and harvest index—source and sink—achieves genetic gains in wheat. *Euphytica* **213**: 257
- Reynolds MP, Pask AJD, Mullan DM, eds. 2012.** Physiological breeding I: interdisciplinary approaches to improve crop adaptation. CIMMYT.
- Richards RA, Cavanagh CR, Riffkin P. 2019.** Selection for erect canopy architecture can increase yield and biomass of spring wheat. *Field Crops Research* **244**: 107649.
- Rutkoski J, Poland J, Mondal S, Autrique E, Pérez LG, Crossa J, Reynolds MP, Singh R. 2016.** Canopy temperature and vegetation indices from high-throughput phenotyping improve accuracy of pedigree and genomic selection for grain yield in wheat. *G3-Genes Genomes Genetics* **6**: 2799-2808.
- Sadras VO, Calderini DF, eds. 2009.** Crop physiology. Applications for genetic improvement and agronomy. Elsevier Science.
- Sadras VO, Lawson C. 2011.** Genetic gain in yield and associated changes in phenotype, trait plasticity and competitive ability of South Australian wheat varieties released between 1958 and 2007. *Crop and Pasture Science* **62**: 533-549.
- Sanchez-Garcia M, Álvaro F, Peremarti A, Trevaskis B, Martín Sánchez JA, Royo C. 2015.** Breeding effects on dry matter accumulation and partitioning in Spanish bread wheat during the 20th century. *Euphytica* **203**: 321-336.
- Sanchez-Garcia M, Royo C, Aparicio N, Martín Sánchez JA, Álvaro F. 2013.** Genetic improvement of bread wheat yield and associated traits in Spain during the 20th century. *Journal of Agricultural Science* **151**: 105-118.

-
- Schulthess AW, Reif JC, Ling J, Plieske J, Kollers S, Ebmeyer E, Korzun V, Argillier O, Stiewe G, Ganai MW et al. 2017.** The roles of pleiotropy and close linkage as revealed by association mapping of yield and correlated traits of wheat (*Triticum aestivum* L.). *Journal of Experimental Botany* **68**: 4089-4101.
- Serrago RA, Alzueta I, Savin R, Slafer GA. 2013.** Understanding grain yield responses to source–sink ratios during grain filling in wheat and barley under contrasting environments. *Field Crops Research* **150**: 42-51.
- Serraj R, Krishnan L, Pingali PL. 2018.** Chapter 1: Agriculture and food systems to 2050: a synthesis. In: World Scientific Publishing Co. Pte. Ltd., ed. *Agriculture & food systems to 2050. Global Trends, Challenges and Opportunities*. World Scientific.
- Shearman VJ, Sylvester-Bradley R, Scott RK, Foulkes MJ. 2005.** Physiological processes associated with wheat yield progress in the UK. *Crop Science* **45**: 175-185.
- Shi S, Azam FI, Li H, Chang X, Li B, Jing R. 2017.** Mapping QTL for stay-green and agronomic traits in wheat under diverse water regimes. *Euphytica* **213**: 246.
- Sinclair TR, Jamieson PD. 2006.** Grain number, wheat yield, and bottling beer: an analysis. *Field Crops Research* **98**: 60-67.
- Sinclair TR, Rufty TW, Lewis RS. 2019.** Increasing photosynthesis: unlikely solution for world food problem. *Trends in Plant Science* **24**: 1032-1039.
- Tang Y, Wu X, Li C, Yang W, Huang M, Ma X, Li S. 2017.** Yield, growth, canopy traits and photosynthesis in high-yielding, synthetic hexaploid-derived wheats cultivars compared with non-synthetic wheats. *Crop and Pasture Science* **68**: 115-125.
- Tian X, Wen W, Xie L, Fu L, Xu D, Fu C, Wang D, Chen X, Xia X, Chen Q et al. 2017.** Molecular mapping of reduced plant height gene Rht24 in bread wheat. *Frontiers in Plant Science* **8**: 1379.
- Tian Z, Jing Q, Dai T, Jiang D, Cao W. 2011.** Effects of genetic improvements on grain yield and agronomic traits of winter wheat in the Yangtze River Basin of China. *Field Crops Research* **124**: 417-425.
- Tilman DG. 1998.** The greening of the Green Revolution. *Nature* **396**: 211-212.
- van Eeuwijk FA, Bustos-Korts D, Millet EJ, Boer MP, Kruijer W, Thompson A, Malosetti M, Iwata H, Quiroz R, Kuppe C et al. 2019.** Modelling strategies for assessing and increasing the effectiveness of new phenotyping techniques in plant breeding. *Plant Science* **282**: 23-39.
- Verma V, Foulkes MJ, Worland AJ, Sylvester-Bradley R, Caligari PDS, Snape JW. 2004.** Mapping quantitative trait loci for flag leaf senescence as a yield determinant in winter wheat under optimal and drought-stressed environments. *Euphytica* **135**: 255-263.
- Vijayalakshmi K, Fritz AK, Paulsen GM, Bai G, Pandravada S, Gill BS. 2010.** Modeling and mapping QTL for senescence-related traits in winter wheat under high temperature. *Molecular Breeding* **26**: 163-175.

-
- Voss-Fels KP, Stahl A, Wittkop B, Lichthardt C, Nagler S, Rose T, Chen T-W, Zetzsche H, Seddig S, Majid Baig M et al. 2019.** Breeding improves wheat productivity under contrasting agrochemical input levels. *Nature Plants* **5**: 706-714.
- Wang E, Brown HE, Rebetzke GJ, Zhao Z, Zheng B, Chapman SC. 2019.** Improving process-based crop models to better capture genotype×environment×management interactions. *Journal of Experimental Botany* **70**: 2389-2401.
- Wang Z, Yin Y, He M, Zhang Y, Lu S, Li Q, Shi S. 2003.** Allocation of photosynthates and grain growth of two wheat cultivars with different potential grain growth in response to pre- and post-anthesis shading. *Journal of Agronomy and Crop Science* **189**: 280-285.
- Wehrmann J, Scharpf HC. 1979.** Der Mineralstickstoffgehalt des Bodens als Maßstab für den Stickstoffdüngerbedarf (Nmin-Methode). *Plant and Soil* **52**: 109-126.
- Witzenberger A, den Boom T von, Hack H. 1989.** Erläuterungen zum BBCH Dezimal-Code für die Entwicklungsstadien des Getreides - mit Abbildungen. *Gesunde Pflanze* **41**: 384-388.
- Wollenweber B, Porter JR, Lübberstedt T. 2005.** Need for multidisciplinary research towards a second Green Revolution. *Current Opinion in Plant Biology* **8**: 337-341.
- World Scientific Publishing Co. Pte. Ltd., ed. 2018.** Agriculture & food systems to 2050. Global Trends, Challenges and Opportunities. World Scientific.
- Wu C, Niu Z, Tang Q, Huang W, Rivard B, Feng J. 2009.** Remote estimation of gross primary production in wheat using chlorophyll-related vegetation indices. *Agricultural and Forest Meteorology* **149**: 1015-1021.
- Wu X-Y, Kuai B-K, Jia J-Z, Jing H-C. 2012.** Regulation of leaf senescence and crop genetic improvement. *Journal of Integrative Plant Biology* **54**: 936-952.
- Würschum T, Langer SM, Longin CFH, Tucker MR, Leiser WL. 2017.** A modern Green Revolution gene for reduced height in wheat. *Plant Journal* **92**: 892-903.
- Würschum T, Leiser WL, Langer SM, Tucker MR, Longin CFH. 2018.** Phenotypic and genetic analysis of spike and kernel characteristics in wheat reveals long-term genetic trends of grain yield components. *Theoretical and Applied Genetics* **131**: 2071-2084.
- Würschum T, Liu G, Boeven PHG, Longin CFH, Mirdita V, Kazman E, Zhao Y, Reif JC. 2018.** Exploiting the Rht portfolio for hybrid wheat breeding. *Theoretical and Applied Genetics* **131**: 1433-1442.
- Xie Q, Mayes S, Sparkes DL. 2016.** Early anthesis and delayed but fast leaf senescence contribute to individual grain dry matter and water accumulation in wheat. *Field Crops Research* **187**: 24-34.
- Xiong D, Chen J, Yu T, Gao W, Ling X, Li Y, Peng S, Huang J. 2015.** SPAD-based leaf nitrogen estimation is impacted by environmental factors and crop leaf characteristics. *Scientific Reports* **5**.
- Yin X, Guo W, Spiertz JH. 2009.** A quantitative approach to characterize sink–source relationships during grain filling in contrasting wheat genotypes. *Field Crops Research* **114**: 119–126.

-
- Yin X, Struik PC, Kropff MJ. 2004.** Role of crop physiology in predicting gene-to-phenotype relationships. *Trends in Plant Science* **9**: 426-432.
- Zhang L, Hu Z, Fan J, Zhou D, Tang F. 2014.** A meta-analysis of the canopy light extinction coefficient in terrestrial ecosystems. *Frontiers of Earth Science* **8**: 599-609.
- Zhang S, Zhao G, Lang K, Su B, Chen X, Xi X, Zhang H. 2019.** Integrated satellite, unmanned aerial vehicle (UAV) and ground inversion of the SPAD of winter wheat in the reviving stage. *Sensors* **19**: 1485.

CURRICULUM VITAE

Contact

Fuchspfad 10
29342 Wienhausen
0175-7472935
c.lichthardt@t-online.de

Date of birth

11.12.1987, in Celle

Nationality

German

Family status

married, one daughter (*30th April, 2017)

PROFESSIONAL CAREER

Since 08/2020

Consultant at the Federal Plant Variety Office, Hannover

11/2019 – 04/2020

Assistant Breeder for phenotypic and marker-assisted selection in hybrid rye
KWS LOCHOW GMBH, Bergen – Wohlde

08/2014 – 03/2020

PhD candidate, Leibniz University Hannover
Institute of Horticultural Production Systems
Topic: “*Impact of breeding innovations in canopy architecture and function on yield formation in winter wheat*” within the BMBF funded project **BRIWECS**

ACADEMIC STUDIES

10/2012 – 07/2014

Crop Science, University of Hohenheim, Stuttgart
M. Sc., Average: 1,7 (B)
Major: Plant Breeding and Seed Science
Master thesis: „*Application of selective sweep mapping to identify resistance genes in a pre-breeding population of sugar beet*“, grade: very good (A)

10/2008 – 06/2012

Agricultural Biology, University of Hohenheim, Stuttgart
B. Sc., Average: 2,0 (B)
Bachelor thesis: „*Characterisation of different Quinoa (Chenopodium Quinoa Willd.) accessions by GBS*“, grade: very good (A)

INTERNATIONAL EXPERIENCES

08/2013

Summer school– Aarhus University (Research Centre Flakkebjerg)
“Advanced methods and techniques in plant science and biotechnology”

01/2011 – 06/2011

ERASMUS – semester abroad
Sveriges lantbruks-universitet (SLU) in Uppsala, Sweden

SCHOOLING

07/2000 – 06/2007

Kaiserin-Auguste-Viktoria-Gymnasium, Celle, Average: 2.6

LIST OF PUBLICATIONS

Reviewed articles

Lichthardt C, Chen T-W, Stahl A, Stützel H, 2019. Co-evolution of sink and source in the recent breeding history of winter wheat in Germany. *Frontiers in Plant Science* 10: 1771.

Voss-Fels K P, Stahl A, Wittkop B, **Lichthardt C**, Nagler S, Rose T, Chen T-W, Zetzsche H, Seddig S, Majid Baig M, Ballvora A, Frisch M, Ross E, Hayes B J, Hayden M J, Ordon F, Leon J, Kage H, Friedt W, Stützel H, Snowdon R J, 2019. Breeding improves wheat productivity under contrasting agrochemical input levels. *Nature plants* 5, 706–714

Conference papers

Lichthardt C, Chen T-W, Stützel H, 2019. Post-anthesis green canopy duration contributes to breeding progress of German winter wheat. 1st International Wheat Congress (*presentation*).

Lichthardt C, Chen T-W, Stützel H, 2018. Post anthesis canopy green area duration contributes to breeding progress of German winter wheat. *Mitteilungen der Gesellschaft für Pflanzenbauwissenschaften Band 29 (presentation)*.

Lichthardt C, Chen T-W, Stützel H, 2018. Increasing wheat yield by focusing on light interception? German Plant Breeding Conference (*poster*).

Lichthardt C, Stützel H, Wittkop B, 2017. Increasing wheat yield by focusing on light interception? 13th International Wheat Genetics Symposium (*poster*).

Lichthardt C, Stützel H, 2017. BRIWECS: Increasing wheat yield by focusing on light interception? PLANT 2030 Status Seminar (*poster*).

Lichthardt C, Stützel H, 2016. Entwicklung in der Lichtaufnahme von Winterweizensorten in der deutschen Züchtungshistorie – erste Ergebnisse und Erkenntnisse. *Mitteilungen der Gesellschaft für Pflanzenbauwissenschaften Band 28 (presentation)*.

Lichthardt C, Stützel H, 2016. BRIWECS: Influence of breeding innovations in crop architecture and canopy light interception on the productivity of winter wheat. PLANT 2030 Status Seminar (*poster*).

Lichthardt C, Stützel H, 2016. Influence of breeding innovations in crop architecture and canopy light interception on the productivity of winter wheat. German Plant Breeding Conference (*poster*).

Lichthardt C, Stützel H, 2015. Innovations in wheat breeding - Impact of innovations in plant architecture and light interception on productivity and stability in wheat cropping systems. *Mitteilungen der Gesellschaft für Pflanzenbauwissenschaften Band 27 (poster)*.

DANKSAGUNG

Zu aller erst möchte ich **Hartmut** für das Vertrauen danken! Die Möglichkeit so selbstständig und fokussiert arbeiten zu können war eine einmalige Gelegenheit und ich habe dadurch sehr viel gelernt. Vielen Dank für dein Interesse an meiner Arbeit und deine Unterstützung! **Andreas** und **Tsu-Wie**, vielen Dank, dass ihr geholfen habt, die Auswertung der Daten und die Interpretation meiner Ergebnisse auf ein wissenschaftliches Niveau zu heben, vielen Dank für kritische Fragen und genaues Hinschauen. Die ehrlichen Diskussionen, eure Zeit und euer Interesse an meiner Arbeit haben wesentlich dazu beigetragen, dass in diesen Kapiteln (vor allem Kapitel 2 und 3) wertvolle Aussagen zu finden sind! Ich bin zudem sehr dankbar für alle fachlichen Diskussionen und das nette Beisammensein bei den BRIWECS Projekttreffen. Vielen Dank an alle **BRIWECS Kollegen** für eure Unterstützung und eure Beiträge zu unserem Teilprojekt. Vor allem auch an **Sophia** ein großes Dankeschön fürs Korrektur lesen und für die gute Zeit in Kanada!

Rückblickend sind es die kleine Gesten, die in Erinnerung bleiben und die Zusammenarbeiten ausmachen, zum Beispiel der Besuch von Hartmut auf dem Feld zur ersten Versuchsernte, dass **Tino** mich im zweiten Versuchsjahr die letzte Parzelle dreschen lies (obwohl ich noch vorher noch nie auf dem Drescher gesessen hatte), die guten Wünsche zur „großen Reise“ nach Kanada... Vor allem diese kleinen Momente tragen dazu bei, dass meine Zeit in Hannover einen wertvollen Platz in meinem Werdegang einnimmt. Ich danke insbesondere **Katharina**, **Tino**, **Petra** und all den fleißigen Hiwis für die fröhliche Unterstützung bei der Arbeit auf dem Feld, **Ilna** für hilfreiche Ratschläge, immer ein freundliches Lächeln und wenn nötig aufmunternde Worte und **Heike** fürs wertvolle „regeln und sich kümmern“, für den Überblick und die freundliche Art.

Von ganzen Herzen danke ich meiner **Familie**, vor allem natürlich David und Leni, die mich in den Zeiten, wo meine Gedanken sich schlecht vom Schreibtisch lösen konnten oft mit Nachdruck an die schönen Dinge des Lebens erinnert haben. Ich bin sehr dankbar, für alle aufmunternden Worte meiner Freunde und euer Verständnis! Ohne die Unterstützung vor allem aber von meinen **Eltern** wäre diese Arbeit nicht zustande gekommen. Allein die Bestärkung und Ermutigung, die Doktorarbeit auch nur zu beginnen, die unermüdlich Unterstützung, euer Interesse und euer Stolz haben unmessbar dazu beigetragen, dass ich durchgehalten habe. Wenn ich selbst nicht mehr daran geglaubt habe, dass es noch was werden könnte, habt ihr es doch getan und nur so hatte ich die Kraft bis zum Ende durchzuhalten.